UNIVERSIDADE DE LISBOA

FACULDADE DE CIÊNCIAS

DEPARTAMENTO DE QUÍMICA E BIOQUÍMICA

Effect of TGFß Signalling on CFTR Protein: Consequences for Epithelial Differentiation in CF

Mestrado em Bioquímica

Especialização em Bioquímica Médica

Margarida Cuco Quaresma

Dissertação orientada por:

Professor Doutor Luka A. Clarke

Professora Doutora Margarida B. Telhada

2015

Index

Acknowlegments/Agradecimentos

Ao terminar este trabalho não posso deixar de agradecer às várias pessoas que contribuiram, de alguma maneira, para a sua realização.

Em primeiro lugar gostaria de agradecer à professora Margarida Amaral por me ter recebido no seu laboratório e grupo de investigação e por sempre ter mostrado um interesse pessoal para comigo e o meu projecto. Gostaria de lhe agradecer por toda a ajuda e orientação e por acreditar em mim e no projecto.

Não posso deixar também de agradecer aos meus orientadores, a professora Margarida Telhada e o professor Luka Clarke. Obrigada pela ajuda, paciência, atenção e preocupação, mesmo quando o tempo era pouco. Obrigada pela confiança e pela simpatia com que sempre se mostraram disponíveis para mim.

Quero também deixar um agradecimento ao professor António Cidadão por me ter convidado para realizar a experiência de H&E no seu laboratório e ao Vítor Proa pela prontidão e amabilidade com que me recebeu e ajudou.

O meu mais sincero agradecimento e reconhecimento vão para o Hugo Botelho, que foi simplesmente incansável a supervisionar de perto todos os passos deste projecto. Sem ele este trabalho não teria metade da qualidade ou coerência. Obrigada por todo o tempo dispendido a discutir protocolos e resultados, por todos os ensinamentos e pela paciência infinita, sempre com boa disposição e vontade de ajudar. Obrigada ainda pela leitura das versões mais cruas da minha tese e por todo o investimento para que ficasse muito melhor.

I also have to thank Ines Pankonien for helping me with a lot of the experiments and for teaching me, always giving me great advice, coffee and keeping my spirits up. Working with her was both instructing and very fun!

Quero também agradecer ao Luís Marques por ter sido verdadeiramente incansável e indespensável a recolher a analisar todas (e eram muitas!) as minhas imagens de microscopia confocal. Obrigada também pelo tempo dispendido a discutir os resultados e a ensinar-me coisas e pelas conversas parvas que fomos tendo pelo caminho.

O meu agradecimento sentido vai também para todos os meus colegas de laboratório que, cada um à sua maneira, me ajudaram com este trabalho. À Veronica por estar sempre disponivel para me ajudar quando desesperava com os meus PCRs; à Sara por responder sempre prontamente a todas as minhas dúvidas (mesmo as parvas); ao João por ter sempre qualquer coisa querida para dizer e alegrar o meu dia (mesmo sendo do Benfica...); ao Zé e ao Simão por me ajudarem com tudo o que precisava e por animarem sempre toda a gente; à Joana, que tinha sempre um conselho para dar quando era preciso; à Susana, com os seus conselhos e ensinamentos de "grown up, que tentava sempre dizer-me para parar de "stressar" e me trazia fruta para manter os níveis de vitaminas elevados; e por fim aos meus eternos parceiros de todas as horas, o João Coelho e a Madalena – sem a irmandade dos "small ones" (incluindo as horas tardias, os vídeos parvos e todos os risos) isto tinha tudo sido bem mais difícil.

Tenho que agradecer também aos meus "migos falsos" por todo o apoio e motivação ao longo do ano, por me obrigarem a ver que o trabalho não é tudo e que os amigos, e os momentos que passamos com eles, são do melhor que levamos desta vida. Especialmente obrigada às melhores amigas de sempre, Ana, Inês, Leonor, Madalena e Sílvia, por tudo. Com

vocês tudo é mais fácil. A vossa amizade consegue sempre ajudar-me a superar todos os desafios e maus momentos. Que estejam sempre presentes!

Obrigada à "família" que escolhi, Eunice, Marta, Vanessa, Bruno, Jorge e Luís. Obrigada pelo apoio, pelo interesse e por me conhecerem tão bem e há tantos anos. Já podem parar de se preocupar com o meu ar cansado e preocupado!

Obrigada ao Tomás por tentar, sempre. Tentar animar-me, tentar ajudar-me, tentar acalmar-me, tentar ser melhor por mim. Sem ele para me apoiar nos dias mais complicados nada seria o mesmo.

Obrigada à minha família, por estarem lá para mim ao fim dos dias compridos, por nunca desistirem de mim, por acreditarem sempre. Por partilharem as minhas vitórias. Obrigada ao meu pai, que é o melhor modelo que conheço de integridade e inteligência e que me motiva sempre a dar o meu melhor. Obrigada à minha mãe pelo carinho infinito que nem sempre sei retribuir. Obrigada ao meu irmão Duarte que quis sempre ler o que andava a fazer, que me ajudou com histologia, que me faz sempre rir e me tenta sempre ajudar ao máximo. Obrigada à minha tia João, a minha "tia fixe", que está sempre lá para tudo. Obrigada ao Simão, por ser o meu eterno companheiro e confidente. Obrigada ao meu avô Amândio por tudo o que me ensinou na vida – depois de tantos anos a aprender, este trabalho também é para ele.

Por fim não posso deixar de agradecer à pessoa mais essencial neste ano de trabalho, a minha melhor amiga e parceira de bancada e de parvoíce, a Madalena. A Madalena traz sempre ao de cima o melhor de mim, motiva-me a ser esforçada, empenhada, a nunca desistir. Mas também me aceita como sou, com todas as falhas e defeitos. Faz-me sempre rir e tem sempre os melhores conselhos. Sem a força e o apoio dela nunca teria sido possível chegar ao fim. Obrigada pela partilha desta jornada tão importante.

A todos o meu mais sincero obrigada!

Abstract

Cystic fibrosis (CF) is the most common life-threatening autosomal recessive disease in Caucasians. CF is caused by mutations in the cystic fibrosis transmembrane regulator (CFTR). The most common one is the deletion of residue phenylalanine 508 (F508del). CFTR is well established as a cyclic AMP-activated anion channel, expressed in the apical surface of epithelial cells of a wide variety of tissues. F508del-CFTR, however, adopts an abnormal conformation which potentiates endoplasmic reticulum retention and degradation of the protein. Most of this protein fails to reach the plasma membrane. CFTR is known to conduct chloride and bicarbonate. In addition to anion transport, CFTR also has a regulatory role towards other epithelial channels, like the epithelial Na^+ channel (ENaC).

CFTR mutations are in the origin of the clinic manifestations of CF. The more severely damaged tissues and organs are the airways, gastrointestinal tract and reproductive system. Pancreatic insufficiency, meconium ileus and liver disease are recurrent symptoms. Male infertility is almost universal. However, most CF morbidity and mortality is associated with the respiratory tract. As a conductance regulator, CFTR influences the ion and water content of the airway surface liquid (ASL) and its dysregulation causes a reduced ASL volume as well as thick and dehydrated airway mucus. This mucus obstructs the small airways and impairs mucociliary clearance, prejudicing the removal of inhaled bacteria and other pathogens. Hence the CFTR defect promotes persistent infections by pathogens resistant to therapy. This generates continuous antigen stimulation which results in exacerbated inflammation and progressive airway damage. This eventually leads to airway fibrosis and destruction.

The poor correlation between CFTR genotype and lung disease phenotype suggests the influence of environmental and secondary genetic factors (CF modifier genes) which affect the development, progression and disease severity. The transforming growth factor beta 1 (TGFβ1) has been among the most studied. TGFβ controls differentiation, migration, and programed cell death. It is a master regulator of immune responses, exerting powerful pro- and anti-inflammatory functions and also has a central role in epithelial remodelling, balancing the extracellular matrix (ECM) production and degradation. Intracellular TGFβ signalling occurs via specific type II receptors (TbR-II) which complex with, and subsequently phosphorylate, type I receptors (TbR-I). The canonical intracellular signalling pathway for TGFβ1 is mediated by a family of transcription factors, the Smad proteins.

TGFβ1 polymorphisms which increase its expression have been found on CF patients and reported to correlate with low lung function and a more severe pulmonary disease. TGFβ1 is therefore speculated to bridge the inflammatory and remodelling pathways in CF, modifying CF lung disease progression.

TGFβ is also a major inducer of epithelial-mesenchymal transitions (EMTs). An EMT is a complex process whereby fully differentiated polarized epithelial cells transition into a mesenchymal phenotype. EMT underlies tissue morphogenesis and organogenesis in the embryo, as well as tissue remodelling and repair in adults. However, it is also an important element in cancer progression and malignancy, such as fibrosis. The transition of epithelial cells into mesenchymal cells occurs through a conserved programme with hallmarks. Firstly, there is the dissolution/disassembly of the epithelial cell–cell junctions, followed by loss of apical–basal polarity. This is followed by reorganization of the cytoskeletal architecture and changes in cell shape, as well as development of cell protrusions and motility and, in many cases, an ability to degrade ECM proteins to enable invasive behaviour. Finally, there is a

downregulation of the epithelial gene expression signature and activation of genes that help defining the mesenchymal phenotype.

Interestingly, CFTR has been described to be not only dependent on but also involved in epithelial differentiation, having reported roles in development, fibrosis and cancer. Importantly, airway epithelial differentiation and regeneration has been reported to be impaired in bronchial epithelial CF cells, even in the absence of airway infection. However exacerbated inflammation can also affect CFTR expression. In a remodelled surface epithelium with severe inflammation, CFTR protein presented either a diffuse distribution in the cytoplasm of ciliated cells or was absent.

Unveiling of TGFβ pathways, including those involved in EMT, has revealed mediators regulating the downstream Smad transcriptional activity. These include the CCAAT-enhancer binding proteins (C/EBP). Among this family, C/EBPβ has been reported to be the dominant DNA binding factor in the adult airway epithelium. C/EBPβ is known to have roles in the differentiation of adipocytes, macrophages and mammary epithelial cells; in metabolic control; in inflammation and acute-phase response; and in promoting cellular proliferation. C/EBPβ possesses distinct types of isoforms, including two transcriptional activators (LAPs) and one transcriptional inhibitor (LIP). LIP represses gene expression, inhibiting LAP isoforms in a dominant negative fashion.

TGFβ signalling is known to induce Smad-dependent inhibition of C/EBPβ function. However, C/EBPβ can also serve as a cofactor for TGFβ signalling: induction of the cyclin-dependent kinase 4 inhibitor B (p15INK4b) and repression of c-Myc (both needed for the cytostatic response of TGFβ) were found to depend on C/EBPβ. Interestingly, a higher level of LIP (and decreased level of LAP) has successfully been linked to a loss of TGFβ-dependent cytostatic responses in metastatic cells from breast cancer patients. LIP increase in several epithelial cells resulted in an increase in proliferation, decrease in differentiation and formation of hyperplasias.

In addition to TGFβ, C/EBPβ is also regulated by miR-155. This miRNA is reported to be involved in numerous biological processes including inflammation and immunity. TGFβ stimulation is also known to enhance miR-155 expression levels, augmenting the TGFβ-dependent EMT. Accordingly, miR-155-mediated loss of C/EBPβ was also found as a mechanism of promotion of breast cancer progression, by shifting the TGFβ response from growth inhibition to EMT, invasion and metastasis. Finally, expression of miR-155 was found to be elevated in CF lung epithelial cells, compared with control cells.

The main goal of the present work was to explore the physiological significance of TGFβ signalling in the absence of functional CFTR, namely its possible role in activating EMT pathways.

To achieve this it was sought to: determine if EMT was a component of CF disease; assessing the localization and status of transcription factor C/EBPβ in the absence of functional CFTR; investigating C/EBPβ's possible role in mediating TGFβ induced EMT; and evaluating the role of miR-155 on these processes. Both lung tissue (from control and CF patients) and cystic fibrosis bronchial epithelial cells (expressing either wt or F508del-CFTR) were used to perform these tasks.

Analysis of the CF tissue revealed tissue remodelling consistent with a chronic inflammation environment in the lung and a loss of epithelial differentiation. Furthermore, the presence of mesenchymal markers and loss of epithelial markers supported the notion of an EMT occurrence.

The differences in the differentiation status seemed to reflect on the C/EBPβ levels. F508del-CFTR CFBE cells show reduced C/EBPβ protein and mRNA levels. Although CFTR and C/EBPβ were not found to interact on protein level, reduction of wt-CFTR at the plasma membrane when C/EBPβ was knocked down suggests an involvement of C/EBPβ in the traffic of CFTR to the plasma membrane. It is still unclear if this is mediated by the LAP or LIP isoform.

TGFβ treatment of both polarized CFBE cell lines resulted in decreases in transepithelial electrical resistance (TEER) and loss of E-cadherin expression, consistent with a TGFβ-induced EMT. Despite the anti-inflammatory and anti-apoptotic roles known for TGFβ, a 48 hour exposure to this cytokine seemed to shift definitively the response towards chronic inflammation and EMT induction. This response is consistent with the findings on CF lung tissue. Accordingly, TEER and C/EBPβ expression were found to be more reduced in F508del-CFTR cells compared to wt after TGFβ treatment. This could be due to more increased LIP levels (which were observed on F508del-CFTR cells) but could also point to the involvement of other dysregulated pathways resulting from the CFTR defect. Accordingly, miR-155 was found to be repressing C/EBPβ on both cell types. However, on F508del-CFTR cells addition of miR-155 had a larger impact on C/EBPβ levels. This could suggest that the CFTR dysfunction produces increased baseline levels of miR-155 which further contributes to decreasing C/EBPβ. This is in agreement with the TGFβ results, which point to additional dysregulated pathways resultant from CFTR defect affecting C/EBPβ levels.

Surprisingly, the wt-CFTR levels increased with TGFβ and miR-155 treatment whereas F508del-CFTR showed no changes in expression. Since this is contradictory to recent findings that TGFβ impairs CFTR biogenesis, CFBE cells could not be the best model to assess CFTR levels in response to TGFβ treatment. This can be because these cell lines are overexpressing CFTR and, in this respect, do not perfectly recapitulate the *in vivo* situation.

This work contributes to our understanding of the regulatory role of CFTR in epithelial differentiation and chronic inflammation in cystic fibrosis.

Key words: CFTR, cystic fibrosis, C/EBPβ, Epithelial-Mesenchymal Transition, TGFβ

Resumo

A fibrose quistica (FQ) é a doença letal autossómica recessiva mais comum na população caucasiana. A doença é causada por mutações na proteina CFTR (do inglês *cystic fibrosis conductance regulator*), a mais comum sendo uma deleção do resíduo de fenilalanina 508 (F508del). A CFTR encontra-se bem estabelecida como um canal iónico activado por AMP ciclico expresso na superficie apical de células epiteliais numa variedade de tecidos. A CFTR F508del no entanto adopta uma conformação anormal que potencia a sua retenção no reticulo endoplasmático e degradação. A maioria desta proteína não atinge a membrana plasmática. A CFTR tem um papel conhecido como transportador de cloro e bicarbonato. Além do transporte aniónico, esta proteina também tem um papel regulador em relação a outros canais na membrana, como a ENaC (do inglês *epithelial sodium channel*).

Mutações na CFTR estão na origem das manifestações clínicas da doença. Os tecidos e orgãos mais afectados incluem as vias respiratórias, o tracto gastrointestinal e o sistema reprodutor. Insuficiencia pacreática, mecónio e hepatopatia são sintomas recurrentes. A infertilidade masculina também é praticamente universal em pacientes. No entanto a maior causa de mortalidade resultante da FQ está associada com as vias respiratórias. Enquanto reguladora de conductância, a CFTR influencia o conteudo em água e iões do ASL (do inglês, *airway surface liquid*) e a sua desregulação causa um volume reduzido do ASL e muco espesso e desidratado. Este muco obstrói as vias respiratorias mais pequenas e afecta a limpeza mucociliar, prejudicando a eliminação das bactérias e outros patogenios inalados. Assim, o defeito na CFTR promove infecções persistentes por patógenios resistentes a tratamento. Isto gera estimulação continua por antigénios que resulta numa resposta inflamatória exacerbada e dano progressivo das vias respiratórias. Eventualmente isto conduz a fibrose e destruição do tecido.

A fraca correlação entre o genótipo da CFTR e a doença pulmonar na FQ sugere o envolvimento de factores ambientais ou genéticos (genes modificadores da FQ) que afectam o desenvolvimento, progressão e severidade da doença. O TGFβ1 (do inglês *transforming growth factor beta 1*) tem sido dos mais estudados. O TGFβ controla a diferenciação, migração e morte celular programada. É também um poderoso regulador de respostas imunes, exercendo funções pro- e anti-inflamatórias e tem também um papel central na remodelação epitelial, equilibrando a sintese e degradação da matriz extracelular (MEC). A sinalização intracelular do TGFβ ocorre através de repectores espicificos tipo II (TbR-II) que complexam com, e subsequente fosforilam, receptores tipo I (TbR-I). A via intracelular canónica para o TGFβ é mediada por uma família de factores de transcrição chamadas as proteínas Smad.

Polimorfismos no TGFβ1 que aumentam a sua expressão foram encontrados em pacientes com FQ e correlacionados com baixa função pulmonar e doença pulmonar mais severa. Assim é especulado que o TGFβ1 funciona estabelecendo uma ponte entre a inflamação e a remodelação epitelial na FQ, modificando a progressão da doença.

O TGFβ é também um importante indutor da transição epitélio-mesenquima (TEM). Uma TEM é um processo complexo em que células epiteliais completamente diferenciadas transitam para um fenótipo mesenquimal. A TEM é responsável pela morfógenese de tecidos e organogénese no embrião, bem como remodelação e reparação do tecido em adultos. No entanto é também um elemento importante na progressão do cancro e outras malignidades, como fibrose. A transição de células epiteliais para mesenquimais ocorre através de um

programa conservado com certos passos. Primeiro ocorre a dissolução das junções celulares, seguido da perda da polaridade apical-basal. Isto é procedido pela reorganização da arquitectura do citosqueleto e alterações na forma celular, bem como desenvolvimento de protusões e motilidade e, em muitos casos, uma capacidade de degradar proteinas da MEC e promover comportamento invasivo. Finalmente, ocorre uma diminuição da expressão de genes/proteinas epiteliais e a activação de genes que ajudam a definir o fenótipo mesenquimal.

Curiosamente, a CFTR já foi descrita como sendo não só dependente de mas também involvida na diferenciação epitelial, possuindo um papel no desenvolvimento, fibrose e cancro. A diferenciação e regeneração das vias respiratórias foi encontrada como estando debilitada na FQ, mesmo na ausência de inflamação. No entanto, a inflamação exacerbada também possui um papel na expressão da CFTR. Num epitélio remodelado com inflamação severa, a expressão de CFTR foi identificada de forma difusa no citoplasma das células ou encontrava-se ausente.

A descoberta das vias de sinalização do TGFβ, incluindo aquelas envolvidas na TEM, revelou mediadores da actividade transcripcional das Smads. Estes mediadores envolvem as proteinas C/EBP (do inglês *CCAAT-enhancer binding proteins*). Desta família de proteinas, o C/EBPβ é o factor de transcrição dominante no epitélio respiratório em adultos. O C/EBPβ tem funções ao nível da diferenciação de adipócitos, macrófagos e células epiteliais mamárias, controlo metabólico, inflamação e resposta de fase aguda e promoção da proliferação celular. O C/EBPβ possui dois tipos de isoformas distintos, incluindo dois activadores de transcrição (LAPs) e um inibidor de transcrição (LIP). O LIP reprime a expressão génica, inibindo as isoformas LAP de forma dominantemente negativa.

A sinalização do TGFβ pode inibir as funções do C/EBPβ através das Smads. No entanto o C/EBPβ é também um co-factor do TGFβ: a indução do p15INK4b (do inglês c*yclin-dependent kinase 4 inhibitor B*) e repressão do c-Myc (ambos necessários para a resposta citóstatica do TGFβ) são dependentes do C/EBPβ. Curiosamente, um nível elevado de LIP (e nível diminuido de LAP) foi ligado a uma perda das respostas citóstaticas dependentes do TGFβ em células metásticas de pacientes com cancro da mama. Consistentemente, um aumento do LIP em vários tipos de células epiteliais resultou num aumento de proliferação, diminuição na diferenciação e formação de hiperplasias.

Além do TGFβ, o C/EBPβ é também regulado pelo miR-155. Este miRNA está envolvido em vários processos biológicos que incluem inflamação e imunidade. A estimulação com TGFβ aumenta os níveis de miR-155, que por sua vez aumenta o TEM dependente do TGFβ. A perda de C/EBPβ mediada pelo miR-155 foi descoberta como um mecanismo de promoção da progressão do cancro da mama por desviar a resposta do TGFβ de morte celular para TEM, invasão e metastase. Além disto, a expressão do miR-155 encontra-se aumentada em células pulmonares de FQ, comparando com os controlos.

O objectivo principal deste trabalho era explorar a significancia fisiológica da sinalização do TGFβ na ausência de CFTR functional, nomeadamente o seu papel na activação de TEM. Com este fim procurou-se: determinar se a TEM era um componente da FQ; avaliar o estado e localização do C/EBPβ na ausência de CFTR funcional; investigar o possível papel do C/EBPβ como mediador do TEM induzido por TGFβ; e avaliar o papel do miR-155 nos processos acima referidos. Tecido pulmonar (de controlos e pacientes de FQ) e células epiteliais bronquicas de

FQ (do inglês, *CFBE*), expressando CFTR normal (CFTR wt) ou com a mutação F508del (CFTR F508del), foram usados para realizar estas tarefas.

Análise do tecido de um paciente com FQ revelou remodelação consistente com inflamação crónica e ainda perda de diferenciação epitelial. A presença de marcadores mesenquimais e ausência/diminuição de marcadores epiteliais era consistente com a ocorrência de TEM.

As diferenças no estado de diferenciação dos dois epitélios reflectiram as diferenças nos niveis de C/EBPβ. Este encontrava-se reduzido (ao nível de proteina e mRNA) nas células com CFTR F508del. Apesar de o C/EBPβ e a CFTR não interagirem ao nível proteico, redução de CFTR wt na membrana plasmática quando a expressão de C/EBPβ foi inibida sugere um envolvimento deste factor de transcrição no tráfego da CFTR para a membrana plasmática. Se este envolvimento é da isoforma LAP ou LIP ainda não é claro.

O tratamento de células CFBE polarizadas com TGFβ reduziu a resistência transepitelial (do inglês, *TEER*) e a expressão da E-caderina, consistente com a indução de TEM. Apesar das funções anti-inflamatórias e anti-proliferativas do TGFβ, uma exposição de 48h a esta citocina parece desviar definitivamente a sua resposta para inflamação crónica e indução de TEM. Isto é consistente com o que foi encontrado no tecido do paciente com FQ. A TEER e a expressão de C/EBPβ encontravam-se mais reduzidas em células com F508del-CFTR após tratamento com TGFβ. Isto pode ser devidos aos niveis de LIP mais elevados encontrados para estas células mas pode também apontar para uma desregulação de outras vias, resultados do defeito na CFTR. Em apoio desta hipótese, observou-se que o miR-155 reprime a expressao de C/EBPβ em ambas as linhas celulares. No entanto nas células com CFTR F508del este impacto foi maior, o que sugere uma desregulação intrínseca dos níveis deste miRNA, podendo esta via estar desregulada sinergicamente com a do TGFβ.

Surpreendemente os níveis de CFTR wt aumentaram com o tratamento com TGFβ e miR-155, enquanto os de CFTR F508del se mantiveram inalterados. Como isto é contraditório a um papel encontrado recentemente para o TGFβ em afectar a biogenese da CFTR, provavelmente o modelo utilizado não foi o melhor para avaliar estes níveis, já que a CFTR se encontra sobrexpressa.

Este trabalho contribuiu para o melhor conhecimento do papel regulatório da CFTR na diferenciação epitelial e inflamação crónica na FQ.

Palavras-chave: CFTR, C/EBPβ, fibrose quística, TGFβ, transição epitélio-mesenquima

Abbreviations

ABC	ATP-binding cassette
Akt	Protein kinase B
AmiR	AntagomiR
AMP	Adenosine monophosphate
APS	Ammonium persulfate
ASL	Airway surface liquid
ATP	Adenosine triphosphate
BALF	Bronchoalveolar lavage fluid
BMP	Bone morphogenic protein
BSA	Bovine serum albumin
C/EBP	CCAAT-enhancer binding proteins
CaCC	Ca^{2+} activated chloride channel
cAMP	Cyclic adenosine monophosphate
CAR	Coxsackie virus and adenovirus receptor
cDNA	Complementary DNA
CF	Cystic fibrosis
CFBE	Cystic fibrosis bronchial epithelial
CFTR	Cystic fibrosis transmembrane regulator
CK18	Cytokeratin-18
COPD	Chronic obstructive pulmonary disease
CRISPR	Clustered regularly interspaced short palindromic repeats
crRNA	CRISPR RNA
DAPI	4',6-diamidino-2-phenylindole dihydrochloride
DMEM	Dulbecco's modified eagle's medium
DMSO	Dimethyl sulfoxide
DNA	Deoxyribonucleic acid
DPBS	Dulbecco's phosphate buffered saline
DSB	Double strand breaks
DTT	Dithiothreitol
E-cadherin/E-cad	Epithelial cadherin
ECM	Extracellular matrix
EMEM	Eagle's minimum essential medium
EMT	Epithelial to mesenchymal transition
ENaC	Epithelial sodium channel
ER	Endoplasmic reticulum
ERK	Extracellular signal-regulated kinase
ESCC	Esophageal squamous cell carcinoma
F508del	Deletion of phenylalanine (F) residue at position 508
FBS	Foetal bovine serum
GDF	Growth and differentiation factor
GSH	Glutathione
GSK3β	Glycogen synthase kinase 3β

H&E	Haematoxylin and eosin
HBE	Human bronchial epithelial
HBSS	Hank's balanced salt solution
HDR	Homology directed repair
HEK	Human embryonic kidney
HRP	Horseradish peroxidase
IL	Interleukin
IP	Immunoprecipitation
IPF	Idiopathic pulmonary fibrosis
I-Smad	Inhibitory Smad
JNK	Jun N-terminal kinase
LAP	Liver-enriched transcriptional activator protein
LB	Lysogeny broth
LIP	Liver-enriched transcriptional inhibitory protein
MAPK	Mitogen-activated protein kinase
miR/miRNA	MicroRNA
MMP	Metalloproteinase
mRNA	Messenger RNA
MSD	Membrane-spanning domain
mTORC	Mammalian TOR complex
NBDs	Nucleotide binding domains
N-cadherin/N-cad	Neural cadherin
NF-κB	Nuclear factor κB
NHEJ	Non-homologous end joining
NSCLC	Non-small cell lung cancer
N-terminal	Amino-terminal
O.C.T.	Optimal cutting temperature
ORCC	Outwardly rectifying chloride channel
PAGE	Polyacrylamide gel electrophoresis
PAM	Protospacer adjacent motif
PAR	Partitioning-defective
PBS	Phosphate buffered saline
PCR	Polymerase chain reaction
PFA	Paraformaldehyde
PI3K	Phosphatidylinositide 3-kinase
PIC	Protease inhibitor cocktail
PM	Plasma membrane
PVDF	Polivinylidene difluoride
qRT-PCR	Quantitative real time polymerase chain reaction
RNA	Ribonucleic acid
ROMK	Renal outer medullary potassium channel
R-Smad	Receptor activated Smad
RT	Room temperature
SDS	Sodium dodecyl sulfate
SHIP 1	Phosphatidylinositol-3,4,5-trisphosphate 5-phosphatase 1

SMURF1	Smad ubiquitylation regulatory factor 1
TEER	Transepithelial electrical resistance
TEMED	Tetramethylethylenediamine
TGFβ	Transforming growth factor beta
TNFα	Tumour necrosis factor α
tracrRNA	Trans-activating crRNA
UTR	Untranslated region
Vim	Vimentin
WCL	Whole cell lysate
wt	Wild type
ZEB	Zinc-finger E-box-binding
β-cat	β-catenin
Ω	Ohm

1. Introduction

1.1. Cystic fibrosis and CFTR

1.1.1. Cystic fibrosis

Cystic fibrosis (CF) is the most common life-threatening autosomal recessive disease in Caucasians, affecting 1 in 2500-4000 new-borns. The frequency of the disease varies among ethnic groups and/or geographic locations[1,2]. In 2004 it was estimated that more than 35000 individuals in Europe were affected by CF[3].

The disease was first described in 1938 by Anderson and collaborators[4], who coined the term cystic fibrosis and also described the disease's autosomal recessive autosomal pattern of inheritance. Throughout the years various studies pointed to a deficiency in chloride transport as being at the origin of the disease. This defect was detected in tissues which are affected in CF, including the lung epithelium[5]. In 1989, the gene responsible for CF was finally identified and was named cystic fibrosis transmembrane conductance regulator (CFTR)[6]. The gene harboured mutations in all CF patients analysed. Even though it was not evident at the time of its discovery, today CFTR is well established as a cyclic adenosine monophosphate (cAMP)-activated anion channel, expressed in the epithelial cells of a wide variety of tissues[1].

The exact symptoms and their severity vary across CF patients and may change or aggravate throughout the patient's life[7]. The more severely affected tissues and organs are the airways, gastrointestinal tract and reproductive system.

Pancreatic insufficiency is a very common CF symptom, as a result of pancreatic duct obstruction. Meconium ileus – a form of intestinal obstruction – and liver disease are also recurrent symptoms. Regarding the reproductive system, male infertility is almost universal and women are also frequently affected[1,7].

Most CF morbidity and mortality however is associated with the respiratory tract: pulmonary insufficiency is responsible for 80% of CF-related deaths[7]. The most commonly accepted explanation for CF airway disease is the "low volume" hypothesis. The airways are lined with a film of liquid and mucus called airway surface liquid (ASL). As a conductance regulator, CFTR influences the ion and water content of the ASL (either by itself or by regulating other epithelial channels) and its dysregulation causes a reduced ASL volume as well as thick and dehydrated airway mucus. This dense mucus obstructs the small airways and impairs mucociliary clearance, the removal of inhaled bacteria and other pathogens through ciliary beating[8]. Furthermore, the absence of CFTR-dependent HCO_3^- secretion lowers the ASL pH, which strengthens mucus adherence to epithelial surfaces[9]. Low pH also inhibits antimicrobial function in the lung, impairing the killing of bacteria[10]. This generates continuous antigen stimulation with chronic airway bacterial infection and exacerbated inflammation and progressive airway damage. As bronchioles become compromised, the pathological process extend to alveolar structures, causing fibrosis and destruction[11].

The process described above is the so-called CF pathogenesis cascade (Figure 1). Upon challenge by viral or bacterial infection (especially by *Pseudomonas aeruginosa*), high concentrations of neutrophils and proinflammatory mediators abound in the airways. In normal individuals, the inflammatory response eradicates the infection and then is itself

resolved. Neutrophils phagocytose and kill the bacteria, undergo apoptosis, and are cleared by macrophages with little residual lung damage. Although at birth the lungs of CF patients are structurally normal, within the first months of life the CFTR defect starts to promote persistent infections which last throughout the patient's life. Moreover, bacteria adapt to the pulmonary microenvironment[12] since they are not eradicated[9], providing a continuing pro-inflammatory stimulus[1,13,14].

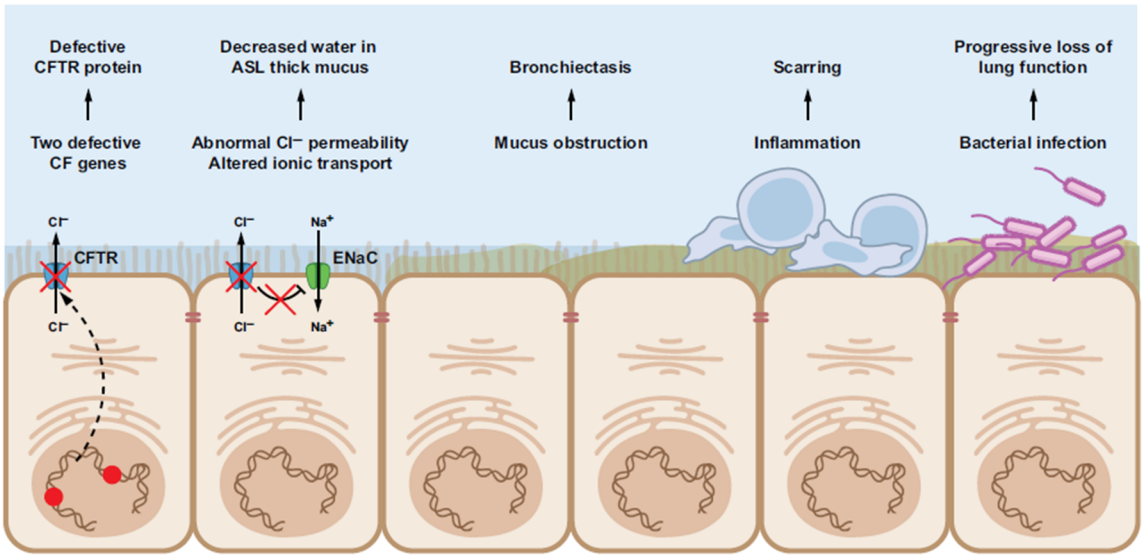

Figure 1 - CF pathogenesis cascade in the lung. *CF dysfunction ultimately leads to loss of lung function. Retrieved from [2].*

One of the inflammatory mediators which intervenes in the exacerbated inflammatory response in the CF lung is interleukin (IL)-8. IL-8, high neutrophil count and neutrophil granulocyte products are found in the sputum, bronchoalveolar lavage fluid (BALF) and sera specimens obtained from CF patients. Further studies in cellular CF models, including nasal cells and bronchial epithelial cells, confirmed these results. Interestingly some of these studies have observed inflammation markers in the absence of CF-related pathogens, which supports the hypothesis that the CFTR defect is sufficient to trigger the inflammatory process related to CF. This could place airway inflammation not simply as a direct consequence of bacterial colonization but as a process which is independent of infection and precedes it[11,13–15]. Direct support for this hypothesis comes from the observation that the specific CFTR inhibitor $CFTR_{Inh}$-172 produced an inflammation profile that resembled that observed in CF patients[16].

1.1.2. CFTR protein structure, mutations and function

The *CFTR* gene resides on the long arm of chromosome 7 (7q31.2) and consists of a TATA-less promoter and 27 exons spanning about 215kb of genomic sequence[17]. When translated, this originates a polypeptide 1480 amino acid residues long which is part of the adenosine triphosphate (ATP)-binding cassette (ABC) protein superfamily. Even though an experimental high resolution 3D structure is not available, the overall topology – proposed by Riordan and his co-workers when the gene was first cloned – is known[6]. CFTR's structure is homologous to other ABC proteins. These proteins conform to a modular architecture, comprising two membrane-spanning domains (MSDs), typically with six α-helices each, and two cytoplasmic

nucleotide binding domains (NBDs). CFTR further encompasses a highly charged cytoplasmic regulatory (R) domain. The R domain links the two homologous halves of the protein, generating the overall domain organization MSD1-NBD1-R-MSD2-NBD2[18] (Figure 2A).

CFTR is synthesized and folded in the endoplasmic reticulum (ER), where it is core-glycosylated. This is an immature form of CFTR (known as band B) and has 145kDa. After this immature CFTR is checked for correct folding, it migrates to the Golgi complex, where it undergoes full glycosylation and acquires a mature functional form (known as band C) with 170kDa (Figure 2B). This mature form can successfully be trafficked to the plasma membrane. F508del-CFTR, however, is known to adopt an abnormal conformation, with most protein failing to fold correctly or form oligomeric structures. This potentiates ER retention and degradation of the protein. Hence this protein does not reach the plasma membrane[19].

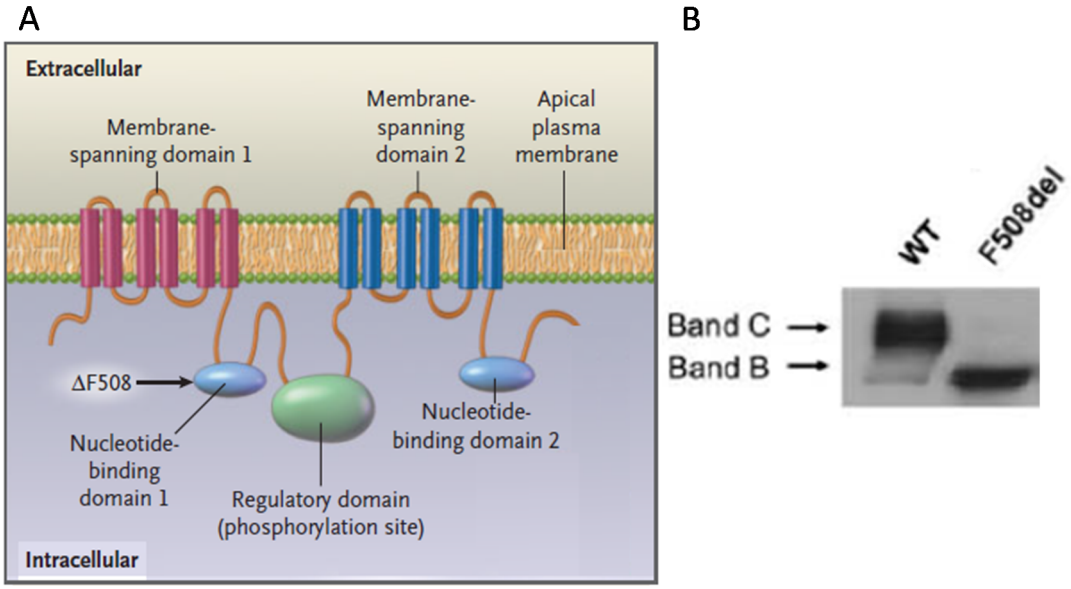

Figure 2 – A) Hypothesized CFTR structure. *The most common CFTR mutation in CF, F508del, occurs in the NBD1 domain of the protein. Adapted from [12].* ***B) Band C and Band B on Western blot for wt and F508del-CFTR (CFBE cells).*** *Adapted from [20].*

CFTR was, for many years, thought to be exclusively a chloride channel. However it has been found that CFTR provides a pathway for apical HCO_3^- efflux as well[21,22]. In addition to anion transport, CFTR also has a regulatory role towards the epithelial Na^+ channel (ENaC), with CFTR and ENaC activities being inversely correlated[23]. CFTR also positively regulates chloride transport by outwardly rectifying chloride channels (ORCC), by triggering the transport of ATP out of cells where it stimulates ORCCs[24]. It has also been reported that CFTR controls the activity of Ca^{2+} activated chloride channels (CaCCs), renal epithelial apical KvLQT-1 K^+ channels and outer medullary potassium channel (ROMK) 1 and 2. CFTR is also able to regulate water channels from the aquaporin family[25,26]. Finally, recent evidence has pointed to glutathione (GSH) flux also being mediated by CFTR, implicating it in the control of oxidative stress in the airways[27].

In CF some or all the above mentioned functions can be compromised by mutations in CFTR. The most common one is the deletion of residue phenylalanine 508 (F508del) at the NDB1 domain[6]. However, by the time this work was written there were 2003 mutations described for the CFTR gene[28]. CFTR mutations can be grouped into six classes, according to

their effects on the CFTR gene or protein. Class I comprises mutations which produce premature termination codons and yield no protein. Class II includes mutants that fail to traffic to the plasma membrane due to misfolding and premature degradation; this class includes the most common mutation, F508del. Class III comprises CFTR mutants that, although reaching the plasma membrane, exhibit defective channel gating, having no function. Class IV mutants display substantially reduced function (channel conductance). Class V includes mainly mutants that allow synthesis of some normal CFTR mRNA (and protein) but at very low levels. Finally, Class VI mutants impair the CFTR stability at the plasma membrane. When rescued to the cell surface (e.g. at ~26^{o}C), F508del-CFTR also behaves as a Class VI mutant due to its intrinsic instability[2].

A range of symptomatic therapies – standardized multisystem treatments comprising antibiotics, mucolytics, high-calorie nutrition, and chest physiotherapy among others[2] – have allowed the life expectancy of CF patients to be raised to over 30 years. Yet, the disease must be treated beyond its symptoms, addressing the CFTR dysfunction and halting its pathological cascade before downstream effects occur. Studies have suggested that 10-15% of normal CFTR, bringing about 20-30% of the activity present in native non-CF epithelia would suffice to avoid CF[19]. Mutation classes have been instrumental in the development of pharmacological therapies for CF[29]. Drugs addressing the basic CFTR defect have only recently become available: Kalydeco, a potentiator compound that overcomes the defective Cl- conductance of G551D-CFTR and 8 other class III mutants); and Orkambi, a combined prescription of VX-809 – a F508del-CFTR folding corrector – and VX-770 – the active principle in Kalydeco – for F508del homozygous patients[30]. Nevertheless, understanding the cellular pathways and genes that affect and/or are affected by CFTR dysfunction in CF is important to enable the development of more effective therapies.

1.1.3. CF modifier genes: TGFβ and consequences for CF

The poor correlation between CFTR genotype and lung disease phenotype suggests the influence of environmental and secondary genetic factors (CF modifier genes) which affect the development, progression and disease severity[17]. Wide phenotypic variation and differences in chloride conductance occur even between monozygotic and dizygotic twins[31].

Modifier gene candidates are generally selected on a mechanistic basis either because they function in key disease-related pathways or have been previously identified as modifiers in similar diseases. Published studies testing candidate modifier genes for CF have examined multiple genetic polymorphisms in immune or inflammatory genes. The transforming growth factor beta (TGFβ) has been among the most studied[32]. TGFβ is known to modulate immune responses, proinflammatory and anti-inflammatory effects, wound healing and enhance host defence and airway repair in response to inflammation. Recent studies have implicated TGFβ1 in the pathogenesis of lung disease including idiopathic pulmonary fibrosis (IPF), chronic obstructive pulmonary disease (COPD), acute respiratory distress syndrome, bronchopulmonary dysplasia and asthma[33,34].

TGFβ1 belongs to the TGFβ superfamily, which comprises TGFβs, bone morphogenic proteins (BMPs), growth and differentiation factors (GDFs), activins and related inhibins, among others. The members of this superfamily act as multifunctional regulators of cell growth and differentiation, controlling cell division, differentiation, migration, adhesion, organization and programed cell death[35]. TGFβ occurs in three isoforms: TGFβ1, TGFβ2 and

TGFβ3. All of them have been shown to be essential for normal embryonic and foetal development and play a role in normal organ homeostasis and function[36].

TGFβ1 is the most prevalent isoform and is almost ubiquitously found in mammalian tissues. The 25kDa polypeptide dimer is produced as part of an inactive latent complex that is targeted to the extracellular matrix (ECM). The activation of TGFβ1 is an important mechanism in several pathophysiologic conditions including proteolysis, thrombospondin and integrin interactions, pH changes, and presence of reactive oxygen species[37]. TGFβ has been shown for example to be activated by the integrin αvβ6, which is highly expressed on airway epithelial cells[35].

Intracellular TGFβ signalling occurs via two receptor serine/threonine kinases that act in sequence. The active form of TGFβ binds to specific type II receptors (TbR-II) which recruit type I receptors (TbR-I) to form tetrameric complexes. In the ligand-bound complex, type II receptor phosphorylates serine and threonine residues in the type I receptor, which then propagates the signal. The canonical intracellular signalling pathway for TGFβ1 is mediated by a family of transcription factors, the Smad proteins. Activation of the type I receptor results in phosphorylation of the receptor activated Smads (R-Smads) - Smad2 and Smad3 - which then form a heteromeric complex with a co-Smad, Smad4. The complex translocates to the nucleus where it activates transcription of target genes by binding to specific promoter elements. Inhibitory Smads (I-Smads) Smad 6 and 7 can antagonize TGFβ signalling by binding to the type I receptor. Under conditions of TGFβ stimulation, Smads constantly undergo phosphorylation and dephosphorylation, shuttling in and out of the nucleus[35–37] (Figure 3). Smads function in association with different protein partners. Each Smad-partner complex targets a particular subset of genes and recruits either transcriptional co-activators or co-repressors. The availability of each cofactor may vary on each cell type, partly determining specific responses to TGFβ[35,38].

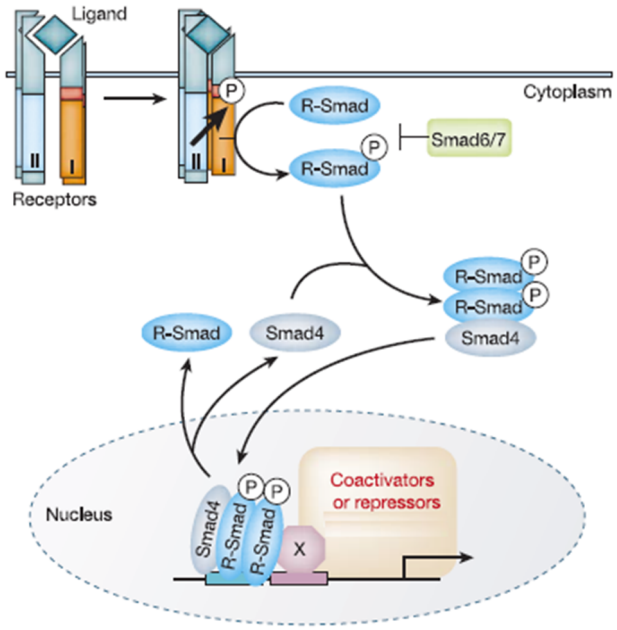

***Figure 3 - General mechanism of TGFβ receptors and Smad activation**. Adapted from [37].*

Smad signalling is essential for most, but not all, TGFβ gene responses. TGFβ has been shown to activate other mediators such as all three mitogen-activated protein kinase (MAPK) pathways: extracellular signal–regulated kinase (ERK), Jun N-terminal kinase (JNK) and p38 MAPK. In addition, TGFβ signalling can also be mediated by PI3K kinases, PP2A phosphatases and Rho family members. Signalling through these pathways may further regulate Smad proteins or mediate Smad-independent TGFβ responses[35,37].

TGFβ polymorphisms regulate its protein levels and have been shown to modify the development and/or severity of fibrotic lung disease, asthma and chronic obstructive pulmonary disease[32]. TGFβ polymorphisms which increase its expression have been found on CF patients and reported to correlate with low lung function and a more severe pulmonary disease[34,39,40]. However the findings conflict in respect to which polymorphisms are responsible for this phenotype[41]. Despite this, it is clear that TGFβ1 activation is markedly upregulated in CF lung disease. Harris and collaborators have shown that TGFβ in BALF is associated with increased airway inflammation (high neutrophil count) and diminished lung function[33]. They also found increased plasma TGFβ1 in CF patients, which was reduced after antibiotic therapy[42].

TGFβ1 is a master regulator of immune responses and exerts powerful pro- and anti-inflammatory functions. It has potent chemoattractive properties and can rapidly recruit macrophages, granulocytes (such as neutrophils) and other cells to the site of inflammation[37]. However, the TGFβ1 (anti-inflammatory) role in downregulating the IL-8-dependent migration of neutrophils has also been shown in CF. Patients with chronic stable disease express high levels of TGFβ1 relatively to those with exacerbations[43]. Consistent with this, inhibition of IL-8 was observed in primary human bronchial epithelial (HBE) cells and suggested to be mediated via the Smad2/3 pathway[44,45].

TGFβ1 also has a central role in remodelling, balancing ECM production and degradation[37]. TGFβ induces the transcription and synthesis of various components of the ECM by immature and mature pulmonary fibroblasts, inhibiting the degradation of the newly formed ECM proteins by decreasing, for instance, the induction of metalloproteinases (MMPs)[36]. TGFβ1 also mediates the transition of fibroblasts into myofibroblasts[46]. In health, myofibroblasts undergo apoptosis after the resolution of tissue injury. In diseases such as IPF, aberrant myofibroblasts persist and result in tissue fibrosis. TGFβ signalling and myofibroblast differentiation have been demonstrated to be increased in the CF lung approaching the pathogenic levels observed in patients with IPF. Hypoxia, persistent epithelial injury and increased protease activity all increase TGFβ1 activity and are present in the CF lung. Furthermore mechanical strain in CF is pronounced due to mucus plugging and chronic cough. The environment of CF lung is therefore well primed for increased TGFβ signalling, myofibroblast differentiation and persistence of pathologic fibroblast behavior[46].

TGFβ1 is therefore speculated to bridge the inflammatory and remodelling pathways in CF, modifying CF lung disease progression[42].

1.2. EMT and CF

1.2.1. CFTR role in epithelial differentiation and EMT

Epithelial-mesenchymal transition (EMT) is a complex process whereby fully differentiated polarized epithelial cells transition into a mesenchymal phenotype, giving rise to apolar fibroblastoid cells, namely fibroblasts and myofibroblasts[47,48].

Epithelia are established as single cell layers or multilayer tissues with various functions. Epithelial cells are tightly packed together, adhere and communicate with each other through specialized intercellular junctions, show apical–basal polarity, and are positioned on a basement membrane[49]. The apical and basal surfaces are structurally different, adhere to different substrates, or have different functions. Mesenchymal cells form structures that are irregular in shape and not uniform in composition or density. Adhesion between mesenchymal cells is weaker, allowing for increased migratory capacity. Mesenchymal cells also have a more extended and elongated shape and possess front-to-back leading edge polarity[50]. This allows for enhanced invasiveness capacity, elevated resistance to apoptosis and greatly increased production of ECM components. The completion of an EMT is signalled by the degradation of the epithelial basement membrane and the formation of mesenchymal cells that have migratory ability[51].

EMT underlies tissue morphogenesis and organogenesis in the embryo, as well as tissue remodelling and repair in adults[47]. However, EMT is also an important element in cancer progression and malignancy as well as in other pathologies that involve organ degeneration, such as fibrosis[52].

According the three distinct biological settings in which EMT is encountered, a classification of EMT into three different biological subtypes was proposed[51]. Type 1 EMT occurs mainly in implantation, embryo formation, organ development and tissue morphogenesis and is therefore generally known as embryonic and developmental EMT. It causes neither fibrosis nor induces an invasive phenotype[47,51,53]. Type 2 EMT underlies tissue regeneration and fibrosis. Consequently it is associated with wound healing, and is essential for tissue homeostasis. Contrary to type 1, type 2 EMT is dependent on inflammation and ceases once it is attenuated, such as after wound repair[47,51]. Type 3 EMT occurs in neoplastic cells that have previously undergone genetic and epigenetic changes, favouring outgrowth and the development of localized tumours. It is responsible for cancer progression, invasion and metastasis, such as in carcinoma cells[51].

At the cellular level, pathological EMTs are very similar to physiological EMTs in that they are governed by similar signalling pathways, regulators and effector molecules[52]. The transition of epithelial cells into mesenchymal cells follows a common and conserved programme with the following hallmarks: the dissolution/disassembly of the epithelial cell–cell junctions; loss of apical–basal polarity and acquisition of a front–rear polarity; reorganization of the cytoskeletal architecture and changes in cell shape (transition to a spindle-shaped morphology); downregulation of the epithelial gene expression signature and activation of genes that help defining the mesenchymal phenotype; development of cell protrusions and motility; and, in many cases, an ability to degrade ECM proteins to enable invasive behaviour (Figure 4). Additionally, cells that have undergone EMT acquire resistance to senescence and apoptosis[49,53].

One of the early events in EMT is the loss of epithelial cell-cell interactions. Epithelial cells contact with each other through subapical tight junctions, adherens junctions and desmosomes at lateral surfaces, and scattered gap junctions at lateral surfaces. Upon the initiation of EMT, these junctions are deconstructed. During the destabilization of adherens junctions, epithelial cadherin (E-cadherin/E-cad) is cleaved at the plasma membrane and subsequently degraded. This is considered one of the most important and universal hallmarks of EMT. As EMT progresses, the expression of junction proteins is transcriptionally repressed, preventing the *de novo* formation of epithelial cell–cell junctions[47,49].

As a subsequent event in EMT, the dissolution of epithelial junctions during EMT affects polarity complexes integrated in the cell junction architecture, disrupting the apical-basal polarity. Partitioning-defective (PAR) complexes and Crumbs complexes define the apical compartment while Scribble complexes define the basolateral compartment. After EMT is initiated, the expression of polarity complex proteins is repressed, which further destabilizes the polarized phenotype. Additionally, to achieve directional polarity, some of these complexes relocalize to the leading edge of the cell, assisting in activating actin polymerization and membrane protrusion formation[49,52,54].

At this point in EMT, loss of apical-basolateral polarity and dissociation of intercellular junctions are accompanied by fundamental remodelling of the actin cytoskeleton. Cells that undergo EMT replace cortical actin with actin stress fibres and reorganize their cytoskeleton so that it enables dynamic cell elongation and directional motility. Lamellipodia, actin membrane projections (protrusions) are generated, facilitating cell invasion. Remodelling of the ECM also occurs at this stage, to enable invasiveness. Changes to the integrin repertoire (downregulation of epithelial integrins and expression of mesenchymal integrins) during EMT correlate with the increased expression of proteases, such as the MMP2 and MMP9, enhancing ECM protein degradation[49,53].

One of the final events in EMT is the repression of genes encoding epithelial cell junction proteins is fully active and accompanied by the activation of another set of genes, the protein products of which promote mesenchymal adhesion. Specifically, the downregulation of E-cadherin is balanced by the increased expression of mesenchymal neural cadherin (N-cadherin), whose interactions are weaker than E-cadherin's and facilitate cell migration and invasion. The intermediate filament composition also changes with the repression of cytokeratin and the activation of vimentin expression. Keratin and vimentin filaments regulate the trafficking of organelles and membrane-associated proteins, but they show differences in the proteins that they target to the membrane (for example keratins direct E-cadherin to the membrane but vimentin does not). These changes in gene expression involve master regulators, including SNAIL1 (SNAIL), SNAIL2 (SLUG), TWIST1, TWIST2 and zinc-finger E-box-binding (ZEB) transcription factors**.** These transcription factors act by binding to E-box DNA sequences through their carboxyl-terminal zinc-finger domains and acting like transcriptional repressors or activators. They act by coordinating histone modifications, specifically methylation and acetylation[49,53,54].

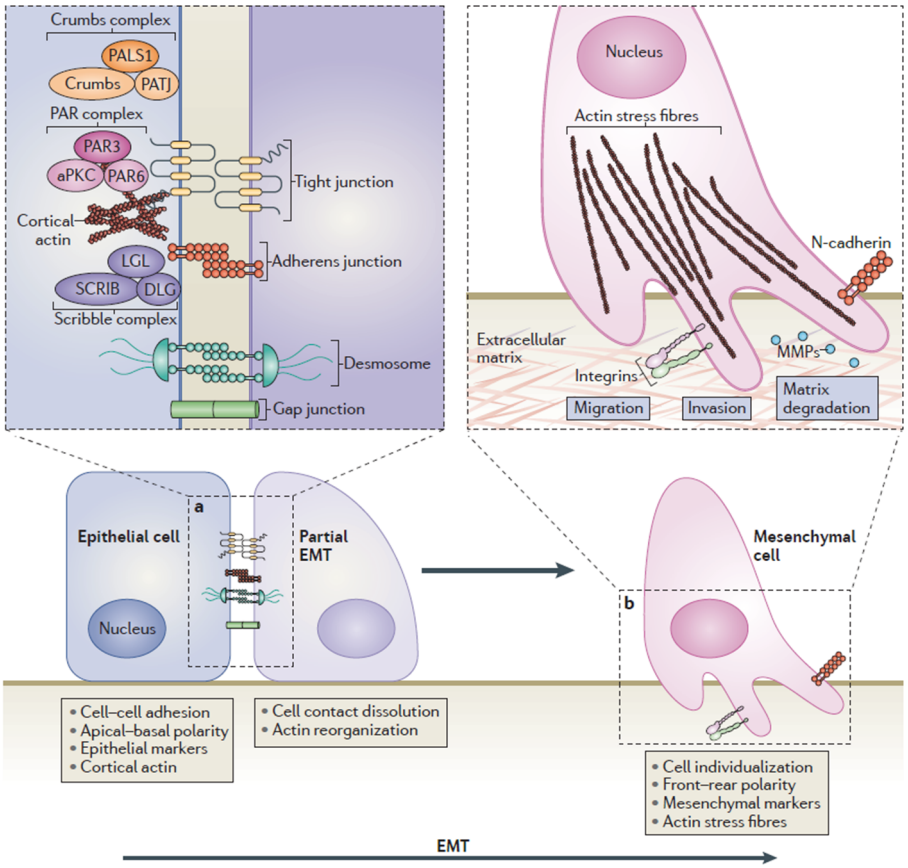

Figure 4 - Cellular events during EMT. *Disassembly of epithelial cell-cell contacts and loss of epithelial polarity are the first steps on EMT. The cytoskeleton then reorganizes and cells acquire migration and invasive and matrix degradation capacities. Retrieved from [48].*

Many studies on CFTR, including its subcellular localization, functions and regulators, have placed it at the centre of the three EMT types. CFTR has been reported to be not only dependent on but also involved in epithelial differentiation, having reported roles in development, fibrosis and cancer. Overall CFTR expression has been shown to increase with cellular differentiation in several cell types[55–57]. Its cellular distribution in the lung was also found to change with the degree of differentiation of the epithelial cells, evolving from diffused expression (in unpolarised cells) to a predominantly apical distribution (in differentiated and polarized cells)[58]. Accordingly, polarized epithelial cells showed an apical localization for the wt protein[59], and treatment of F508del-CFTR cells (where most CFTR fails to traffic to the plasma membrane), with an epithelial differentiating agent (dimethyl sulfoxide, DMSO) and/or growing cells as polarized monolayers, significantly increased CFTR levels at the plasma membrane[60]. Furthermore, CFTR-mediated chloride transport was shown to require cellular polarization; specifically, an apical localization of CFTR[61]. More recently it was established that CF epithelia had impaired differentiation[62]. Expressing wt-CFTR (in a parental cell line without CFTR) significantly increased the transepithelial electric resistance (TEER, a measurement of the epithelial tightness and hence differentiation) whilst expressing F508del-CFTR had no effect[63].

In addition to differentiation, several studies reported wound healing and tissue repair to be abnormal in CF. Wound healing is an essential process which includes several steps:

spreading and migration of the basal cells neighbouring the wound; proliferation and active mitosis; squamous metaplasia and progressive redifferentiation. In the case of bronchial epithelium, there is the further emergence of preciliated cells, ciliogenesis and complete regeneration of a pseudostratified mucociliary epithelium. Any delay or disturbance in the repair process may start fibrotic responses[64]. Tissue fibrosis can be seen as an abnormal wound healing process which, due to persistent inflammation, is not stoped[47,51]. In this setting of chronic inflammation, type 2 EMT can be continuously activated[50].

Surface epithelium remodelling and inflammation were found to affect the expression and distribution of wt-CFTR. While an epithelium with diffuse inflammation was mainly characterized by an apical CFTR protein distribution in ciliated cells, in a remodelled surface epithelium with severe inflammation, CFTR protein presented either a diffuse distribution in the cytoplasm of ciliated cells or was absent. This distribution was similar to that present in F508del homozygous CF respiratory tissue, implying that CFTR distribution in CF respiratory tract may not only be associated with the gene mutations but also with the surface epithelium inflammation, dedifferentiation and remodelling[65]. However, airway epithelial differentiation and regeneration has been reported to be impaired in bronchial epithelial CF cells even in the absence of airway infection[62]. Cell proliferation was, on the other hand, shown to be higher in the regenerating CF epithelium[62,66]. Selective inhibition of wt-CFTR was found to produce a significant delay in wound repair, with lower migration rate and lamellipodia protrusion[67]. Accordingly, airway epithelial cells from CF patients repaired slower than non-CF cells. Whenever the CFTR defect was corrected (by transduction of wt-CFTR or pharmacologically) the wound healing process significantly improved[68]. Even if it is still unclear whether the inability of CF airways to regenerate themselves is due to a basic repair defect of CF airway epithelia or to infectious and inflammatory mediators, it is very clear that this dysregulation is present in the airways of patients.

CFTR has also been reported to have an important role in lung development. In mice and pigs, defects in the cartilaginous rings, decreased contractile response, a reduced breathing rate, decreases in lumen size and circularity and increases in smooth muscle were found. Similar congenital malformations occur in young human patients[69,70].

There is an increasing interest in the association of cancer incidence with the genetic variations in the CFTR gene. A large cohort studies in North American and European patients with CF, involving 41188 cases of CF patients who were followed over 20 years, reported a higher risk of digestive tract cancer as well as an increased risk for testicular cancer and lymphoid leukaemia and a decreased risk of melanoma (on F508del homozygous patients)[71]. Hence, CFTR may function as a tumour suppressor or tumour promoter, depending on the type of tumour. Accordingly, a protective role for the CFTR (consistent with a tumour suppressor role) has been found for breast cancer[72], prostate cancer[73] and non-small cell lung cancer (NSCLC), where a reduced CFTR expression points to its role as tumour suppressor[74,75]. CFTR was found to be absent from the apical surface of cancer cells, being diffusely distributed in the cytoplasm[72]. Differences in samples size, study design and various CFTR mutations in the individual studies can contribute to the contradicting roles of CFTR in cancer progression.

1.2.2. C/EBPβ at the core of TGFβ mediated EMT

Consistent with its roles in inflammation and remodelling, TGFβ is a major inducer (and maintainer) of EMT[48,53]. In development, TGFβ1 and TGFβ2 expression are associated with

EMT-like events in the formation of endocardial cushions, whereas TGFβ3 drives EMT that mediates palate fusion. Postnatally TGFβ1 induces EMT in wound healing, fibrosis and cancer[48].

There are three major pathways through which TGFβ modulates EMT: the Smad pathway, the MAPK pathway and the phosphatidylinositide 3-kinase (PI3K)/protein kinase B (Akt) pathway (Figure 5). The distinction between Smad-dependent and Smad-independent mechanisms is not always clear since there is a significant cross talk between these pathways[48]. On the Smad pathway, TGFβ induces: SNAIL1 expression through Smad3-dependent transcription (inducing repression of E-cad); Smad3-Smad4 complexes' interaction with ZEB1 and ZEB2; and Smad3-Smad4 complexes' mediated enhancement of TWIST expression and activity. Additionally, TGFβ can also induced Smads to directly activate mesenchymal genes like those encoding fibronectin, vimentin and collagen αI[49,54]. As for the MAPK pathways, TGFβ induces the ERK MAPK pathway, resulting in increased repression of E-cad, activation of N-cad and MMP expression[49,53], and stabilization of SNAIL1 activity by inhibiting glycogen synthase kinase 3β (GSK3β)[49], (which results in β-catenin accumulation in the nucleus and consequent activation of mesenchymal genes[48]). TGFβ also induces other MAPK pathways: JNK mediated activation of c-JUN which cooperates with Smad3-Smad4; and finally, the Ras/Raf/MEK/MAPK pathway, which is required to maintain EMT in several cell types[53]. As for the PI3K/Akt signalling, TGFβ activates Akt through PI3K, which results in the activation of mammalian TOR complex I and II (mTORC1, mTORC2) which contribute to increased cell size, protein synthesis, motility and invasion[54]. Additionally, TGFβ induces phosphorylation of PAR6, which recruits E3 ubiquitin ligase Smad ubiquitylation regulatory factor 1 (SMURF1) that mediates degradation of RHOA and dissolution of the tight junctions and the actin cytoskeleton[49,53]. RHOA itself is also induced, regulating cytoskeletal and adherens junctions' rearrangement[48].

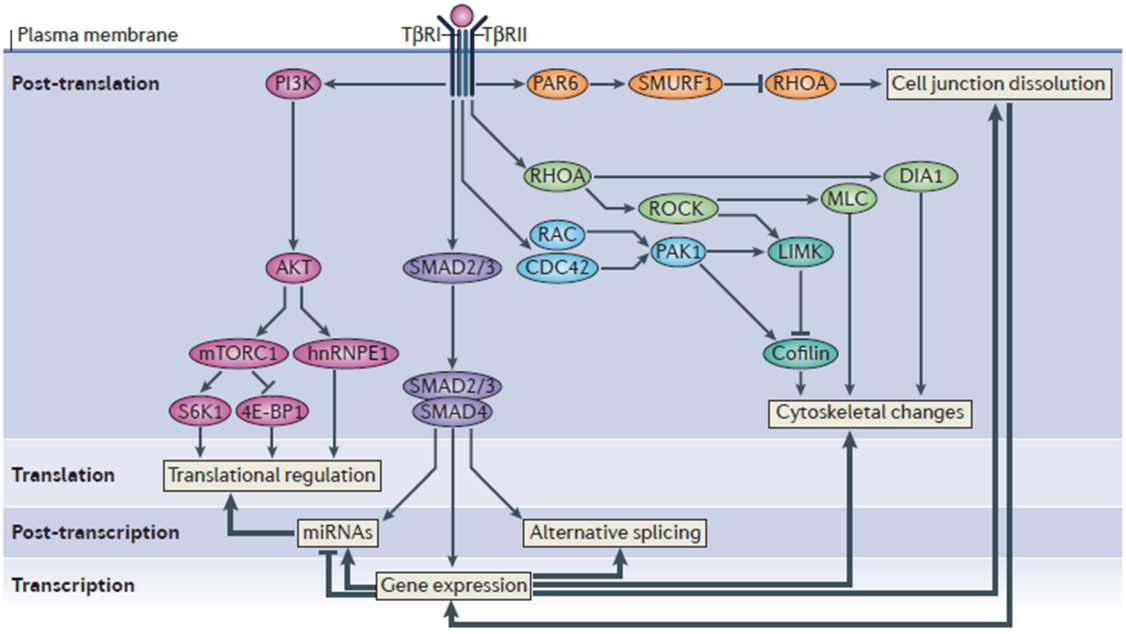

Figure 5 - Molecular mechanisms of TGFβ signalling in EMT*. Smad-mediated and non-Smad signalling are depicted. Ultimately, TGFβ signalling results in cell junction dissolution, cytoskeletal changes and mesenchymal gene expression. Retrieved from [48].*

The unveiling of these TGFβ pathways has revealed mediators regulating the downstream Smad transcriptional activity. These include the CCAAT-enhancer binding proteins (C/EBP). C/EBPs regulate energy metabolism, innate and adaptive immunity, inflammation, cellular proliferation and differentiation (haematopoiesis, adipogenesis) and apoptosis[76]. They share a highly conserved, C-terminal, leucine-zipper dimerization domain, adjacent to a basic DNA-binding region, together referred to as b-ZIP. The N-terminal domain contains the transactivation domains which interact with different components of the basal transcription apparatus and thereby stimulate transcription[77] (Figure 6B). The first C/EBP protein to be identified (C/EBPα) was a heat-stable factor in rat liver nuclei that was capable of interacting with the CCAAT box motif present in several cellular gene promoters[78,79] (Figure 6A). During the following decade, five additional members were identified in mammalian species and subsequently named C/EBPβ, γ, δ, ε, ζ)[80].

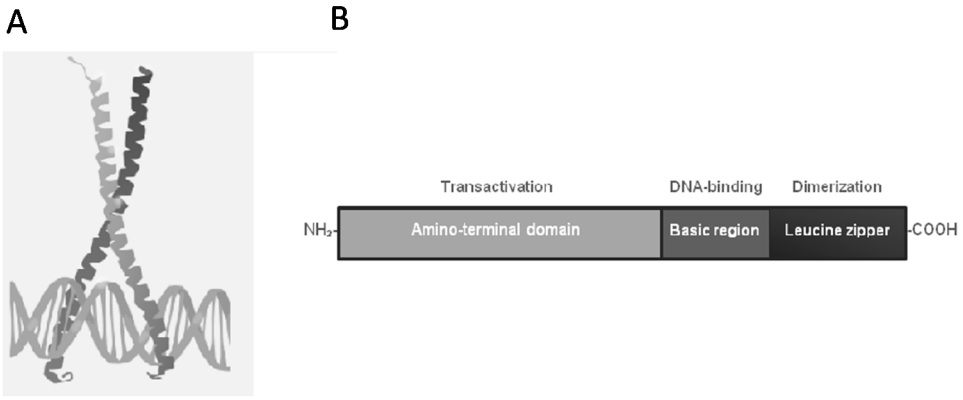

Figure 6 - Protein structure of CCAAT/Enhancer-binding proteins. *A) Model of binding of C/EBP dimer to DNA through bZIP domains. B) Domain topology of the C/EBPβ protein. Retrieved from [79].*

C/EBPβ was initially described as a nuclear factor that binds to an IL-1-responsive element in the IL6 gene[76]. C/EBPβ is known to have roles in the differentiation of adipocytes, macrophages and mammary epithelial cells; in metabolic control, namely in glycogen mobilization; in inflammation and acute-phase response; and in promoting cellular proliferation. Constitutive expression of C/EBPβ is particularly high in the liver, intestine, lung, adipose tissue, spleen, kidney and myelomonocytic cells[78]. Among the C/EBP family, C/EBPβ has been reported to be the dominant DNA binding factor in the adult airway epithelium[80]. Relating to CF, C/EBPβ was recently found as a primary hit in a screen searching for F508del-CFTR traffic regulators in bronchial epithelial cells. (Hugo M. Botelho, unpublished data)

The C/EBPβ mRNA is intronless and can be translated as multiple proteins by leaky ribosome scanning and the alternative use of multiple translation initiation codons in the same mRNA[77] (see Appendices, Figure 32). Three C/EBPβ isoforms have been identified, the 38kDa liver-enriched transcriptional activator protein (LAP*/LAP1), the 35kDa LAP/LAP2 and the 20 kDa liver-enriched transcriptional inhibitory protein (LIP). LIP lacks the transactivation domain and represses gene expression, suggestively by inhibiting the function of other C/EBP isoforms in a dominant negative fashion[78]. C/EBPβ is normally maintained in a repressed state by negative regulatory domains, which sterically inhibit its transactivation domains. Phosphorylation within the inhibitory domains can abolish this repressive effect, and in many cases, leads to an increase in the transcriptional activity of C/EBPβ[78]. C/EBPβ phosphorylation

occurs on numerous residues and is regulated via numerous signalling pathways, which include Ras–MAPK, growth factors, GSK3β, and protein kinases A and C, among others[77].

C/EBPβ activity is implicated in the regulation of lung cytokine expression, myofibroblast differentiation, and collagen deposition[81]. C/EBPβ-binding sequences were found in regulatory regions of several genes associated with the acute-phase response and inflammation[76]. Interestingly the *CXCL8* promoter element (which encodes for IL-8) contains C/EBPβ binding sites[82]. C/EBPβ has been implicated as a critical regulator of IgG immune complex-induced inflammatory responses and injury in the lung and its knockout led to a significant attenuation of the lung neutrophil accumulation in BALF[83]. Mesenchymal-specific deletion of C/EBPβ in the lung of mice showed significant reduction of pulmonary fibrosis when injury was promoted. No significant differences in inflammatory/immune cell influx were noted, but a reduction in myofibroblast differentiation was noticeable[81].

Several reports have indicated that TGFβ signalling induces Smad3/4-dependent inhibition of C/EBPβ function, namely in adipose differentiation. However, C/EBPβ can also serve as a cofactor for TGFβ signalling: induction of the cyclin-dependent kinase 4 inhibitor B (p15INK4b) and repression of c-Myc were found to depend on C/EBPβ[84]. The TGFβ cytostatic effect is based on elevating the expression of the CDK inhibitors p15INK4b, p21CIP1 or p57KIP2 and concurrently repressing Myc growth promoting factors and ID antidifferentiation factors. Induction of p15INK4b requires a Smad-FoxO-C/EBPβ transcriptional complex and Smad-E2F4/5-C/EBPβ targets c-Myc for repression. Hence, C/EBPβ coordinates the induction of p15INK4b and the repression of c-Myc by Smads, emerging as a fundamental member in the TGFβ cytostatic program[35,85]. Interestingly, a higher level of LIP has successfully been linked to a loss of TGFβ-dependent cytostatic responses in metastatic cells from breast cancer patients[85]. Because an increase in LIP expression antagonises LAP2 activity, a high LIP:LAP ratio favours the inactivation of p15INK4b, activation of Myc and proliferative behaviour in metastatic breast cancer cells[77].

The LIP:LAP ratio and its involvement in oncogenesis has been further studied. LIP increase in mammary epithelial cells resulted in an increase in epithelial proliferation, decrease in differentiation and formation of mammary hyperplasias. LIP expression had also been observed in some human breast cancers, potentiating more highly proliferative and aggressive tumours[86]. More recently, LIP was reported to be abnormally overexpressed and correlated with cancer metastasis in human esophageal squamous cell carcinoma (ESCC)[87]. However, LAP upregulation has also been linked to human primary breast tumours, which showed markers of having undergone EMT[88].

Additionally, C/EBPβ has also been reported as an essential mediator of skin tumorigenesis involving oncogenic Ras signalling[89,90] and cyclin D1-dependent tumours[91].

1.2.3. Role of miR-155 in regulating C/EBPβ and EMT

MicroRNAs (miRNAs) are a class of evolutionary conserved single-stranded non-coding RNA molecules of 19-24 nucleotides that control gene expression at a post-transcriptional level, functioning as negative regulators of gene expression. miRNAs have been predicted to target and control the expression of at least 30% of the entire mammalian genome[92]. miRNAs bind to regions of complementary in the 3'untranslated region (3'UTR) of target mRNAs and trigger either their degradation or the inhibition of translation, depending on the degree of

complementarity between miRNA and its target mRNA[93]. However miRNAs are increasingly being reported in other noncoding regions such as promoter or intronic regions[94].

MiR-155 in particular is reported to be involved in numerous biological processes including haematopoiesis, inflammation and immunity. Accordingly, deregulation of miR-155 has been found to be associated with cardiovascular diseases, viral infections and different kinds of cancer. MiR-155 was found to be overexpressed in several solid tumours, such as B-cell lymphoma, thyroid carcinoma, breast cancer, colon cancer, cervical cancer, pancreatic ductal adenocarcinoma and lung cancer[92,93].

MiR-155 has also been identified and characterized as a component of the primary macrophage response to different types of inflammation mediators[92]. Mice without expression of this miRNA are immunodeficient and display increased lung airway remodelling[95].

Some findings point to a role of TGFβ in regulating miR-155 expression. Upon TGFβ stimulation, Smad4 can enhance miR-155 expression levels, augmenting the TGFβ-dependent EMT. Furthermore, a key molecule in EMT, RhoA, is a miR-155 target[93]. MiR-155-mediated loss of C/EBPβ was also found as a mechanism of promotion of breast cancer progression, by shifting the TGFβ response from growth inhibition to EMT, invasion and metastasis. Furthermore, loss of C/EBPβ enhanced invasion and metastatic dissemination of the mouse mammary tumour cells to the lungs[96]. The expression of C/EBPβ protein correlated with cytokine production in tumour-activated monocytes and with sustained reduction of miR-155[97]. Accordingly, exposure of macrophages and mice to LPS lead to an upregulation of miR-155 with the confirmation of C/EBPβ as a direct target for this miRNA[98].

miR-155 upregulation was further associated with recurrence and poor survival in NSCLC[99]. Interestingly, miR-155 was one of only 2 miRNAs found to be upregulated in both breast and lung cancer, implying that these miRNAs may be part of a common mechanism in the development of cancer in these organs[94].

Finally, expression of miR-155 was found to be more than 5-fold elevated in CF lung epithelial cells, compared with control cells. Clinically, miR-155 was also highly expressed in CF lung epithelial cells and circulating CF neutrophils biopsied from CF patients. Interestingly, a reduction in miR-155 levels reduced IL-8 expression in CF cells, suggesting a regulatory role for miR-155 in the inflammation processes in the lung[100].

1.3. Objectives of the present work

The main goal of the present work was to explore the physiological significance of TGFβ signalling in the absence of functional CFTR, namely its possible role in activating EMT pathways.

The aims of the present work included

- Determining if EMT was a component of CF disease;
- Assessing the localization and status of transcription factor C/EBPβ in the absence of functional CFTR;
- Investigating C/EBPβ's possible role in mediating TGFβ induced EMT;
- Evaluating the role of miR-155 on these processes.

This work contributed to our understanding of the regulatory role of CFTR in epithelial differentiation and chronic inflammation in cystic fibrosis.

2. Materials and Methods

2.1. Generation of a new cell line by the CRISPR system

The CRISPR system is a novel technique which addresses the need for precise and efficient genome-engineering technologies. It is based on the RNA-guided Cas9 nuclease from the type II prokaryotic clustered regularly interspaced short palindromic repeats (CRISPR) adaptive immune system[101]. This technology involves generating DNA double strand breaks (DSBs) in specific genomic locations which are targeted by nucleases. The downstream repair mechanisms involve homologous recombination events which can be used to engineer the genomic locus[102]. The main advantage of this system is its ability to target any genomic location in a vast range of organisms. For instance, it has been shown that this *Streptococcus pyogenes* II CRISPR system can be heterologously reconstituted in mammalian cells[101].

CRISPR RNA (crRNA) fused to a normally trans-encoded tracrRNA is sufficient to direct the Cas9 protein to sequence-specifically cleave target DNA sequences matching the crRNA[103]. With this knowledge, a straightforward system was created for gene engineering. The first step is to select the desired locus. Then, the nuclease activity of the CRISPR/Cas9 system is recruited by two noncoding RNA elements: a 20 bp crRNA target sequence (spacer) and a tracrRNA (trans-activating crRNA). This crRNA:tracrRNA duplex (also termed guiding RNA or gRNA) directs Cas9 nuclease to target DNA in the genome via complementary base pairing between the spacer on the crRNA and the complementary sequence (protospacer) on the target DNA. The CRISPR/Cas9 then introduces a double strand break in the DNA. These breaks are repaired by cellular mechanisms, either non-homologous end joining (NHEJ) or the homology directed repair (HDR). Both pathways have specificities, which can be taken advantage of for the desired genome engineering. HDR repair requires a template and is therefore used when specific nucleotide changes are to be introduced in the target gene. In the absence of a repair template the default pathway is the NHEJ repair. During this process a variety of mutations can occur: point mutations, indels ranging from one to hundreds of nucleotides, interchromosomal translocations, pericentric inversions, palindrome-catalysed deletions and microhomology-mediated deletions. These often disrupt open reading frames, effectively creating gene knockouts[102].

By including this system in the present work, the aim was to create C/EBPβ knockouts to further study their effect on CFTR expression and EMT.

2.1.1. gRNA design and synthesis

As referred above, the first step in the CRISPR/Cas9 system is to choose a target sequence in the genome. This target sequence is a 23 bp genomic site with the form 5'-N_{20}NGG-3' near the intended target site (the sequence may reside on the + or - strand). Cas9 target specificity relies on the presence of specific nucleotides 3' to the protospacer sequence, termed the protospacer adjacent motif (PAM). The Cas9 RNA-guided endonuclease from *Streptococcus pyogenes*, spCas9, requires a 5'-NGG–3' PAM, hence the need for this NGG sequence in the genomic site. However this PAM is only present in the genomic region and it is not included in the gRNA.

To generate C/EBPβ gene knockouts, its genomic DNA sequence (from the NCBI database[104]) was analysed. All 23bp genomic sites matching the criteria were blasted using NCBI's nucleotide BLAST tool, so as to choose the most exclusive for the C/EBPβ gene. The sequences were also run by E-CRISPR, an online software tool to design and evaluate target sites (from the German Cancer Research Institute). Two different gRNAs matched all the criteria: TCATGCAACGCCTGGTGGCC (with a TGG PAM) and AGCCCGTACCTGGAGCCGCT (with a GGG PAM).

2.1.2. Bacteria transformation

Three plasmids were used to transfect the cells in order to implement the CRISPR/Cas9 system: a plasmid coding for the gRNA, one encoding Cas9-GFP and one which confers hygromycin resistance (vector maps are depicted in the appendices, Figure 33). The gRNA expression cassette for C/EBPβ was synthesized by GeneArt (LifeTechnologies) and subcloned into a pMTA vector. The construct for the enzyme Cas9 was purchased from Addgene (plasmid #44719) and was already available in the laboratory. In order to amplify the plasmids, XL1-Blue (Stratagene, 200315) bacterial cells were transformed.

100ng of DNA from the plasmid stocks were added to the cells. Uptake was performed for 30min on ice and stopped by heat shock, 90s at 42^{o}C and 2min on ice. Lysogeny broth (LB) medium (NZYTech, MB02803) was then added and left for 60min at 37^{o}C with agitation (220rpm). A centrifugation step was performed (2min at 6000rpm) and the supernatant discarded. Cell pellet was resuspended and added to a plate of LB-agar (Sigma-Aldrich, L2897) with the appropriate antibiotic for each plasmid selection [ampicillin (Sigma, A9518) or kanamycin (Sigma, K1377)]. Plates were incubated overnight at 37^{o}C and the following day stored at 4^{o}C. Then, selected clones were resuspended in LB medium and grown overnight at 37^{o}C with agitations (220rpm). The following day plasmid DNA was extracted and purified.

2.1.3. DNA extraction

The plasmid DNA purification was performed using the NZYMiniprep kit (NZYTech, MB010). This kit is based on alkaline lysis of bacterial cells followed by selective adsorption of DNA to a silica gel-based column. The protocol involves removal of impurities such as proteins, salts, nucleotides and oligos. Purified DNA concentration was assessed with a Nanodrop ND1000 Spectrophotometer (absorbance at 260nm).

2.2. Cell culture and tissues

2.2.1. Cell lines, culture conditions and treatments

Cell lines and culture conditions

In this work, studies were performed in airway epithelial cell lines derived from parental cystic fibrosis bronchial epithelial cells (CFBE41o-). CFBE cells are an excellent preclinical model for CF because they were derived from bronchial epithelial cells from an F508del-CFTR homozygous CF patient[105]. Since the parental cell line does not express CFTR at detectable levels, in the present work cells stably transfected with wt or F508del-CFTR were used, so as to model control and CF tissue respectively. A full description of the development of these cell lines a and relevant functional studies is available elsewhere[106]. From this point on, these cells

will be generally be referred to as CFBE cells. This line also allowed the development of other cells lines used in this study, namely CFBE mCherry-FLAG CFTR cells (in both the wt and F508del-CFTR variants). These cells possess a tet-on promoter for CFTR expression, and feature a mCherry tag at the N-terminus of CFTR and a FLAG tag in the fourth extracellular loop. A full explanation of the generation, characteristics and advantages of these cells is available elsewhere[107]. From this point on this cell line will be referred to as CFBE mCherry FLAG cells.

CFBE cells were grown in Eagle's Minimum Essential Medium (EMEM) with L-glutamine (Lonza, BE12-611F) supplemented with 10% (v/v) Foetal Bovine Serum (FBS) (Gibco, 10270) and the antibiotic puromycin (Sigma-Aldrich, P8833) at 2.5µg/mL for selection. At times PenStrep (penicillin:streptomycin solution, Gibco, 15070) 1% (v/v) was also added to the cells as an antibacterial agent. CFBE mCherry-FLAG cells were grown in Dulbecco's Modified Eagle's Medium (DMEM) with 4.5 g/L Glucose and L-glutamine (Lonza, BE12-604F) supplemented with 10% FBS and the antibiotics blasticidin (InvivoGen, ant-bl-1) 10µg/mL and puromycin 2µg/mL (for cell selection). Doxycycline (Sigma-Aldrich, 9891) 1µg/mL was added whenever CFTR expression was desired. For the CFBE mCherry FLAG wt-CFTR cell line, doxycycline was added for 24h before cells were analysed. For the CFBE mCherry FLAG F508del-CFTR cell line, the incubation time with doxycycline was 48h.

All cell lines were cultured in an incubator with humidified atmosphere of 5% CO_2 at 37°C. Cells were kept in diverse plastic flasks or plates. When the cells reached appropriate confluence (generally 100%) they were rinsed twice with Dulbecco's Phosphate Buffered Saline (DPBS) (Lonza, BE17-512F), dissociated with Trypsin EDTA (Lonza, BE17-161E), resuspended and redistributed into new flasks/plates. Frozen cells stocks were kept in cryotube vials (Thermo Scientific, 340 711) at -80^{o}C. When thawing was necessary the process was done very quickly, submerging the vials in water at RT, washing the cells with fresh media without antibiotics and subsequently seeding them. When it was necessary to freeze cells, the cell pellet was isolated by centrifugation and resuspended in 40% (v/v) of the respective media, 50 % (v/v) FBS and 10 % (v/v) dimethyl sulfoxide (DMSO) (Sigma-Aldrich, 41640), to prevent the formation of ice crystals. Cells were then placed in -80^{o}C in a freezing container, to avoid abrupt freezing and damage.

CFBE mCherry FLAG CFTR cells were used in the C/EBPβ knockdown studies and characterized regarding its protein levels. They were also used to study the effects of miR-155 and its antagomiR. CFBE cells were the main model of this study and were used for the CRISPR technique, co-immunoprecipitation studies and all experiments with polarized cells. These cells were also characterized regarding its C/EBPβ protein and transcript levels.

Polarized cells

To achieve polarization, CFBE cells were grown on collagen IV (Sigma-Aldrich, C7521) coated transwell permeable supports (Costar, 3460; Costar 3470) at a density of $1.25x10^5$ or $2.5x10^5$ cells, depending on the diameter of the filter (6.5mm or 12 mm insert, 0.4um pore size). Cells took two days to polarize after which they were rinsed with Hank's Balanced Salt Solution (HBSS) (Gibco, 24020) and the amount of FBS in the media was changed from 10% to 2%. After the switch, the transepithelial electric resistance (TEER) was measured regularly. The TEER measurement is widely used as an indicator of integrity and permeability of cell monolayers and so it was used in the present work to assess cell differentiation on filters. These measurements were carried out using a volt-ohmmeter (Millicell-ERS, Millipore, MER5000001). The filters were maintained in liquid-liquid interface (*i.e.* submerged). The

experiments were generally conducted when the TEER values had peaked and stabilized (around day 6 or 7 after the switch to 2% FBS).

TGFβ treatment

Cells were incubated with human TGFβ1 from HEK293 (human embryonic kidney) cells (PeproTech, 100-21) for 24 to 48h (TGFβ was added to both basolateral and apical compartments). The incubation was performed when the TEER values had peaked and stabilized for both cell lines. Protein, RNA samples or cells for immunofluorescence (see below) were subsequently collected at desired time points. TEER was monitored throughout.

TGFβ was added to cells at a final concentration of 15ng/ml. To achieve this, the stock solution (500ng/mL) was diluted in EMEM 2% FBS and added to the filters. The stock was prepared by diluting the lyophilized 10µg of TGFβ in 20mL of a solution of 10mM citric acid (Sigma-Aldrich, 251275) (pH 3) and 0.1% bovine serum albumin (BSA) (Sigma-Aldrich, A9647). This solution was previously filtered with a syringe driven filter unit (0.22um pore size, Millex GV, SLGV033NS) for fine particle removal. TGFβ final stock was aliquoted in small volumes and stored at 80^{o}C until use.

Cell transfections

For C/EBPβ knockdown and assessment of miR-155 effect, CFBE mCherry FLAG cells were chosen because of their mCherry and FLAG tags which allow the probing of total CFTR and plasma membrane CFTR in the same experiment. This makes it possible to assess if a treatment rescues F508del-CFTR to the plasma membrane or if the knockdown of a gene negatively affects the amount of wt-CFTR at the plasma membrane.

On the first day of the experiment, cells were seeded on 8-well chambered coverslips (Nunc, 155411) (immunofluorescence assay), 37500 cells per well, or 12-well plates (Thermo Scientific, 130185) (Western blot assay), 180000 cells per well.

On the second day scrambled RNA (4390827), siRNA for C/EBPβ (ID2891, ID2892, 4427037) miR-155 (MC12601, 4464066), antagomiR-155 (MH12601, 4464084) and negative control (AM17010) (all from Ambion) were prepared and added to the cells. All the stocks were reconstituted according to the manufacturer's instructions. The final concentration added to the cells was approximately 0.02µM for scrambled and C/EBPβ siRNA and approximately 0.025µM for negative control, miR-155 and antagomiR-155.

A mix of opti-MEM I Reduced Serum Medium (opti-MEM) (Gibco, 31985) and Lipofectamine 2000 transfection reagent (Invitrogen, 11668-019) was added to another mix of opti-MEM and each of the treatments. Lipofectamine:RNA ratio was approximately 1:8 for scrambled and siRNAs and 1:3 for miR, antagomiR and the negative control, following the manufacturer's recommendations.

24h after the treatments F508del-CFTR cells were induced to express CFTR. 48h after the treatments wt cells were induced. 72h after the treatments immunostaining was performed and/or protein was extracted. 72h was found to be the time point at which the knockdown was more efficient (see appendices, Figure 35).

For the CRISPR system cell transfection, cells were seeded on the first day of the experiment. CFBE wt or F508del-CFTR cells were seeded in T25 flasks (Thermo Scientific, 130189), 8x10^{5} cells/plate. The next day cells were transfected with all three plasmids from the CRISPR system. A total of 5µg of DNA were added to the cells: 2.25µg of the cas9 plasmid and the gRNA plasmid and 0.5µg of the hygromycin resistance plasmid. The DNA was suspended in NaCl 150mM (Polyplus, 702-50) and mixed with JetPei transfection reagent (Polyplus, 101-

40N) also resuspended in NaCl 150mM. The full mix was left for 15 to 30min before being added to the plates. This mix was left on the cells for 6h when an equal volume of EMEM with 10% FBS was added. Media was changed the next day. Cells were trypsinized and passaged to P100 plates 48h after transfection and hygromycin (Sigma-Aldrich, H7772) was added, 200µg/ml. Media was changed every two days, with puromycin 2.5µg/mL being further added for selection. Cells started dying from the antibiotic selection. Hygromycin was removed from the cells approximately 10 days after the transfection. Around the same time some individual colonies were picked. This was done using scienceware cloning discs (Sigma-Aldrich, Z374431) with trypsin. The individual clones were seeded on 24 well-plates and kept in culture. This process was repeated one more time so the maximum number of clones was individualized.

Clones were kept on 24-well plates (Thermo Scientific, 930186) until confluence was achieved. Then, cells were passed to a 6-well plate (Thermo Scientific, 130184). When confluence was, once again, reached, the cells were passed to a T25 which was then kept growing until the cells were ready to freeze, and a 24-well plate to extract protein for C/EBPβ level analysis (as described in section 2.4). The process for all the clones took about three months. Around 40 clones total were frozen.

2.2.2. Human lung tissue

Access to explanted lungs was established through a collaborative project between the Faculty of Sciences of the University of Lisboa and the Cardio-Thoracic Surgery Department of the Hospital de Santa Marta (Lisboa), which received approval from the hospital's Ethics' Committee. The tissue samples used in the present work were already available at the host laboratory.

Control and CF lung bronchial tissue was processed in the mammalian cell culture under the laminar flow hood. The control tissue belonged to a drug user and was homozygous for wt CFTR. The CF patient was F508del CFTR homozygous. Sections of interest, mostly containing secondary or tertiary bronchi and their surrounding regions, were embedded in a cryoprotective embedding medium, Tissue-Tek optimal cutting temperature (O.C.T.) compound (Sakura, 4583) with the appropriate orientation and snap frozen in liquid nitrogen. Upon freezing, water still remaining in the sample expands and form crystals which damage the tissue. Upon sectioning, the presence of water crystals results in multiple holes and loss of cell contents in the sections, depending on the size and degree of crystal formation. Most of the samples used in the present work were snap frozen in liquid nitrogen, as this effect can occur in slow freezing. Afterwards, the sections were stored at -80^{o}C until further use.

Tissue sections were cryocut using a Leica CM1850 UV cryostat. Cryosections 8 to 15µm thick were generated on silane-prep slides (glass slides coated with aminoalkylsilane, Sigma-Aldrich, S4651) and used immediately away for immunohistochemistry or haematoxylin and eosin (H&E) staining or stored at -20^{o}C until they were stained.

H&E staining was performed at the Histology and Development Biology Institute in the Faculty of Medicine of the University of Lisbon, with local materials and reagents. In this procedure hemalum (in the haematoxylin solution) colours the nuclei of cells blue. The nuclear staining is followed by counterstaining with eosin, which colours the remaining tissue structures in various shades of red, pink and orange. This technique was used in this study for a better comprehension of the histological features of wt and CF lung tissue.

Slides with cryosections were warmed to room temperature before being submitted to the following treatment: 5min in distilled water, 3min in Harris haematoxylin, rinsing with distilled water, 30s in 0.2% (v/v) ammonia water, 30s in warm water, 30s in 70% ethanol, four immersions (1s each) in eosin, 30s in 70% (v/v) ethanol, 30s in 96% (v/v) ethanol, 30s in 100% (v/v) ethanol, 15min in xylol. Slides were then mounted with Quick-D mounting medium (Klinipath, 7281).

Images were acquired at Faculty of Sciences, using an Olympus BX51 microscope which, instead of regular bright-field microscopy, allows for coloured image collection. Image processing, including a stitching of the collected images, was performed on Adobe Photoshop software, available in the laboratory.

2.3. Immunofluorescence

2.3.1. Non-polarized cells

For C/EBPβ knockdown and assessment of miR-155/antagomiR-155 effect studies, cells were stained with anti-FLAG and anti-C/EBPβ antibodies (see Appendices for antibody dilutions and general information, Table 1 and 2). Hoechst 33342 (Sigma-Aldrich, B2261) staining was also performed to stain the nuclei. The cells already possessed a mCherry tag on the N-terminus of CFTR (when induced).

Cells were taken out of the incubator and washed once with phosphate buffered saline (PBS) [137 mM NaCl (Calbiochem, 7760); 2.7 mM KCl (Sigma-Aldrich, P9541); 10 mM Na_2HPO_4 (Sigma-Aldrich, S9763); 1.8 mM KH_2PO_4 (Fluka, 60229); pH 7.4] supplemented with 0.7mM of $CaCl_2$ (Merck Millipore, 172570) and 1.1mM of $MgCl_2$ (Merck Millipore, 105833) (henceforth termed PBS++) at 4^{o}C. For the FLAG staining, the anti-FLAG antibody was added for 1h at 4^{o}C. All antibodies were prepared in a solution of BSA 1% (w/v). Cells were then washed again 3 times with PBS++. A fixation step was performed with paraformaldehyde (PFA) (Merck Millipore, 14003) 3% (v/v) for 20min. For the C/EBPβ staining, the cells were first fixed and then permeabilized with a 0.1% (v/v) Triton X-100 (Amersham Biosciences, 17-1315-01) solution for 5min, before adding the antibody for 30min. After the cells were fixed (in both cases) all the steps were performed at room temperature. The secondary antibodies, Cy5 or Alexa Fluor 647 (A647) were added to the cells and left for 1h. The final step was the Hoechst staining (1:5000) for 1h. Cells were left in PBS++ at 4^{o}C until imaging.

2.3.2. Polarized cells

CFBE cells were polarized as previously described in section 2.1.1. Immunostaining was performed when TEER values peaked and stabilized.

Filters were washed 3 times for 5min with warm HBSS. All remaining washes and solutions were performed with PBS. All the treatments were applied to both to the apical and basolateral sides. The cells were fixed with PFA 4% (v/v) for 30min. Then Triton X-100 0.5% (v/v) was added for 15min for permeabilization. A blocking step was performed for 20min with BSA 1% (w/v). Only then were the filters removed from their supports using a scalpel. Filters were split in pieces and each piece placed in an individual well of a 24-well plate. These were then incubated overnight at 4^{o}C with primary antibodies in 1% (w/v) BSA. In between antibodies a more thorough washing step was performed with a solution of Triton X-100

0.05%. A mix of the secondary antibody and nuclear dye ToPro3 Iodide (Life Technologies, T3605) (1:750) was then applied (1h, RT). Finally filter sections were mounted on slides with Vectashield Antifade Mounting Medium (Vector Laboratories, H-1000).

The antibodies used for the immunostainings are described in the Appendices, Table 1 and 2.

2.3.3. Tissues

Slides containing lung cryosections were warmed to RT for 5min. Individual sections were isolated with a liquid blocker (PAP pen, Sigma-Aldrich, Z377821), allowing the same slide to be probed with different antibodies or antibody concentrations. All solutions were diluted in PBS. The fixation step was performed with a PFA 4% (v/v) solution for 10min at RT. The permeabilization was achieved with Triton X-100 0.2% (v/v) for 10min. Autofluorescence arising from abundant elastin in the connective tissue[108] was quenched with sodium borohydride (Sigma-Aldrich, 452882) 1mg/mL (1% w/v). Slides were washed 3 times for 10min with freshly prepared sodium borohydride solution. Afterwards sections were blocked with BSA 1% (w/v) for 30min and incubated with the primary antibody (diluted in 1% (w/v) BSA) overnight at 4^{o}C (in a wet chamber and kept in the dark). The next day the secondary antibody (diluted in 1% (w/v) BSA) (2h, 4^{o}C) incubation was performed and the nuclear dye 4',6-diamidino-2-phenylindole dihydrochloride (DAPI) (Sigma-Aldrich, D9542) was added. Sections were immersed in a solution of DAPI 5µg/mL in 0.1% (v/v) Triton X-100 for 2min and washed for 20min with a higher concentration PBS for a salting out effect. For confocal imaging the nuclear dye ToPro3 was used instead, and this dye was added 1:750 diluted in the secondary antibody solution. Slides were mounted with Vectashield.

Between every step the slides were washed 3 times for 10min with PBS supplemented with 0.1% (v/v) Tween 20 (PBST) (Sigma-Aldrich, P1379).

The antibodies used for the immunostainings are described in the Appendices, Table 1 and 2.

2.3.4. Image acquisition, processing and analysis

Images were acquired using two different systems: either a Leica DMI6000B system equipped with a metal halide light source (EL6000) and a DFC365 FX CCD camera (Leica) or a Leica TCS SPE confocal microscope with a 63x oil objective. On the first system, fluorescence was assessed in three different channels – DAPI/Hoechst, mCherry and A647. For non-polarized cells a contrast-based autofocus step was also performed with the Hoechst channel. On the second system, fluorescence was also assessed in three different channels – Alexa Fluor 488 (A488), Alexa Fluor 568 (A568) and ToPro3.

For tissues, most images were analysed using open source software FIJI for background subtraction, contrast optimization and channel merging. For polarized cells, image analysis was performed using Visage Imaging Amira 5.3.3 for section's 3D reconstruction, made available by Professor Sólveig Thorsteindóttir at DevEM/CE3C. This software was also used to analyse some of the tissue images. Confocal image acquisition and edition were kindly performed by Luís Marques. At last, for non-polarized cells, the image processing and analysis was performed with open source software tools (CellProfiler and R) using specific pipelines. These pipelines comprised an algorithm for background subtraction for all channels (applied to all the images)

and an algorithm for quantification of mCherry (CFTR) or Alexa Fluor 647 (FLAG or C/EBPβ) signal, as previously described[107]. These pipelines were kindly designed by Hugo M. Botelho.

2.4. Protein analysis

2.4.1. Protein extracts

Cells were grown on plates, flasks or filters until they reached the appropriate confluence. Protein was collected by washing cells twice with cold PBS and then adding the appropriate amount of volume of sample buffer [31.25 mM Tris HCl (Sigma, 30721) pH 6.8; 1.5% (v/v) sodium dodecyl sulfate (SDS) (Gibco, 15553); 5% (v/v) glycerol (Sigma, 92025); 0.02% (w/v) bromophenol blue (Sigma-Aldrich, B0126); 50 mM dithiothreitol (DTT) (Sigma, D0632)]. Benzonase (Sigma-Aldrich, E1014) 25 U/mL was then added to shear the DNA, in the presence of $MgCl_2$ 3mM. Cells were scraped to collect the protein extract. SDS-polyacrylamide gel electrophoresis (SDS-PAGE) was performed immediately or the extracts were stored at -20^{o}C or -80^{o}C until further use.

2.4.2. Protein quantification

Bradford method was used to quantify the total protein for SDS-PAGE. 15µL of the protein extract was diluted to a final volume of 800µL using sterile water for irrigation (Aqua B. Braun ecotainer, 0082479E). 200µL of Bradford reagent (BioRad, 500-0006) were incubated with each sample for 5min. Protein concentration was determined by measurement of A595 on a spectrophotometer (Amersham Biosciences, Ultrospec 1100) after calibration with BSA standards of increasing concentrations (0 to 35µg/mL). Typically, 10µg of total protein were loaded on each SDS-PAGE well.

2.4.3. Western blot

The samples were separated by SDS-PAGE. For stacking samples were run in 4% gels [125 mM Tris HCl pH 6.8; 4% (v/v) acrylamide:bisacrylamide (Bio-Rad, 1610154); 0.1% (v/v) glycerol; 0.1% (v/v) SDS; 0.075% (v/v) ammonium persulfate (APS) (Bio-Rad, 1610700); 0.08% (v/v) tetramethylethylenediamine (TEMED) (Sigma, T9281)]. For separation 7 or 10% (w/v) gels were used, depending on the protein band resolution required [for 7%: 375 mM TrisHCl pH 8.8; 7% (v/v) acrylamide; 0.1% (v/v) glycerol; 0.1% (v/v) SDS; 0.075% (v/v) APS;0.06% (v/v) TEMED]. Samples were run on a 10-fold dilution of 10x TGS buffer (Bio-Rad, 161-0772) for 90 to 210min at 65 to 120V.

This was followed by transfer onto polivinylidene difluoride (PVDF) membranes (Merck Millipore, IPVH00010), using a cold 10-fold dilution of 10x TG Buffer (Bio-Rad, 161-0771), for 90min at 400mA. Membranes were first activated with methanol (Fisher Scientific, 412).

The membranes were blocked for 1h with 5% (w/v) skimmed milk (Nestlé, Molico) in PBST. This was followed by incubation with the primary antibody overnight at 4º C, with gentle shaking (40-60rpm). After washing the membranes with PBST (3 times 10min) they were incubated with horseradish peroxidase (HRP)-conjugated secondary antibodies for 1h at RT. Membranes were washed once again before being developed. All the antibodies were diluted in blocking solution. Antibodies used are described in the Appendices, Table 1 and 2.

Membrane luminescence was detected on the Chemidoc XRS+ system (BioRad, 170-8265) using a 1:1 mixture of peroxide:luminol/enhancer solution (BioRad, 170-5061). The quantification of the band intensity was performed using the Image Lab software (BioRad, 170-9690), which integrates peak area. Calnexin was used as an internal control, against which all measurements were normalized.

2.4.4. Co-immunoprecipitation

A co-immunoprecipitation (co-IP) was performed to detect interactions between C/EBPβ and CFTR at the protein level. Eight P100 (Thermo Scientific, 130182) dishes (each) were grown for CFBE wt cells and CFBE F508del-CFTR cells. From that point onward the protocol was performed at 4^{o}C. When 100% confluence was reached the cells were washed 3 times with cold PBS and then with 0.5 mL of PD-buffer [50 mM Tris HCl pH 7.4; 100 mM NaCl; 1% (v/v) glycerol; 1% (v/v) Nonidet P-40 (NP-40) (Roche, 11332473001); 1x Protease Inhibitor Cocktail (PIC) (Roche,11697498001)], scraped and collected. Cells were then centrifuged for 10min at 10000rpm (for cellular debris removal) and the supernatant was collected. At this point whole cell lysate (WCL) samples were collected from each tube, adding 20μL of the supernatant to 20μL of sample buffer. These samples were frozen immediately and stored at -20^{o}C until further use. To the remaining supernatant, 40μL of Protein G Agarose beads (Life Technologies, 20398) were added for pre-clearing of nonspecific proteins, with 1h of rotation. Afterwards the samples were centrifuged 1min at maximum speed (13200rpm) and the beads were discarded. CFTR (1μL) or C/EBPβ (6μL) antibody was added to some of the samples while others were used as a control. The antibody was left incubating overnight with rotation. The following day beads were again added (to isolate antibody-protein complexes) and samples incubated for 2h with rotation. Beads were then washed 3 times with wash buffer [100 mM Tris HCl pH 7.4; 300 mM NaCl; 1% (v/v) Triton X-100]. Protein was eluted with 40μL of sample buffer for 1h rotating at room temperature. The samples were then stored at -20^{o}C until further use.

Samples were spun-down and run in SDS-PAGE 10% (w/v) gels as previously described (section 2.4.3.). When the pulldown for CFTR had been done C/EBPβ protein levels were assessed and vice-versa.

2.5. mRNA analysis

2.5.1. RNA extraction

Cells were grown until they reached the appropriate confluence and then RNA was collected. Cells were first washed twice with cold PBS and then the NucleoSpin kit for DNA, RNA and protein purification (Machery-Nagel, 740955) was used to extract the RNA. First the cells were scraped, lysed and the lysate was cleared. Then the RNA was bound to a silica membrane, which was desalted. The next step was digesting the DNA and washing and drying the silica membrane. The final step was the elution of RNA. RNA concentrations, as well as sample purity, were then evaluated with a Nanodrop ND1000.

2.5.2. cDNA generation

RNA was used to generate cDNA to perform qPCR. The reaction was performed with NZY M-MuLV Reverse Transcriptase (Nzytech, MB08301) according to the manufacturer's instructions. To a mix of 0.2µg of random primers and 0.5mM dNTPs (mix of dATP, dGTP, dCTP and dTTP, Nzytech, MB08701) 1ug of the RNA was added, followed by addition of water for a total volume of 16µL. The tubes were then heated at 65^{o}C for 5min. 100U of the reverse transcriptase, RNase inhibitor (MB08402) and reaction buffer (all diluted in water) were then added to each tube. The total volume was 20 µL.

Reverse transcription of cDNA was performed on a PCR machine at the following temperatures: 10min at 25^{o}C, 50min at 37^{o}C and 15min at 70^{o}C.

cDNA was then diluted 1:5 so that the final concentration for each cDNA was approximately 150ng/µL.

2.5.3. Quantitative real-time PCR

For mRNA expression analysis, quantitative real time polymerase chain reaction (qRT-PCR) was performed in a Bio-Rad CFX96 system. According to the manufacturer, the total qRT-PCR reaction mixture was 20µl per well containing 5µl of the template cDNA, 250nM of the primer mix and 1x SsoFast Evagreen Supermix (Bio-Rad, 172-5201). Hard-Shell 96-well PCR plates were used (Bio-Rad, HSP9601). The protocol was optimized for the primers used (see appendices, Table 3) considering the optimized cycling conditions for Evagreen: 1min at 95^{o}C (for enzyme activation), 10 sec at 95^{o}C (cDNA denaturation) and 30 sec at 55^{o}C (for annealing and extension). The denaturation, annealing and extension steps were repeated 40 cycles. Melting curves with a temperature gradient from 65 to 95^{o}C were obtained to confirm amplification of unique specific products.

Relative abundance of mRNA was measured using the Bio-Rad CFX Manager 2.0 software (Bio-Rad, 1845000).

With standard curve amplification (using a series of 1:5 dilutions of cDNA – from 10ng/µL to 0.016ng/µL) it was found that all the primers showed approximately 100% efficiency. Primer efficiency was calculated with the formula E (%) = $10^{(-1/\text{slope})-1}$x100. Such high efficiencies allowed the type of analysis used and described below.

Transcript levels were calculated by normalizing the gene of interest against the control endogenous gene. The mean CT (threshold cycle) of the gene replicates was subtracted from the mean CT of the control gene, giving the ΔCT. The mean ΔCT was then calculated for a chosen condition, considered the reference value (normally wt). This mean ΔCT was calculated from several replicates and it was then subtracted from the individual ΔCT for each assay, giving the ΔΔCT for each gene compared to the chosen condition. The fold difference in gene expression (experimental/control) was then given by $2^{-\Delta\Delta CT}$.

2.6. Statistical analysis

Data is presented as mean ± SEM. Statistical Analysis Student's t-test for unpaired samples was performed when necessary. When $p<0.05$ results were accepted as significant.

3. Results and discussion

3.1. Chronic inflammation features and EMT markers in bronchial epithelial tissue from CF patients

3.1.1. Chronic inflammation in CF lung tissues

CF patient tissue explants are an excellent resource to study at first-hand the pathological and molecular events occurring in disease as close as possible to the *in vivo* situation. To characterize the histology of bronchial epithelium of healthy controls and CF patients, explanted secondary bronchi samples were stained with haematoxylin and eosin and analysed (Figure 7). Tissue stained with this protocol presents purple cell nuclei and the remaining structures in various shades of pink, according to their protein content. The CF patient whose lung was analysed had an F508del homozygous CFTR genotype.

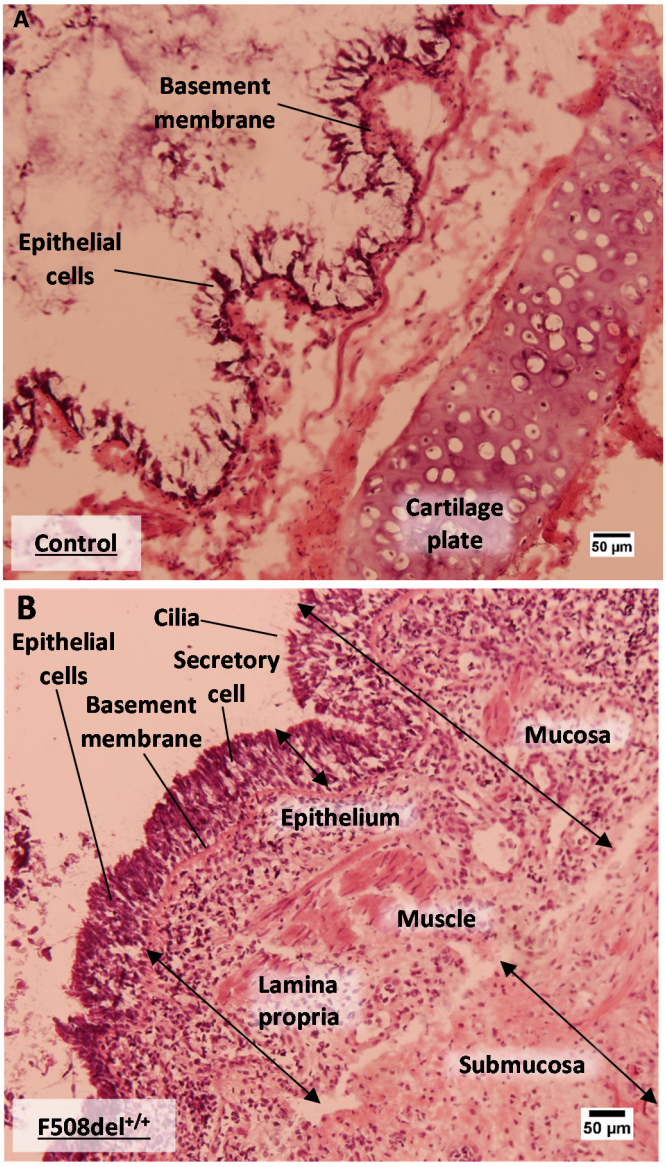

Figure 7 – A. Control and B. CF bronchial epithelium with H&E staining. *Characteristic epithelial structures are identified.*

The tissue samples showed the epithelium lining the bronchial wall, some discontinuous smooth muscle around it and cartilage plates (Figure 7). The bronchi possess a ciliated, pseudostratified columnar epithelium with ciliated, basal and goblet cells. A pseudostratified epithelium is actually a simple epithelium (one cell layer thick) but appears stratified (two or more cell layers): although some of the cells do not reach the surface, all rest on the basement membrane[109]. This was observable in the control sample (Figure 7A). The basement membrane is located beneath the epithelium and is part of the lamina propria, where some loose connective tissue and smooth muscle were visible (Figure 7B). The epithelium and lamina propria constitute the mucosa. Below the mucosa there is another layer, the submucosa. This is where the cartilage plates (visible in Figure 7A) localized.

Although these structures were visible, the control sample appeared not to have been appropriately cryopreserved, presenting gaps within the tissue. Nevertheless, the epithelial cell layer – the focus of the characterization – was not affected. These artefacts could be prevented by, for example, submerging the samples in isopentane cooled to -80ºC, which avoids the formation of vapour barriers, by slowing down the cooling process[110].

Although for the control epithelium (Figure 8A) it was difficult to separate the nuclear staining from the cytoplasmic staining, it seemed to show mainly the expected pseudostratified epithelial structure with ciliated cells touching the basement membrane. No secretory cells were detected in the tissue sections. In the CF epithelium the pseudostratified epithelial structure had been lost (especially seen Figure 8B - arrow). Basal cells had proliferated resulting in a mass of undifferentiated cells with several layers, unlike the normal structure of the epithelium. In the same picture, an area of cell shedding was visible, consistent with extreme epithelial damage (Figure 3B, arrowhead). Other areas of the epithelium (depicted on Figure 8C, arrows) showed signs of secretory cell hyperplasia, with a significant increase in the number of these cells. Some cells were bigger in size, a sign of mucus hypersecretion. Despite this, some areas of the epithelium appeared structurally normal (Figure 8C, arrowhead), suggesting a co-existence of different stages of inflammatory damage and remodelling.

It is now widely accepted that a setting of chronic inflammation in the bronchi is accompanied by damage and remodelling of the epithelium. A study on the ultrastructure of the bronchial epithelium in chronic inflammation identified at least four pathomorphological stages of inflammation: 1) no signs of structural damage; 2) variations of the abundance of each cell type with conservation of the pseudostratified structure (such as hyperplasia of secretory cells and basal cells); 3) loss of the pseudostratified structure with incomplete cell differentiation; and 4) variants with a metaplastic structure (including squamous metaplasia)[111]. Most of these manifestations were found in the CF tissue analysed, as would be expected in the setting of chronic inflammation in the CF lung. Previous histological analyses of CF lung sections have also shown secretory and basal cell hyperplasia, as well as squamous metaplasia, all consistent with tissue remodelling. The analyses also detected areas of extended and severe epithelial shedding. Some areas retained a normal architecture, indicating variable injury severity among areas and patients[68]. These results are also in agreement with the present work.

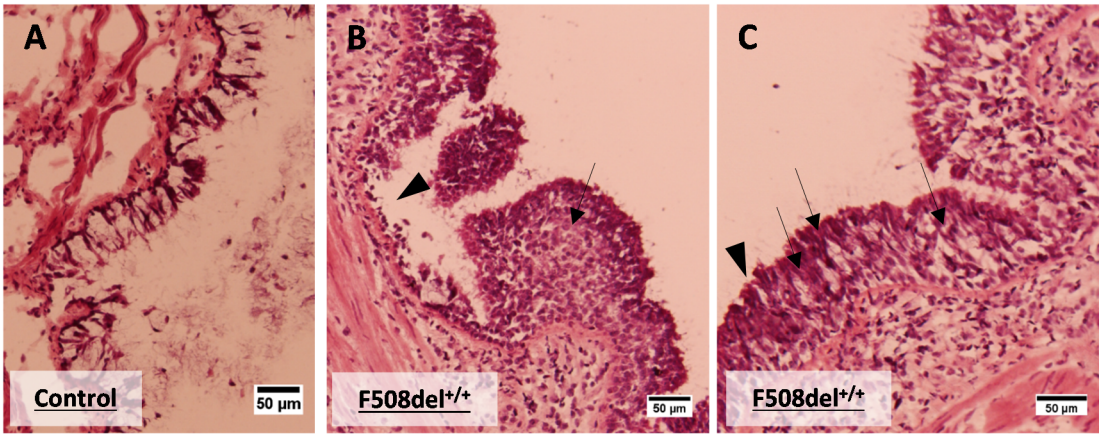

Figure 8 - Histological analysis of the basic defects in CF lung epithelium as a result of chronic inflammation and remodelling. *A. healthy pseudostratified epithelium; B. CF epithelium with cell shedding (arrow head) next to an area of basal cell proliferation and loss of pseudostratified structure (arrow); C. CF epithelium with normal structure (arrow head) next to areas of secretory cell hyperplasia and hypertrophy (arrows).*

3.1.2. Assessment of EMT markers in CF

Since the structural changes observed in CF bronchi can be associated with a loss of airway differentiation, it was sought to compare the expression of epithelial and mesenchymal markers in control and CF tissue. A study conducted in the laboratory of Jonas Fuxe, related miR-155 with loss of C/EBPβ and shift in the TGFβ response from growth inhibition to EMT promotion in breast cancer[96]. Given the common elements, some of the markers used were also transposed into this study. Hence, a panel of markers was selected for differentiated epithelial cells [E-cadherin (E-cad), coxsackie virus and adenovirus receptor (CAR), β-catenin (β-cat) and cytokeratin-18 (CK18)] and undifferentiated mesenchymal cells [N-cadherin (N-cad) and vimentin (vim)]. Additionally, expression of CFTR and a proliferation marker (KI67) expression were also assessed.

On pages 30 to 37, Figures 9 to 16, a side by side direct general comparison can be made between the expression patterns in both CF and control respiratory epithelium. Although CFTR localization for control tissue was difficult to pinpoint at reduced magnification, for CF it is apparent that it localized in the cytoplasm of almost all the cells in the epithelium, without any distinction between apical and basal or membrane expression (Figures 10 and 12). Under increased magnification, CFTR expression in the control tissue was observed to be stronger in the apical component of the epithelium, although some internalization of the protein is also visible. CF tissue, on the other hand, showed dysregulated CFTR expression, with abundant CFTR in the cytoplasm of most epithelial cells, and no distinguishable expression differences in the apical or basal distribution (Figures 14 and 16). An important study characterizing the wt and F508del-CFTR in human respiratory epithelia found a clear CFTR signal in the apical plasma membrane of surface columnar cells in the wt bronchial airways. Intracellular CFTR was low in most ciliated cells. On the other hand, in CF bronchial tissue the authors failed to detect specific CFTR immunostaining. This may be due to the fact that they excluded any areas with distinct inflammation features, focusing only on structurally normal epithelium. However, when some of the metaplastic tissues were analysed, intracellular CFTR staining was observed in some non-differentiated cells, which is consistent with the findings of the present work. As for the CFTR internalization found in the control, since the control tissue used in this work belonged to a drug user, it is possible that fibrotic changes and inflammation are a

consequence of the subject's lifestyle. Inflammation was previously found to affect the expression and distribution of wt-CFTR, showing a diffuse distribution or absence of CFTR in the cytoplasm of ciliated cells[65].

Figures 9 to 12 depict the epithelial markers with reduced magnification. Expression in all of them wass restricted to the epithelium (including staining on the epithelium of a bronchiole and blood vessel for E-cad and β-cat CF, respectively). The most striking difference was that for the control all the markers seem to be highly expressed in comparison with CF, where all markers were reduced or even inexistent. However, in Figures 11 and 12, when the levels of mesenchymal markers (first two rows) were analysed, the opposite is shown: their expression seems increased in CF and decreased in the control. The difference for N-cadherin was more evident, since with the reduced magnification of these images, vimentin expression in the basal cells of the CF epithelia (and its absence in the control) was difficult to see.

As for the proliferation marker, KI67, it appeared to be increased in the CF epithelium where it is not restricted to the basal cells but also to undifferentiated cells in the epithelium. For the control, all the stained cells followed a line consistent with the basal cells. Since KI67 is present during all active phases of the cell cycle (G1, S, G2 and mitosis), but absent from resting cells (in G0), and since its expression is restricted to the nucleus (in interphase) or chromosome surface (in mitosis), it is an excellent marker for the identification of proliferating cells[112]. KI67 has previously been used to assess the level of cell proliferation in F508del cells[62]. This proliferation has been reported to be higher in the regenerating CF epithelium[62,66] compared to control, and these results are consistent with the present work.

In Figures 13 to 16, control and CF epithelium are shown at higher magnification, using either widefield or confocal microscopy. Here, it was possible to observe the expression pattern and localization of the markers in both epithelia.

CAR localized in the membrane of basal epithelial cells in control tissue and was absent in CF. Although its increased expression in a more differentiated epithelium, and decrease in a more undifferentiated one, are in agreement with the literature, the subcellular localization is surprising, since CAR is reported as a marker for epithelial tight junctions, where it promotes cell-cell adhesion and regulates epithelial permeability[113].

E-cadherin had one of the most striking differences in expression between the control and CF. Whereas in the control its expression was restricted to the membrane of the ciliated epithelial cells (at lateral cell-cell contacts), in CF the expression was not only reduced but abnormal. E-cadherin was present in the membrane of the undifferentiated cells with a disrupted pseudostratified structure. This reveals the undifferentiated status of the CF epithelium and the great loss of structural organization which prevents normal function. E-cadherin has long been shown to complex with β-catenin in order to link the tight junctions to the actin cytoskeleton[53]. This complex is known to play a crucial role in epithelial cell-cell adhesion and maintaining the tissue architecture and differentiated status. Perturbations in this complex have been related with cancer (including lung cancer) and invasive cell behaviour. This is partly because upon dissolution of the complex, β-catenin can translocate into the nucleus where it participates in the Wnt pathway, activating genes that can promote neoplastic growth[114,115]. Hence it is not surprising that β-catenin expression followed a similar pattern to that of E-cadherin, being present in the lateral cell-cell contacts of epithelial cells in control tissue, but reduced and abnormally expressed in CF. However, no nuclear staining for β-catenin is observed in CF, which suggests loss of differentiation but no acquisition of an

invasive phenotype. Interestingly, staining of CF epithelium revealed the presence of proliferating polygonal cells flat on the surface of the epithelial layer. This is a documented sign of squamous metaplasia [ultrastructure], which has been previously reported in CF[68], especially in patients with poor clinical condition, being described as the final stage in the transition from inflammatory changes to fibrosis[116]. Surprisingly, the control tissue also had some areas (although rare) with the same pattern consistent with squamous metaplasia (flat polygonal cells are visible). Similarly to the CFTR internalization, this could be attributed to a slight increase in the inflammatory response in this subject, with presence of fibrosis. Nevertheless, the E-cadherin staining of the control tissue was consistent with the expected pseudostratified structure, with only one layer of cells which touch the basement membrane, confirming it as viable model for a healthy control.

As for the mesenchymal markers, in the control epithelium there was no vimentin present, whereas in the basal cells of the CF epithelium some was observed. In EMT, vimentin is known to replace cytokeratins in the composition of the intermediate filaments in the epithelium, contributing, for example, to decreased or absent trafficking of E-cadherin to the membrane[49]. An increase in vimentin in CF was consistent with the reduction in CK18 expression. N-cadherin, which in the control was almost inexistent and disperse, in CF was not only increased but depicted a pattern of expression consistent with a replacement of E-cadherin. In CF tissue, N-cadherin localized in the membrane of the epithelial cells, suggesting a role in cell-cell adhesion. The replacement of E-cadherin with N-cadherin (downregulation of E-cadherin and increased expression of N-cadherin) is consistent with EMT, promoting weaker cell adhesion that can potentiate migration[54].

Overall the results suggest a loss of differentiation in CF epithelium compared to the control. This is consistent with previous reports that the differentiation processes in CF are impaired[62]. Since inflammation was present, it is not possible to conclude if this defect is due to the CFTR defect or the exacerbated inflammation in the CF lung. Interestingly, a recent study discovered that a significant set of differentiation genes are differentially expressed in CF vs non-CF nasal epithelial cells, with a set of genes related to epithelial cell differentiation being among the most significantly disturbed in CF. Genes involved in cellular proliferation were found to be upregulated in CF[117]. This is all in agreement with the findings of the present work.

Owing to the limited quality and availability of control tissue, a quantitative comparison with CF samples was not possible. Since the CF tissue presents increased epithelial height and higher number of epithelial cells, the cell number could be used for normalizing the marker's fluorescence. Since it was not possible to access control tissue from different donors and the main focus of this work was the characterization of molecular inflammatory markers in CF, this approach was not pursued any further.

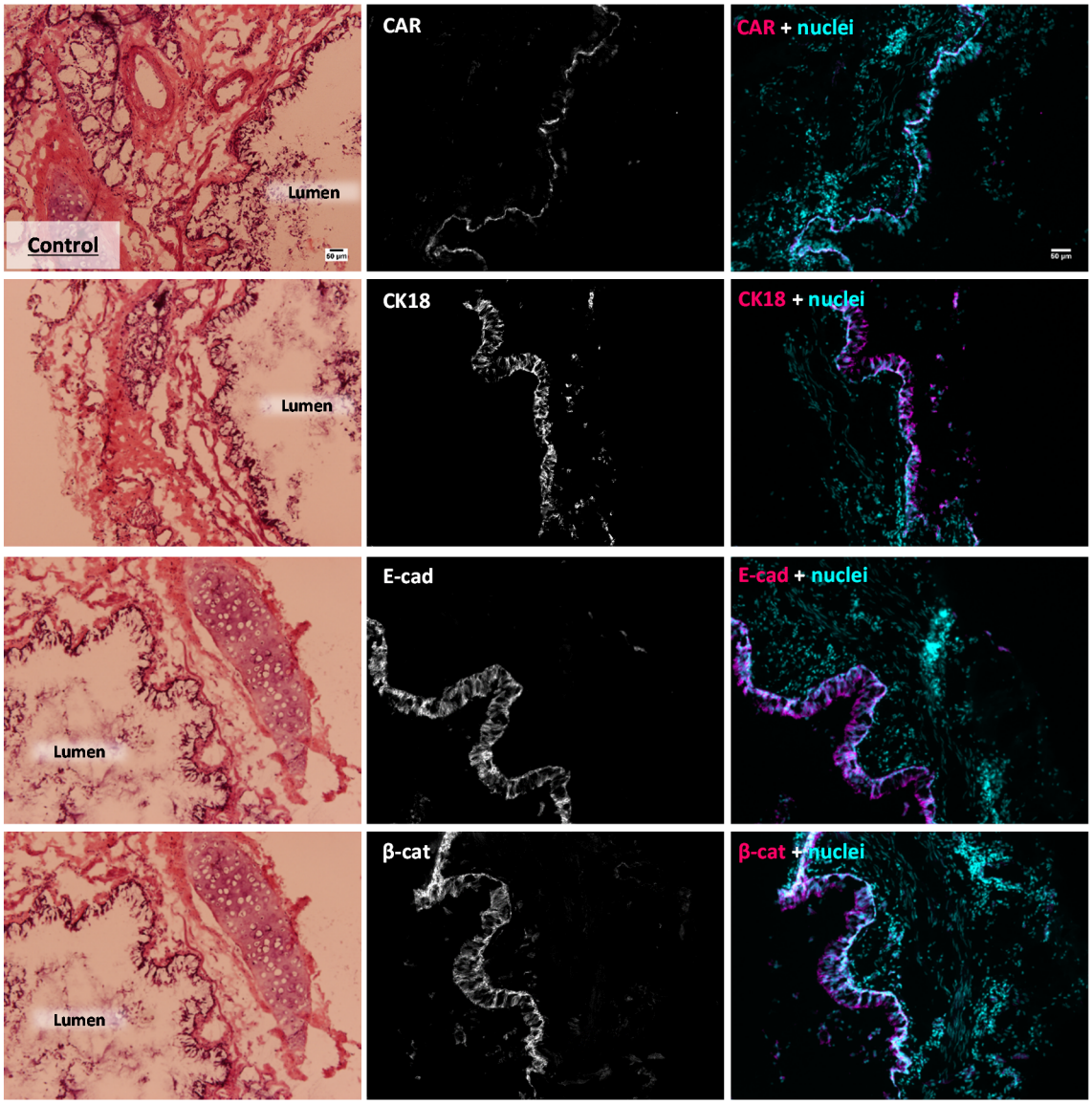

Figure 9 - Epithelial differentiation markers in the control epithelium. *Tissue was stained for CAR, CK18, E-cadherin and β-catenin. Nuclei were stained with DAPI. In merged pictures, nuclei are depicted in cyan and proteins in magenta. Scale bar represents 50 µm. H&E and fluorescence images were obtained from different section but with an equivalent morphology.*

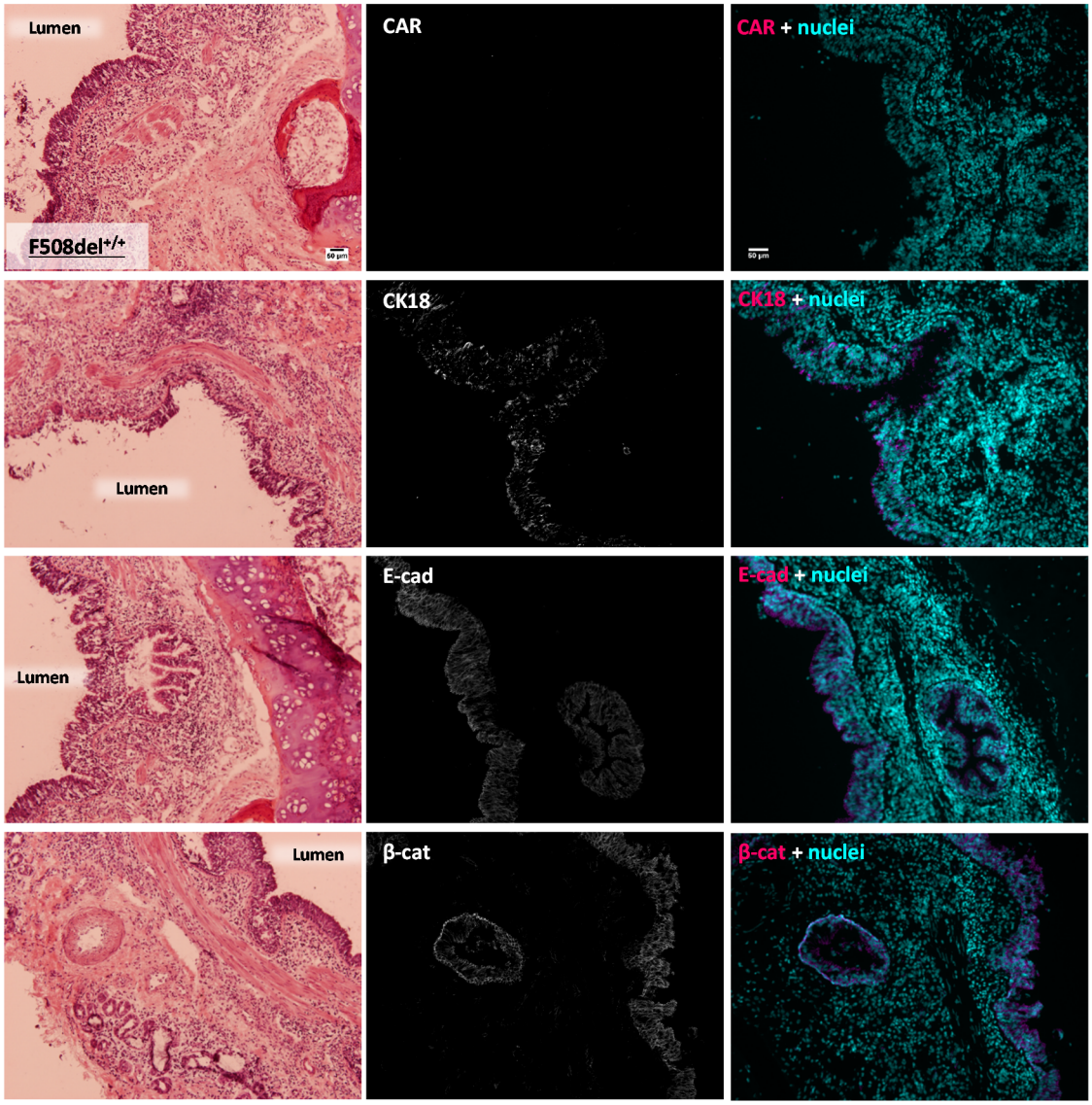

Figure 10 - Epithelial differentiation markers in the CF epithelium. *Tissue was stained for CAR, CK18, E-cadherin and β-catenin. Nuclei were stained with DAPI. In merged pictures, nuclei are depicted in cyan and proteins in magenta. Scale bar represents 50 µm. H&E and fluorescence images were obtained from different section but with an equivalent morphology.*

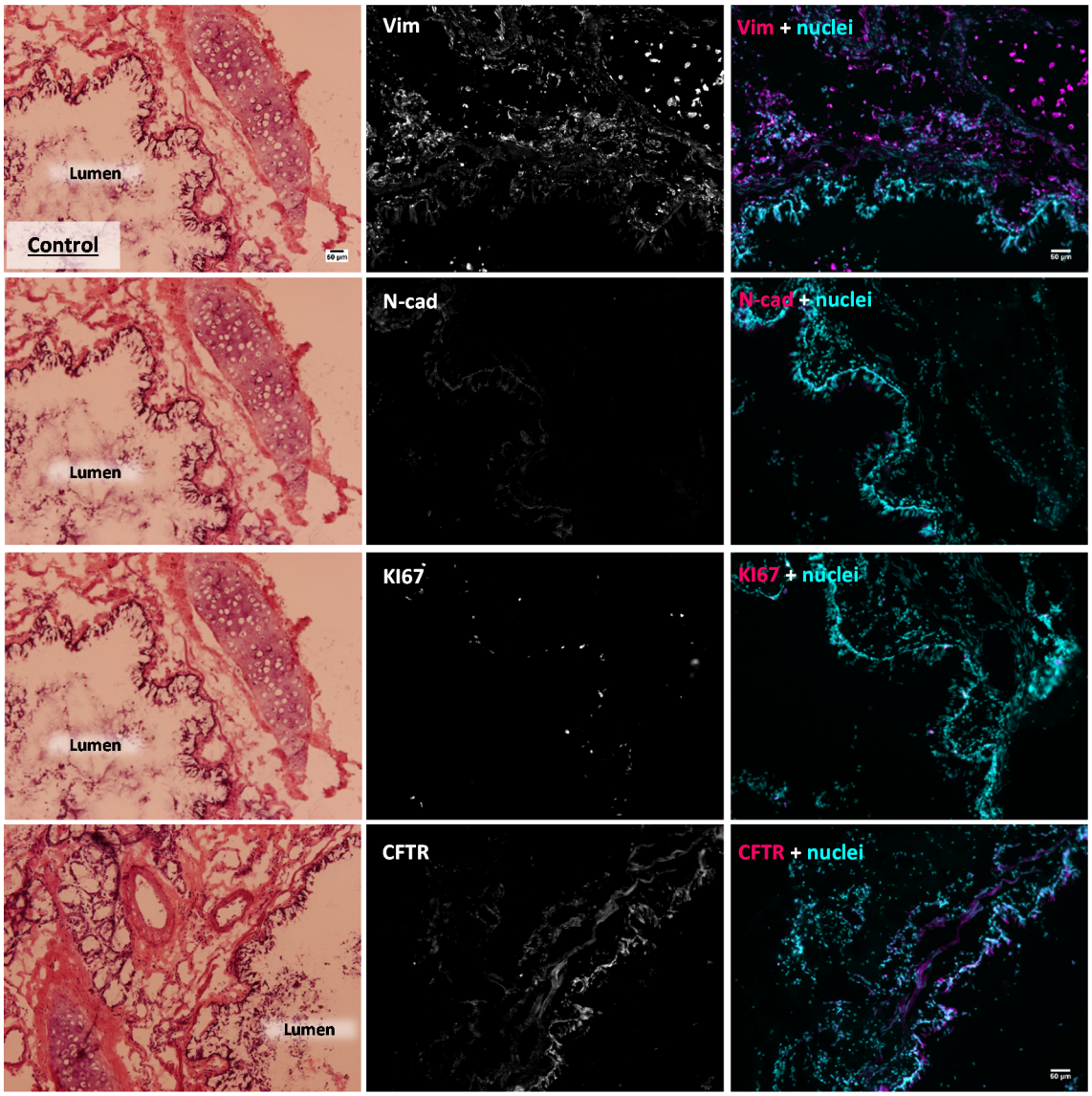

Figure 11 - Mesenchymal markers, proliferation marker and CFTR expression in the control epithelium. *Tissue was stained for vimentin, N-cadherin, KI67 and CFTR. Nuclei were stained with DAPI. In merged pictures, nuclei are depicted in cyan and proteins in magenta. Scale bar represents 50 µm. H&E and fluorescence images were obtained from different section but with an equivalent morphology.*

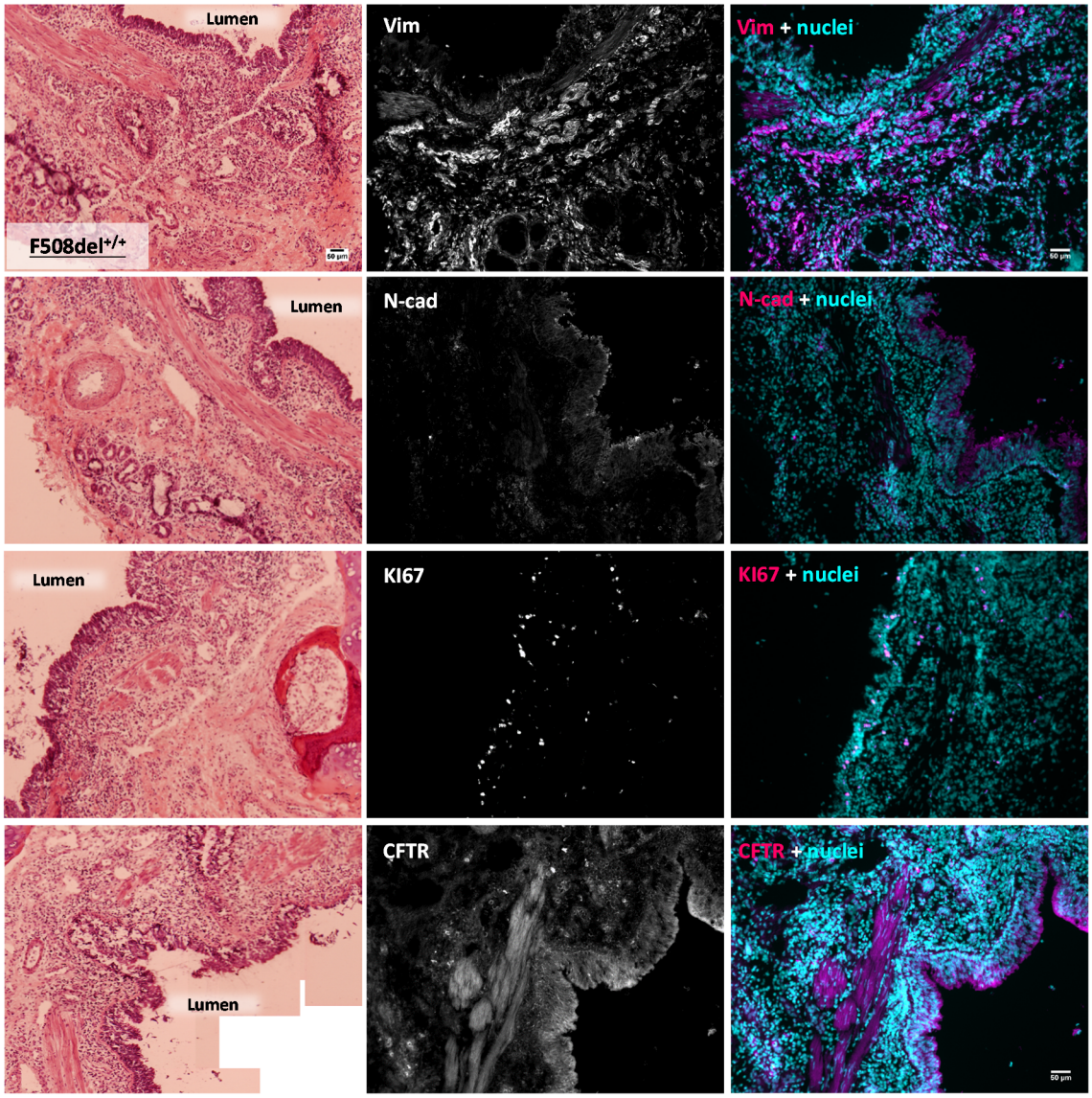

Figure 12 - Mesenchymal markers, proliferation marker and CFTR expression in the CF epithelium. *Tissue was stained for vimentin, N-cadherin, KI67 and CFTR. Nuclei were stained with DAPI. In merged pictures, nuclei are depicted in cyan and proteins in magenta. Scale bar represents 50 µm. H&E and fluorescence images were obtained from different section but with an equivalent morphology.*

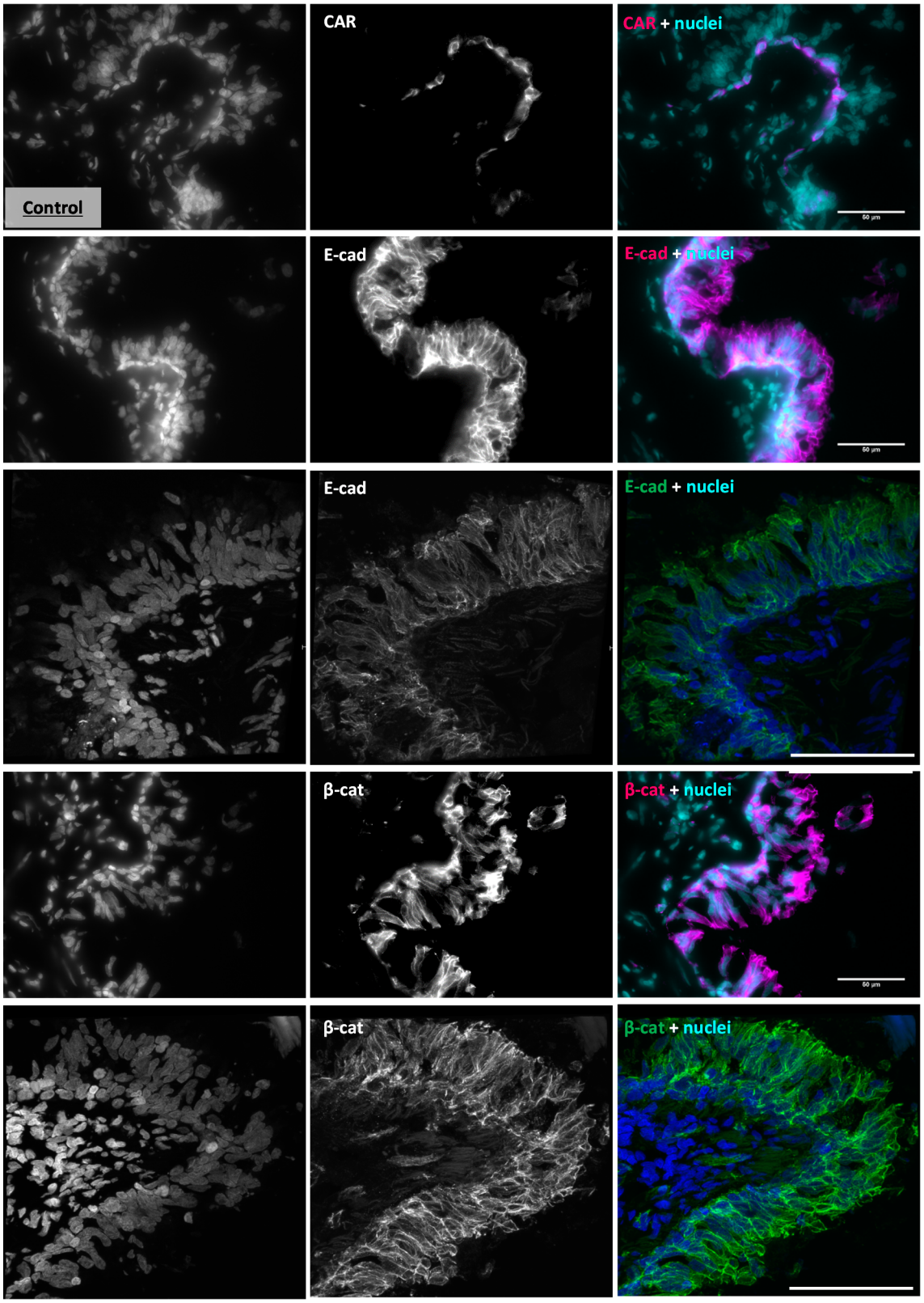

Figure 13 - Epithelial differentiation markers in the control epithelium (magnification). *Tissue was stained for CAR, E-cadherin and β-catenin. Nuclei were stained with DAPI or ToPro3. In merged pictures, nuclei are depicted in blue and proteins in magenta (widefield images) or green (confocal images). Scale bar represents 50 µm. Confocal images were kindly collected and edited by Luís Marques and are maximum intensity projections (MIPs).*

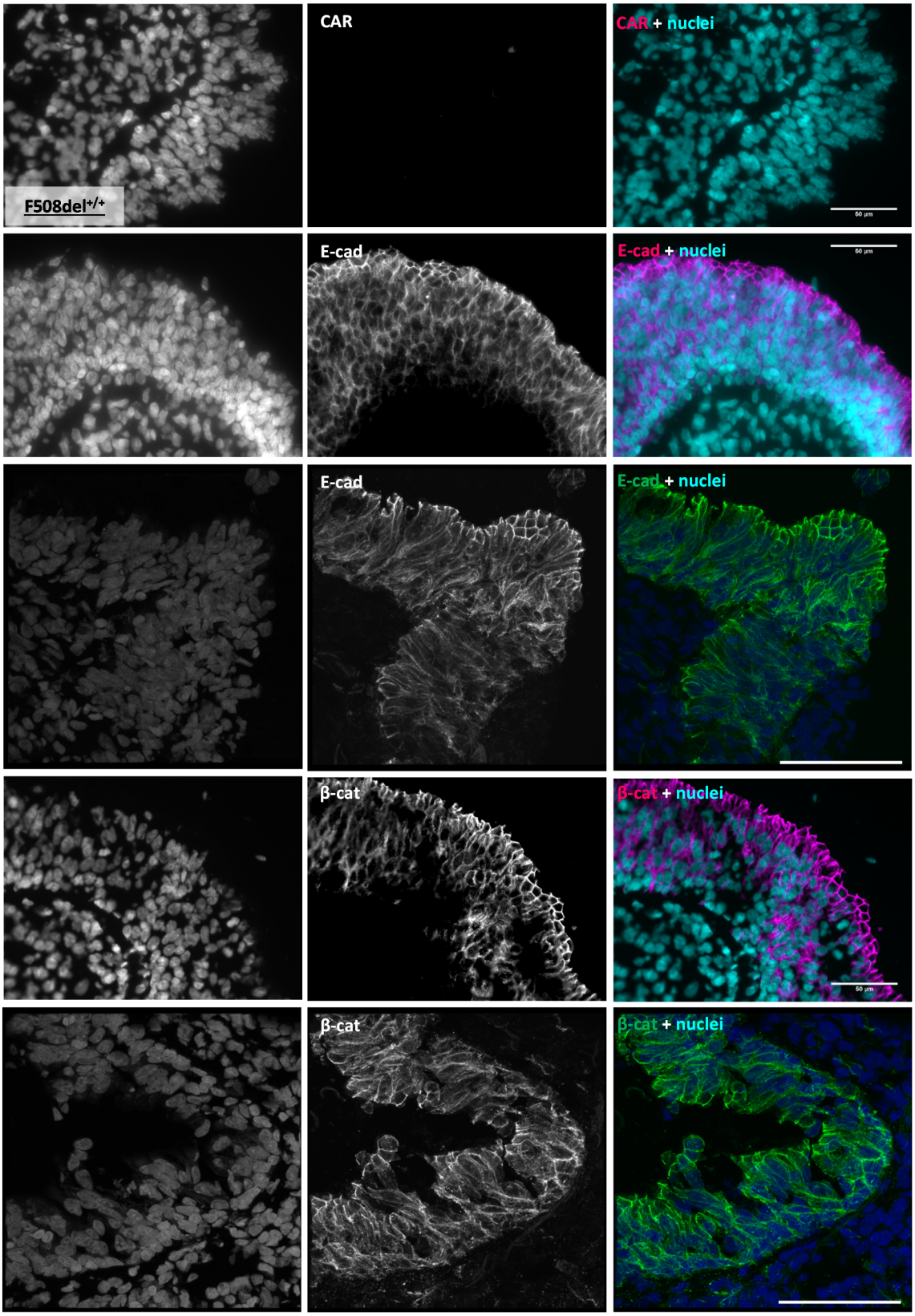

Figure 14 - Epithelial differentiation markers in the CF epithelium (magnification). *Tissue was stained for CAR, E-cadherin and β-catenin. Nuclei were stained with DAPI or ToPro3. In merged pictures, nuclei are depicted in blue and proteins in magenta (widefield images) or green (confocal images). Scale bar represents 50 µm. Confocal images were kindly collected and edited by Luís Marques and are maximum intensity projections (MIPs).*

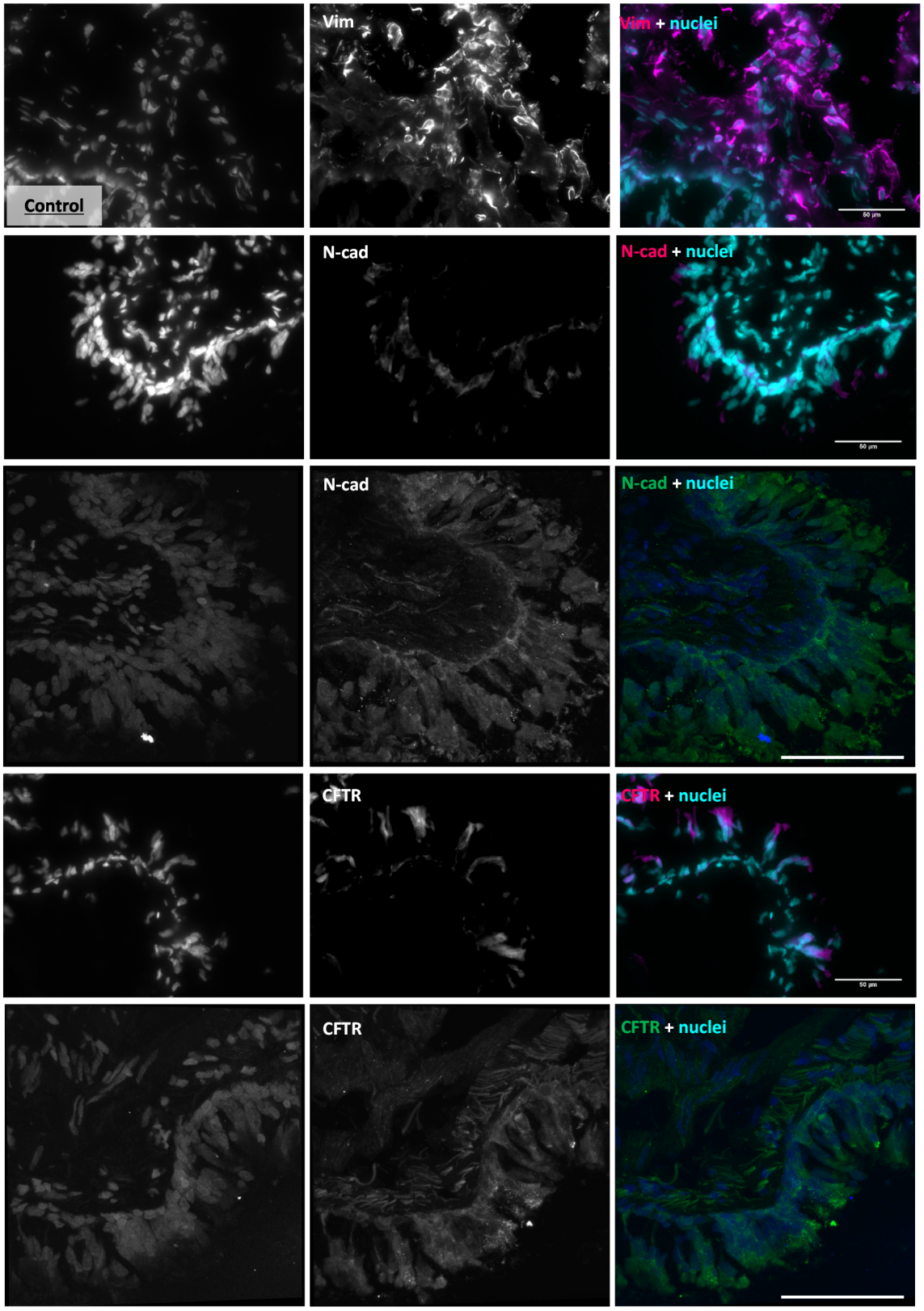

Figure 15 - Mesenchymal markers and CFTR in the control epithelium (magnification). *Tissue was stained for vimentin, N-cadherin and CFTR. Nuclei were stained with DAPI or ToPro3. In merged pictures, nuclei are depicted in cyan and proteins in magenta. Scale bar represents 50 µm. In merged pictures, nuclei are depicted in blue and proteins in magenta (widefield images) or green (confocal images). Scale bar represents 50 µm. Confocal images were kindly collected and edited by Luís Marques and are maximum intensity projections (MIPs).*

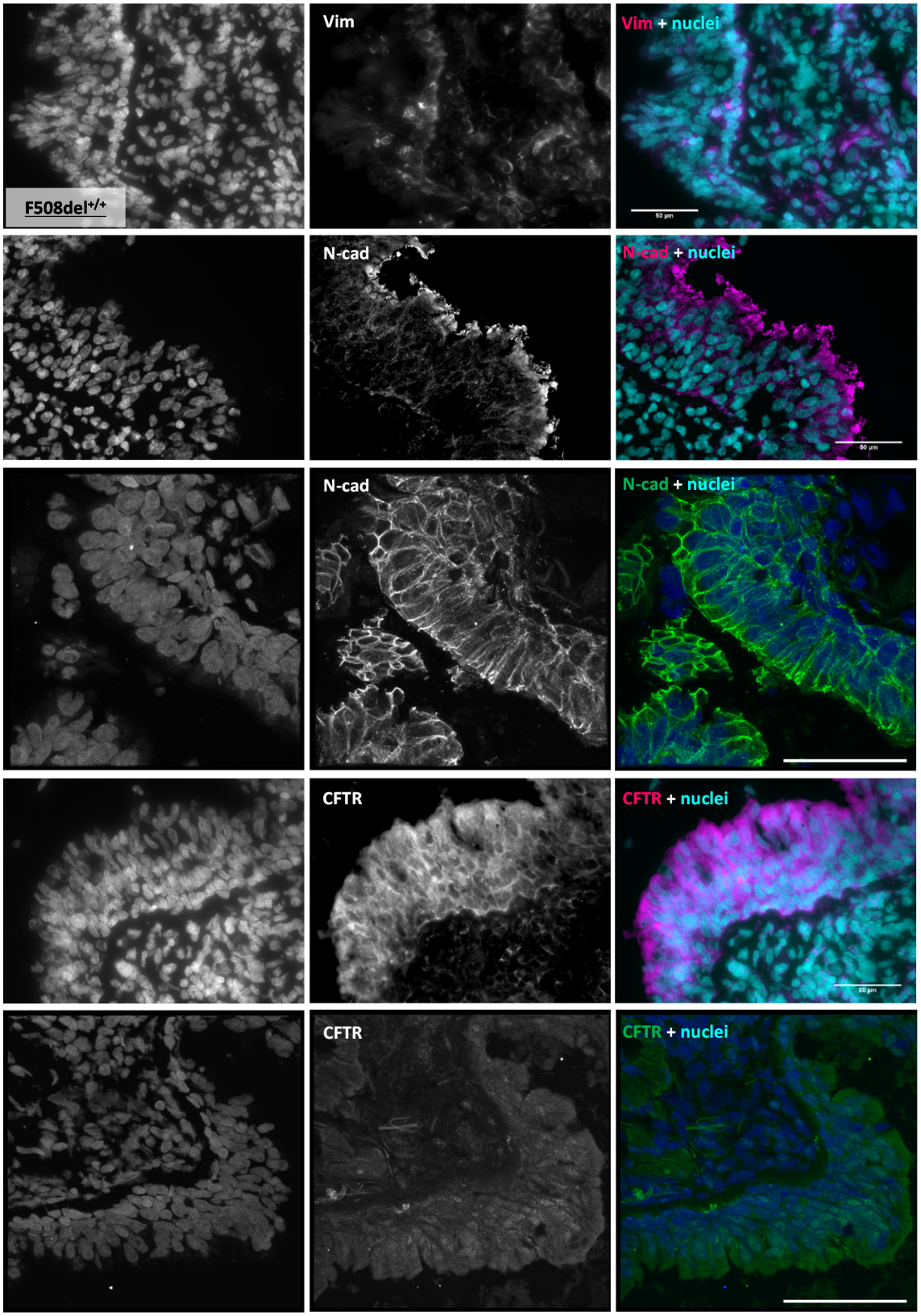

Figure 16 - Mesenchymal markers and CFTR in the CF epithelium (magnification). *Tissue was stained for vimentin, N-cadherin and CFTR. Nuclei were stained with DAPI or ToPro3. In merged pictures, nuclei are depicted in blue and proteins in magenta (widefield images) or green (confocal images). Scale bar represents 50 µm. Confocal images were kindly collected and edited by Luís Marques and are maximum intensity projections (MIPs).*

3.2. C/EBPβ expression in tissue and wt and F508del-CFTR CFBE cells

Since C/EBPβ has several roles in cellular differentiation and TGFβ signalling and since preliminary data suggests a role for C/EBPβ as F508del-CFTR traffic regulator in bronchial epithelial cells, the cellular localization of this transcription factor in control and CF bronchial tissue was determined.

Laser scanning microscopy was used to identify the subcellular localization of C/EBPβ in the bronchi. The results pointed to the nuclear localization that would be expected for a differentiation factor (Figure 17). The C/EBPβ fluorescence observed outside of the nuclei is likely to be nonspecific.

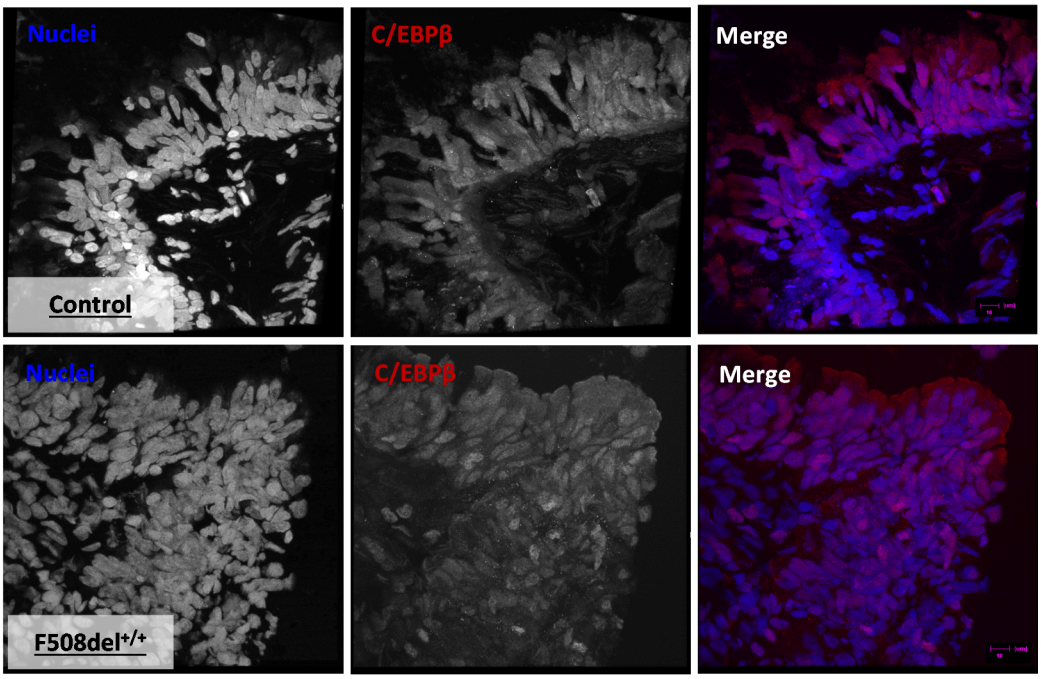

Figure 17 - Nuclear C/EBPβ expression in control and CF lung. *Nuclei were stained with ToPro3. In merged pictures, nuclei are depicted in blue and C/EBPβ in red. Scale bar represents 10 µm. These images were kindly collected and edited by Luís Marques and are maximum intensity projections (MIPs).*

Owing to the limited amount of bronchial tissue available, further characterization was performed using CFBE cell lines. Firstly, the ability of the cell lines to recapitulate the CFTR and C/EBPβ expression levels observed in tissues was validated. wt-CFTR cells showed a pronounced band C and some band B, whereas F508del-CFTR cells only exhibited a faint band B characteristic of immature CFTR (Figure 18A). This is in accordance with the findings in tissue and is also consistent with the literature[19].

As for C/EBPβ, LAP (the C/EBPβ transcriptional activator isoforms) protein expression was significantly increased in wt-CFTR compared to F508del-CFTR cells (figure 18A) and analysis of the mRNA levels confirmed this tendency with borderline significance (p=0.0579, Figure 18B). In addition to the reported LAP* and LAP isoforms another potential isoform was also consistently detected in the experiments [LAP (?)]. This is thought to be a different isoform and not an nonspecific band for two reasons: the presence of more than two start codons very close together in the region coding for the LAP isoforms (and the known leaky ribosome

scanning in C/EBPβ translation) and the fact that siRNAs targeting C/EBPβ eliminated the presence of this band (see below section 3.4). The LAP levels throughout this work were considered as the sum of all the LAP isoforms detected. Interestingly, in polarized cells, the levels of C/EBPβ LAP in F508del-CFTR cells increased and approached the levels in wt-CFTR cells (Figure 19). Due to the role of increased LIP (the C/EBPβ transcriptional inhibitor isoform) expression in cancer and its role in inhibiting LAP, its levels were also evaluated. However, this proved very challenging throughout the work. An analysis of the LAP:LIP ratio in wt and F508del-CFTR cells was performed (Figure 20). Since LAP is much more abundant than LIP, it is not possible to simultaneously detect both protein bands in a Western blot experiment. Therefore, the LAP:LIP ratio was measured using an indirect approach: the luminescence arising from LAP and LIP bands was measured at increasing exposure times and a linear fit was performed to the initial data points. The LAP:LIP ratio corresponds to the ratio of both slopes (Figure 20). For wt-CFTR cells, LAP was approximately 110 times increased compared to LIP, and for F508del-CFTR cells this ratio was approximately 96. This difference between wt and F508del-CFTR cells could potentially have implications in the pathology of CF disease. However, as the LIP expression is so reduced in these cells this can merely be a reflection of the differences in LAP levels.

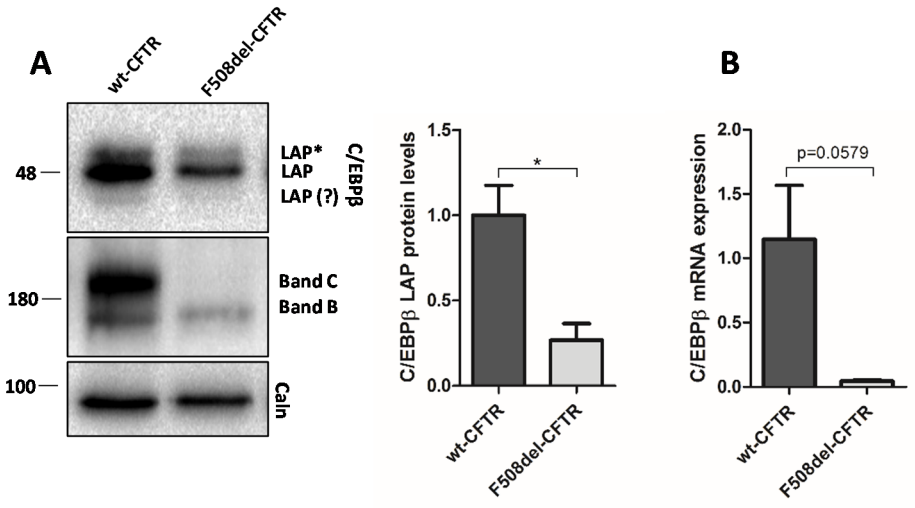

Figure 18 - A. CFTR and C/EBPβ LAP protein expression in CFBE wt and F508del-CFTR non-polarized cells. B. C/EBPβ mRNA expression in CFBE wt- and F508del-CFTR non-polarized cells. *Western blot and qPCR were performed to determine protein and mRNA levels (respectively). 10μg of protein were added per well. Significant differences were found for protein levels ($p<0.05$) and borderline significant differences ($p=0.0579$) for mRNA levels. (n=3)*

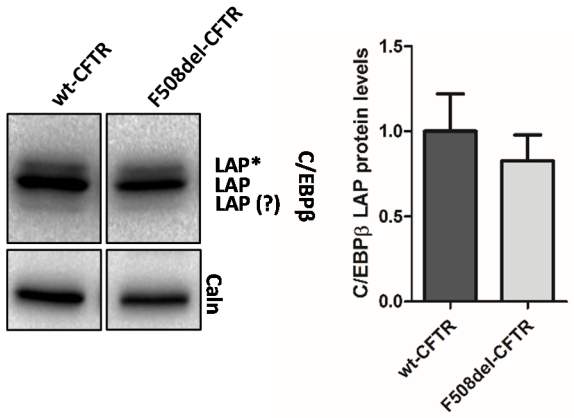

Figure 19 - C/EBPβ LAP protein expression in CFBE wt and F508del-CFTR polarized cells. *Western blot was performed to determine protein levels. 10µg of protein were added per well. These differences were not significant. (n=6)*

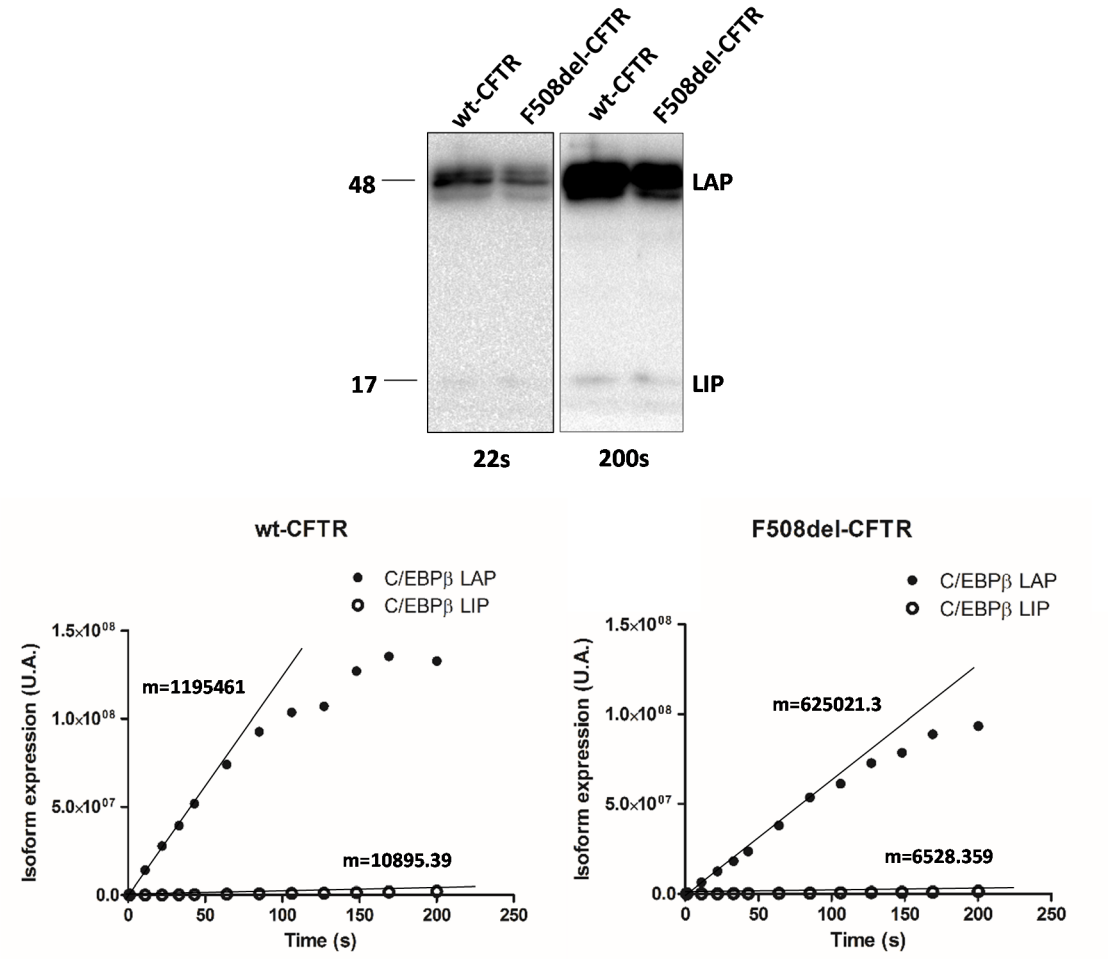

Figure 20 - C/EBPβ LAP and LIP differential expression with exposure time (s) for CFBE wt and F508del-CFTR cells. *Western blot was performed to determine protein levels. 20µg of protein were added per well. Linear regressions performed and slopes for each are represented. (n=1)*

Since C/EBPβ is a major differentiation factor in the lung, the fact that its expression is diminished in F508del-CFTR cells is consistent with the previous observations of this work that F508del-CFTR cells have a more undifferentiated phenotype. Accordingly, in the literature, the

decrease in LAP levels is usually attributed to carcinoma cells which have lost their differentiated phenotype. This is related to an increase in the LIP ratio[86,87] which has a dominant inhibitory effect in the activating isoform[77,78]. However, LIP levels were found to be severely reduced or even absent in most of the protein analysis performed in this work. Although the LIP expression is said to be decreased in relation to LAP, the LAP:LIP ratio was previously found to be 5:1[118], which is highly different from the present data. However, the expression may vary for different cell types. The 5:1 ratio was found in mammary mouse cells whereas the present work was performed in human bronchial epithelial cells. The reduced LIP expression in these cells does not necessarily mean that it is not present or exerting inhibitory effects. Even though the epitope recognized by the antibody used is the C-terminus of the protein (which is common to both LIP and LAP), most of the tests with this antibody (available on the product's website) emphasize the detection of the LAP isoform. It is possible that the antibody used has somehow increased specificity for the LAP isoform, especially if the antibody solution is used more than once (which it usually is) and in a concentration which is not high enough to recognize this isoform.

Interestingly, the C/EBPβ LAP levels were slightly increased in CFBE F508del-CFTR cells when these were polarized. This could be due to the fact that polarized cells have a more differentiated phenotype than non-polarized cells. A similar finding was observed for the CFTR protein by other authors, which saw that F508del-CFTR expression increased at the plasma membrane of polarized cell monolayers[60].

As CFBE mCherry-FLAG cells were also used in the present work, they were also characterized for their CFTR and C/EBPβ expression. As shown in Figure 21, these cells do not express CFTR unless they have been induced (with the addition of doxycycline). When they are, the expression pattern is similar to CFBE cells, except for an additional band in F508del-CFTR cells. This band is a result of alternative translation initiation (unpublished data, Inna Uliykina). Electrophysiological characterization has confirmed an expected CFTR response for these cells[107]. LIP was not found in these cells. As for C/EBPβ LAP expression, it followed the previous observations, with a decreased expression for the F508del-CFTR cells. LAP levels seem to be increased in cells were CFTR expression was not induced (versus the corresponding induced cells), although the difference was not statistically significant.

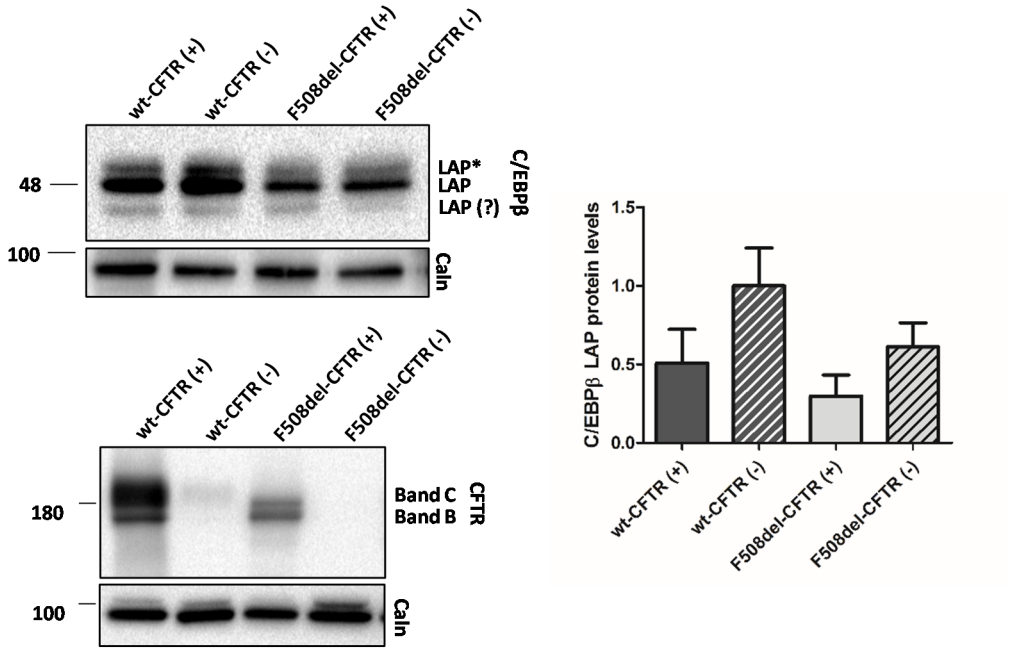

Figure 21 - C/EBPβ LAP expression in CFBE mCherry FLAG wt- and F508del-CFTR cells. *Western blot was performed to determine protein levels. 10µg of protein were added per well. No significant differences were found (n=3)*

3.3. C/EBPβ and CFTR protein interaction

Since one of the main goals of the present work was to elucidate a possible relationship between C/EBPβ and CFTR, a co-IP was performed to check for interactions between the two proteins. Although for the whole cell lysate C/EBPβ was present in all the samples, C/EBPβ and CFTR did not co-immunoprecipitate (Figure 22, left). Accordingly, CFTR also did not co-immunoprecipitate with C/EBPβ (Figure 22, right).

These results show that C/EBPβ and CFTR do not bind at protein level. However, an interaction may still exist at the DNA level, since it has been previously reported that the CFTR promoter possesses a CCAAT-enhancer binding protein (C/EBP) binding site[119]. Another possible scenario is that C/EBPβ interacts with other genes that regulate CFTR. A chromatin IP (ChIP) assay, which could elucidate these hypotheses, was beyond the scope of this work.

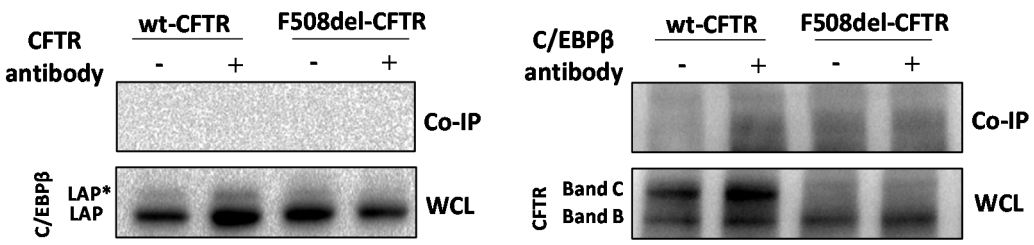

Figure 22 - Co-IP results. *On the left, C/EBPβ was not detected with co-IP with anti-CFTR; on the right CFTR was also not detected with co-IP with anti-C/EBPβ. Proteins were detected on WCL. 20µL of protein were added per well for the WCL and 40µL of protein were added per well for the co-IP. (n=2)*

3.4. Effect of C/EBPβ knockdown on CFTR levels

Since in many pathological contexts C/EBPβ expression is reduced, siRNA assays were performed in order to determine the effect of C/EBPβ knockdown on CFTR expression. Protein levels were assessed by immunofluorescence and Western blot assays. CFBE mCherry-FLAG cells were used in order to assess the total levels of CFTR and the levels of CFTR at the plasma membrane (PM CFTR) in the immunofluorescence assay. Since C/EBPβ isoforms are originated by leaky ribosome scanning and the use of alternative use of multiple translation initiation codons in the same mRNA[77], the C/EBPβ mRNA was targeted with a pool of two siRNAs, targeting either the 5'-UTR mRNA region or the 3' region (see Appendices, Figure 34). With this approach it was expected to knockdown both LAP and LIP isoforms.

As shown in Figure 23B, immunofluorescence analysis revealed a knockdown rate of approximately 20% for wt cells and 35% for F508del-CFTR cells (which represented a significant difference). This resulted in an increase in total CFTR in both wt and F508del-CFTR cells but a slight decrease in plasma membrane wt-CFTR (all with borderline significance). No effect in plasma membrane CFTR was observed in F508del-CFTR cells. This result is consistent with an impairment in wt-CFTR traffic when C/EBPβ is knocked down. Thus, according to these findings, knocking down C/EBPβ not only did not rescue F508del-CFTR [as had been previously found in an F508del-CFTR traffic screen (unpublished data, Hugo M. Botelho)] but also decreased the amount of wt-CFTR at the plasma membrane. This quantitative analysis seems to be in accordance with what is observed in the images in Figure 23A.

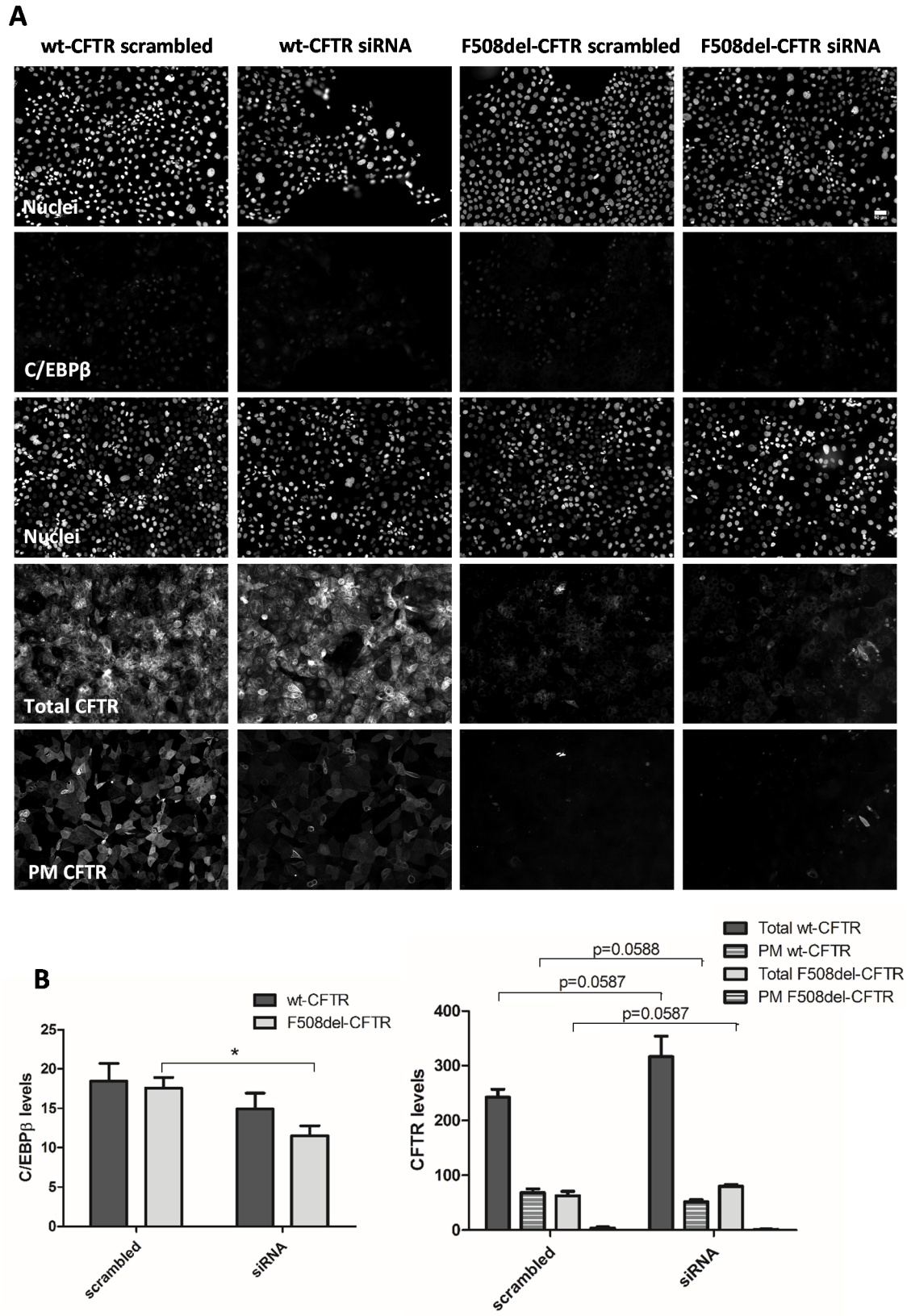

Figure 23 – A. Immunofluorescence assessment of C/EBPβ, total CFTR and plasma membrane (PM) CFTR in CFBE mCherry FLAG cells, upon treatment with C/EBPβ siRNAs. *Antibodies for C/EBPβ and FLAG were used for cell staining. Nuclei were stained with Hoechst. Scale bar represents 50 µm.* ***B. Quantification of the immunofluorescence data.*** *C/EBPβ and CFTR (total and PM) expression were analysed. Differences were significant ($p<0.05$) for C/EBPβ levels (in F508de-CFTR cells) and borderline significant ($p=0.0587$, $p=0.0588$) for total CFTR (both cell lines) and PM CFTR (wt-CFTR cells). (n=2, images analysed per assay=5).*

Western blot was also performed in parallel with the immunofluorescence assay to attempt further confirmation of results (Figure 24). This analysis showed no significant differences in C/EBPβ LAP expression or, as a consequence, on CFTR expression, which was surprising since the siRNA, cells seeded and volume ratio were similar in the two assays. However, the C/EBPβ expression pattern, as measured by immunofluorescence, is heterogeneous in the cellular population. Recent studies in pluripotent cells have shown that heterogeneous transcription factor gene expression is present, being linked to differences in the propensity of individual cells either to self-renew or commit towards differentiation. This heterogeneity may arise from different modes of transcriptional regulation as well as post-transcriptional events such as protein synthesis. Although pluripotent cells are a very different model from CFBE cells, the authors argue that this heterogeneity could be present in other systems and that finding its molecular basis is important[120]. Hence, individual cell C/EBPβ expression is an important aspect to consider, especially in siRNA assays, where although some cells were affected by the knockdown, others retained full expression of the protein. In the quantitative analysis of the immunofluorescence assay, individual cells and their protein expression levels were evaluated, which is a sensitive method of analysis. However in Western blot an ensemble of all the cells was used for protein level assessment, which could dilute the effects of the siRNA, especially if only a small fraction of the cells was affected by the knockdown (which is what was observed in the immunofluorescence assay). Once again, LIP expression was absent (results not shown). As previously mentioned (in section 3.2), the LAP (?) band disappeared with the addition of siRNAs which suggests that this band represents a LAP isoform instead of a nonspecific band.

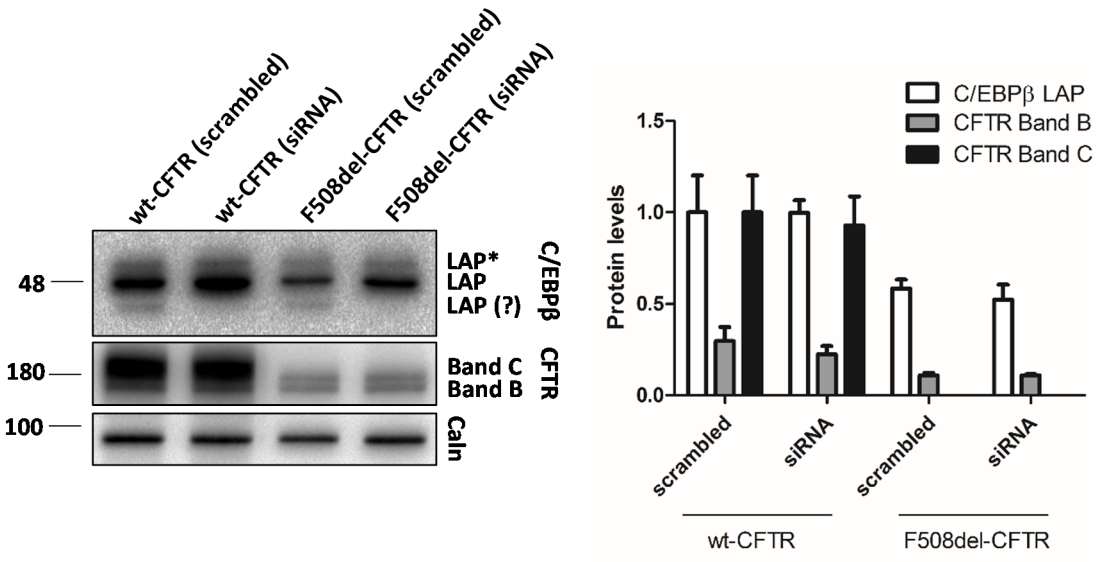

Figure 24 - Assessment of C/EBPβ LAP and CFTR protein levels upon treatment with C/EBPβ siRNAs. *Western blot was performed to determine protein levels.10μg of protein were added per well. No significant differences were observable. (n=3)*

Hence for this set of experiments it can concluded that immunofluorescence is a more sensitive way to determine knockdown effects, at least for C/EBPβ. It has the additional advantage of allowing (with these particular cells) for the detection of PM CFTR, which can provide useful information about the traffic of CFTR and which proteins affect it. Additionally,

it should be interesting to evaluate the separate effects of both siRNAs, in order to determine the individual contributions of the LAP and LIP isoforms for CFTR expression. Since LIP expression is reduced in these cells (expression was not found via Western blot) it was probably the LAP knockdown which resulted in the reduction in PM CFTR in wt cells. Accordingly, if only LIP were to be knocked down, this would potentially increase the LAP levels, which could have beneficial effects on the rescue of F508del-CFTR to the plasma membrane. Interestingly, the siRNA used in the screen where C/EBPβ was a primary hit targeted the LIP region of the C/EBPβ mRNA, which is further in agreement with this hypothesis.

Even though RNAi is a powerful tool to study the biological role of individual genes, it does not provide full mRNA silencing. So, in order to improve the C/EBPβ knockdown, the CRISPR system was used to generate C/EBPβ knockout cells. Such cells would not express C/EBPβ at all and, therefore, the roles of this protein in the overall dysfunction that occurs in CF – including in epithelial differentiation – could thereby be more clearly identified.

Knockout efficiency was evaluated by assessing C/EBPβ levels of CRISPR clones by Western blot. Since C/EBPβ is a differentiation factor, the cell confluence at the time the samples were collected, and the time that cells were kept in culture (which varied between clones) can influence the differentiation level and hence C/EBPβ expression. It is generally accepted that effects of monolayer culture on cell differentiation depend on a number of factors, including time in culture and confluence. Arguably, both time and confluence play an important role in cell communication and thus in differentiation, possibly affecting C/EBPβ expression. A study in Caco-2 cells (human epithelial colorectal adenocarcinoma cells) observed that cell growing density was at least partially responsible for the problems of reproducibility in the experiments performed on this cell line. The degree of cell confluence was also found to influence the cells' differentiation properties[121]. All the cells were collected when 100% confluence was achieved. At this confluence, CFBE cells can start to spontaneously differentiate, even in monolayers. This could affect the C/EBPβ levels, *e.g.* increasing them. Additionally, to avoid degradation, protein extracts were stored at -80ºC before analysis.

After normalization against the calnexin band, at least one of the clones (wt 6, Figure 25B) seemed to be a knockdown (C/EBPβ LAP levels were about 50% decreased compared to control). In this clone in particular, the reduction in LAP levels led to a high increase in CFTR expression. This is consistent with the previous findings, where C/EBPβ knockdown increased the total amount of CFTR. On the F508del-CFTR clones, clone 43 and 44 (which showed a slightly decreased LAP expression, Figure 25A) also demonstrated an increase in CFTR compared to control. However, clone 55, for example, seemed to have an increased CFTR expression with no knockdown of C/EBPβ, so this relationship was not completely straightforward in the CRISPR clones. Consistently, some of the clones where C/EBPβ LAP seemed to be overexpressed in relation to the control levels (clones 29, 46, 55 and 56, Figure 25A) were probably samples where a higher confluence and differentiation was present (as explained above).

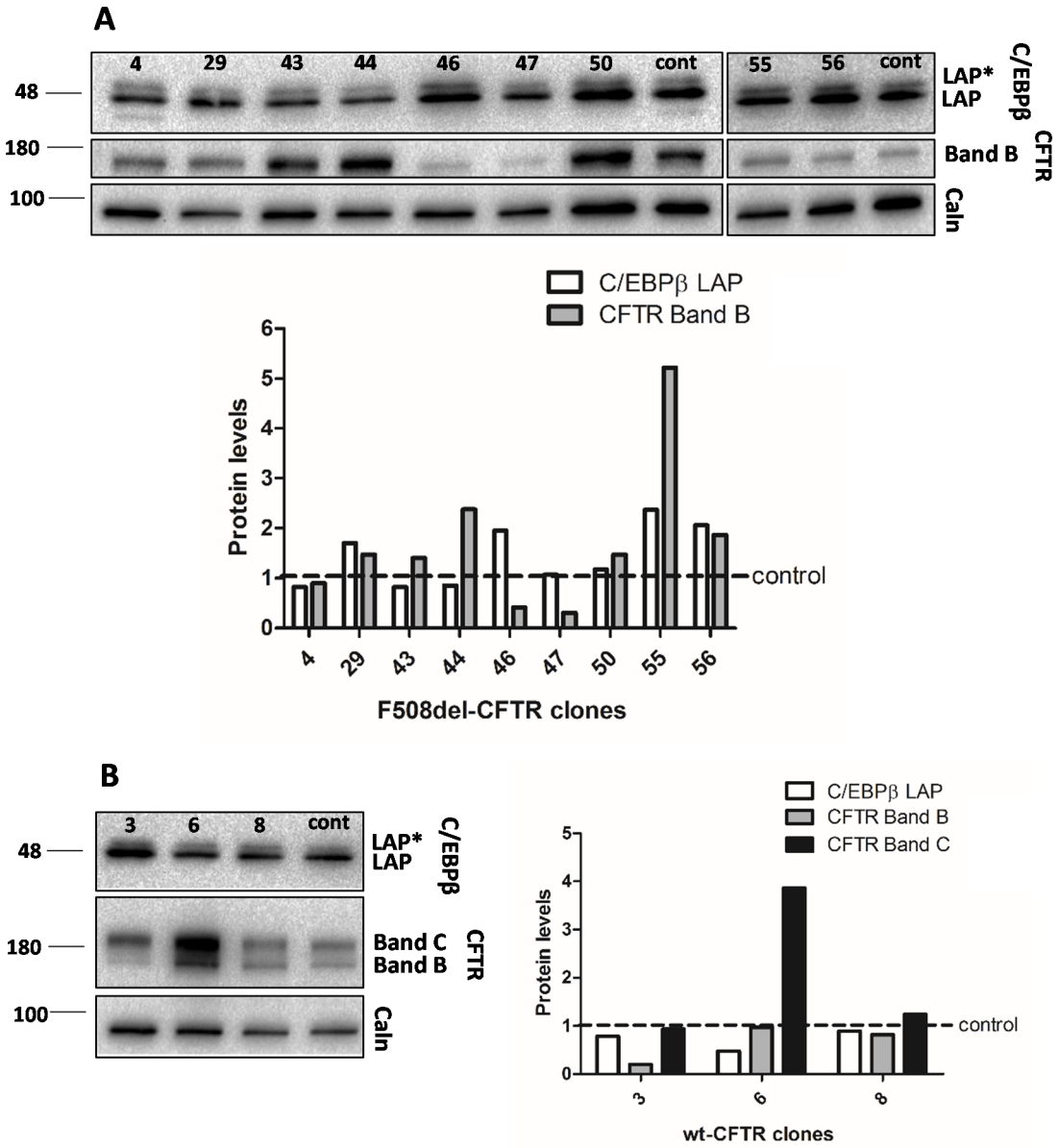

Figure 25 – A. Protein analysis of C/EBPβ LAP and CFTR levels for F508del-CFTR CRISPR clones. B. Protein analysis of C/EBPβ LAP and CFTR levels for wt-CFTR CRISPR clones. *Western blot was performed to determine protein levels. 40µL of protein were added per well. (n=1)*

This results of this experiment demonstrate the need for standardizing the culture conditions when analysing C/EBPβ expression in these. Further experiments are required to generate the knockout cell lines. This could be improved by using, for example, cell sorting methods to separate transfected cells from non-transfected cells. This is possible due to the GFP tag present in the Cas9 vector. Since the transfection rate is very low in CFBE cells, this approach could help to select clones where plasmid uptake was efficient. This would also eliminate the need to use the hygromycin resistance plasmid as a selection marker. Since the CRISPR system needed uptake of all three plasmids to succeed, some of the problems found in this work could be due to the uptake of the hygromycin resistance plasmid but not of the gRNA

and Cas9 plasmids. Hence the clone populations would survive but no genome editing would actually occurred.

In addition, it would be beneficial to extract gDNA from the clones to assess the differences made by the CRISPR system in the C/EBPβ gene. gDNA from CFBE wt and F508del-CFTR cells was extracted and analysed but this showed no productive results (data not shown). This analysis is difficult due to the high GC content of the C/EBPβ gene as well as at least 50% homology with other genes, which are more highly expressed in these cells. In the future, a suitable pair of primers should be designed in order to successfully amplify the C/EBPβ gene region and evaluate correctly the modifications produced by the CRISPR system in these cells.

3.5. Effect of TGFβ on epithelial differentiation and levels of C/EBPβ and CFTR in polarized CFBE cells

In this part of the work, it was sought to investigate the differentiation status in polarized CFBE cells expressing wt or F508del-CFTR and its regulation by TGFβ1. The effects on epithelial differentiation were firstly evaluated by measuring the transepithelial electric resistance (TEER) in the absence of TGFβ1. These measurements are generally accepted as an indirect measure of formation of tight junctions and are often used as a marker of disruption of the epithelial layer. Accordingly, they have proved helpful in assessing the differentiation status of human bronchial epithelial cell culture systems[122].

In Figure 26 are represented the TEER measurements for wt-CFTR and F508del-CFTR epithelia in the days preceding TGFβ addition. Interestingly, differentiation seemed to be impaired in the F508del-CFTR cells; their TEER measurements were always lower than wt-CFTR's for the same time point. This is consistent with the delay in differentiation previously reported by other authors, who found that after epithelial remodelling, while 80% of non-CF epithelial grafts were covered by well-differentiated epithelium, only 18.7% was observed for CF grafts[62].

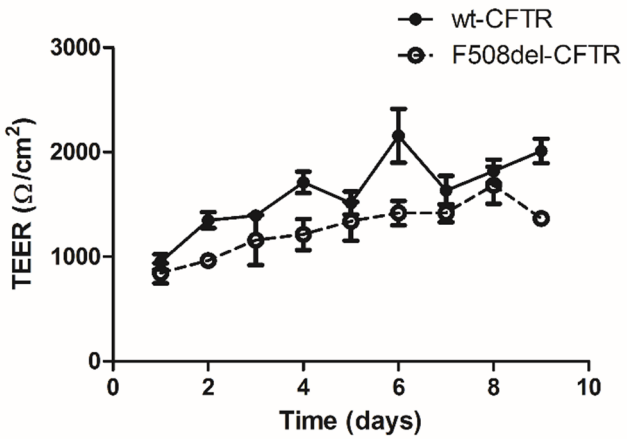

Figure 26 - TEER measurements in the days prior to TGFβ induction for wt and F508del-CFTR polarized CFBE cells. *(n=4)*

It was then analysed how exposure to TGFβ1 modulated the transepithelial electrical resistance (Figure 27). Upon TGFβ addition a reduction in the TEER levels was noticeable after 24h, becoming more pronounced with 48h exposure. Interestingly, this response was differential in wt and F508del-CFTR cells. In wt cells, at 24h, the decrease in TEER levels had only decreased slightly; this effect became more pronounced with continuous exposure to TGFβ. In F508del-CFTR on the other hand, a steady decrease in TEER was observable throughout time. Consistently, the final TEER level was significantly more reduced in F508del-CFTR cells compared to wt, suggesting that the CFTR defect somehow increases the sensitivity of these cells to the TGFβ treatment.

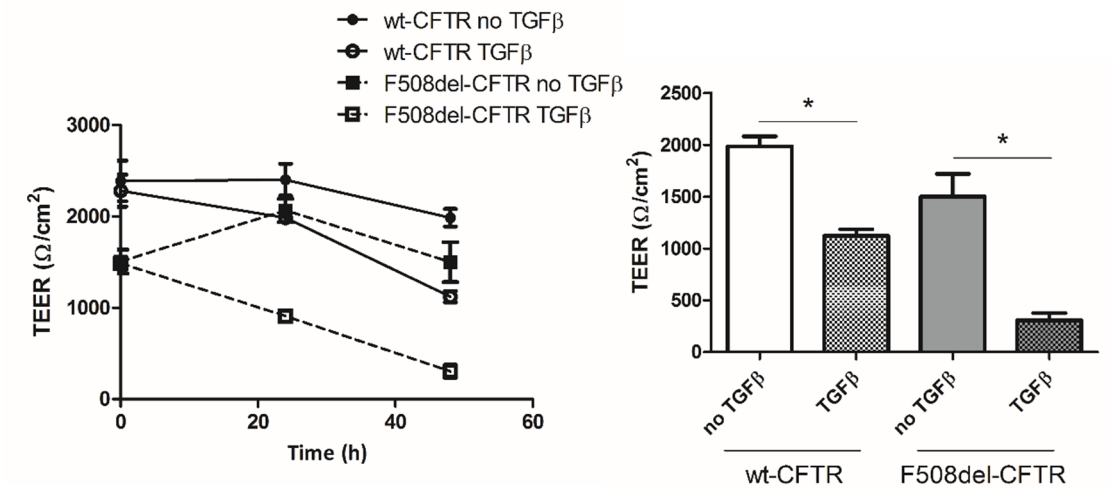

***Figure 27 - TEER values upon TGFβ addition**. Differences at 48h between the TEER of cells without TGFβ compared to cell treated with TGFβ were significant (p<0.05) for both cell types. (n=4)*

These results were validated by analysing the expression of E-cadherin – a major agent of epithelial tightness, which is lost during EMT - in wt and F508del-CFTR cells before and after 48h exposure to TGFβ using laser scanning microscopy. This approach allowed accurate mapping of the subcellular distribution of E-cadherin throughout the polarized epithelial monolayer. At 0h E-cadherin expression was high (Figure 28A) consistent with that seen on tissue, and the protein localized to cell-cell junctions, on the lateral sides of the polarized cells (Figure 28C). For F508del-CFTR cells, E-cadherin's expression was more reduced (Figure 28E) and localized around the cells, without apical/basal distinction (Figure 28G). This was in agreement with the reduced TEER observed for these cells and their impairment in differentiation. After 48h TGFβ incubation, E-cadherin expression was reduced for both cell types (Figure 28B and 28D and 28F and 28H). This was consistent with the EMT-inducing role of TGFβ.

The dual role of TGFβ in cells has received a lot of interest from researchers. Although TGFβ can cause epithelial cells to undergo growth arrest and apoptosis, it can also induce EMT and mediate fibroblast activation[123]. It is commonly accepted that in healthy cells, TGFβ acts as an inhibitor of cellular proliferation. However in abnormal cells (such as cancer cells), this response is lost and there is a shift from growth inhibition to promotion. These cells can then use the TGFβ signalling to their own advantage. Increases in TGFβ signalling are common in invasive cancer cells, which use this pathway to promote angiogenesis, supress the immune

system responses and increase interaction with the extracellular matrix (ECM). This is known as a biphasic role of TGFβ[124]. Accordingly, a shift in the normal anti-inflammatory response of TGFβ to a pro-inflammatory one can also be observed in disease. In the present work, the continuous stimulation with TGFβ had harmful effects consistent with said shift in the inflammatory TGFβ response and promotion of EMT. This is probably due to the fact that 48h stimulation mimics a pathological setting of chronic inflammation. Since both exacerbated inflammation and increased TGFβ levels have been reported in CF patients, partly due to the presence of polymorphisms which increase TGFβ signalling (see introduction), this TGFβ stimulation is potentially a good model for the environment in CF lung. Hence, the results are in agreement with increased TGFβ signalling in the setting of chronic inflammation, which could be potentially inducing (or helping to induce) EMT in the lung of CF patients. Interestingly, this inflammation was enough to cause distress to wt cells as well as F508del-CFTR cells. This could mean that dysregulated inflammation is in itself sufficient to induce EMT. Whether the defect in CFTR also plays a direct role in EMT or in mediating the inflammatory response that causes it is an issue that needs to be addressed for a better understanding of the pathology of CF lung disease.

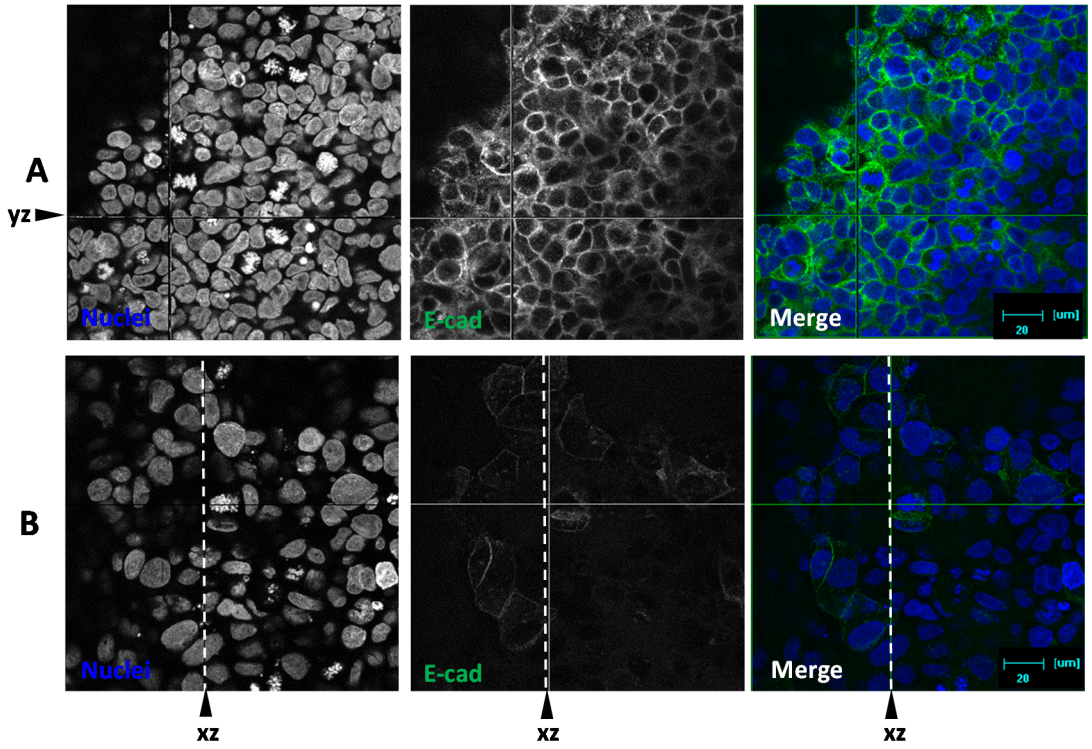
A
yz
Nuclei
E-cad
Merge
20
[um]
B
Nuclei
E-cad
Merge
20
[um]
xz
xz
xz

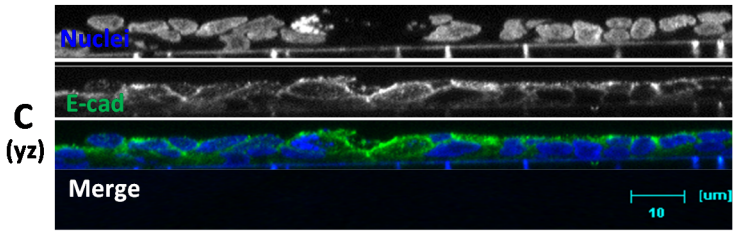
C
(yz)
Nuclei
E-cad
Merge
10
[um]

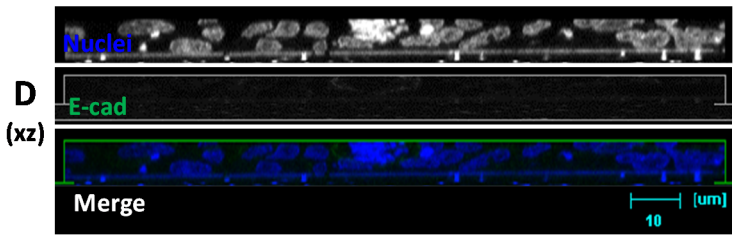
D
(xz)
Nuclei
E-cad
Merge
10
[um]

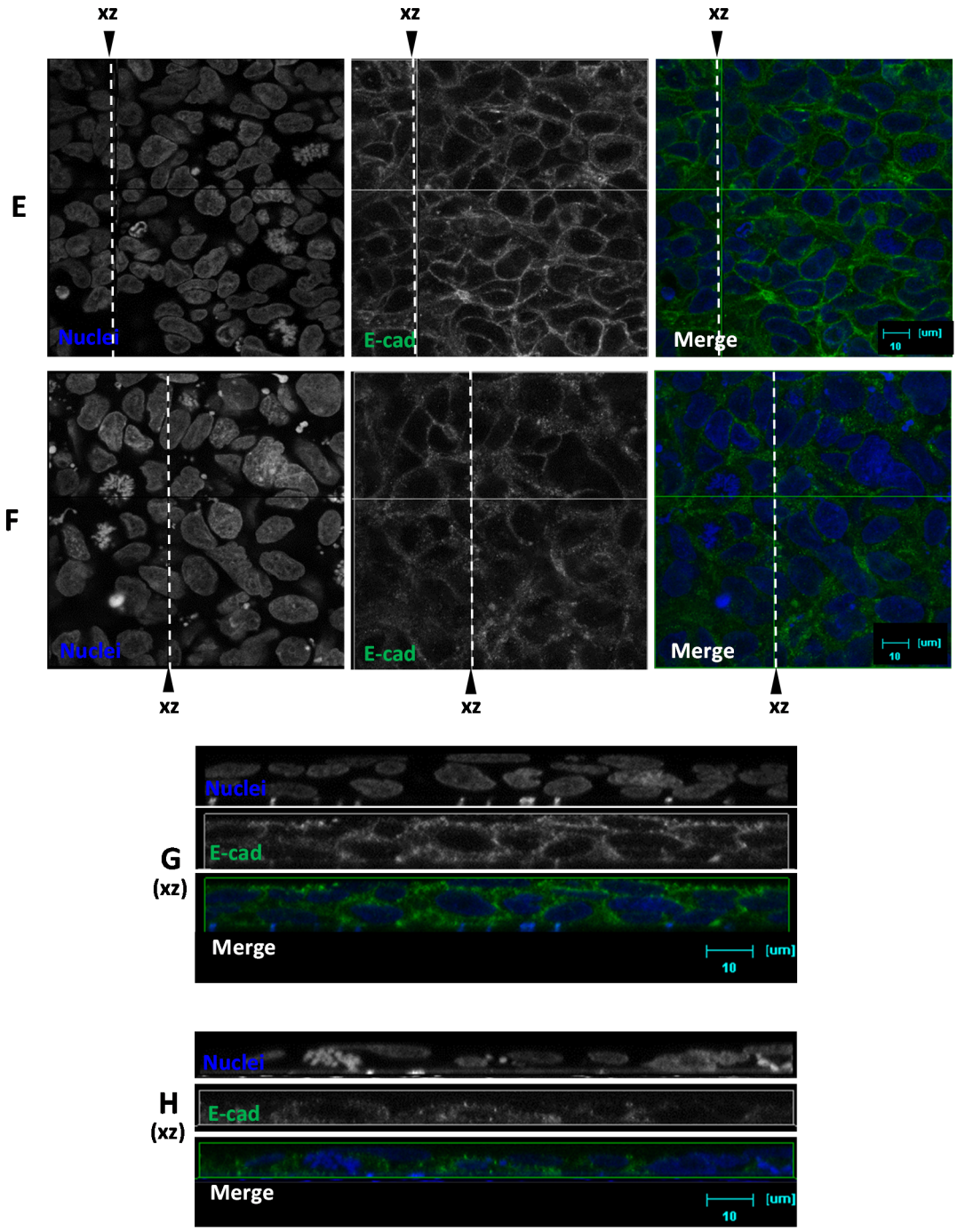

Figure 28 - E-cadherin expression levels in wt and F508del-CFTR cells without TGFβ addition and after 48h of TGFβ presence. *A. xy representation of wt-CFTR polarized cells without TGFβ addition. B. xy representation of wt-CFTR polarized cells with TGFβ addition for 48h. C. yz representation of wt-CFTR polarized cells without TGFβ addition. D. xz representation of wt-CFTR polarized cells with TGFβ addition for 48h. E. xy representation of F508del-CFTR polarized cells without TGFβ addition. F. xy representation of F508del-CFTR polarized cells with TGFβ addition for 48h. G. xz representation of F508del-CFTR polarized cells without TGFβ addition. H. xz representation of F508del-CFTR polarized cells with TGFβ addition for 48h. Polarized cells were stained for E-cadherin. Nuclei were stained with ToPro3. In merged pictures, nuclei are depicted in blue and E-cadherin in green. Scale bar represents 20 µm (A. and B.) or 10 µm (remaining panels). These images were kindly collected and edited by Luís Marques.*

C/EBPβ and CFTR protein levels were also analysed in the context of TGFβ stimulation (Figure 29). For both wt and F508del-CFTR cells, C/EBPβ LAP levels peaked after 24h of induction with TGFβ and decreased at 48h. For F508del-CFTR cells, the levels at 48h were lower than the initial value. In this assay, LIP expression could be evaluated, although it was only present in two of the four replicates. Its expression was elevated in F508del-CFTR cells compared to wt-CFTR cells, where it followed the LAP expression pattern, increasing at 24h – where both isoforms were almost equally abundant - and then decreasing at 48h. In wt-CFTR cells, on the other hand, an increase in LIP levels was still observed at 48h. As for CFTR expression, no significant alterations were observed in the F508del-CFTR cells whereas in wt-CFTR cells the CFTR expression significantly increased with continuous TGFβ exposure.

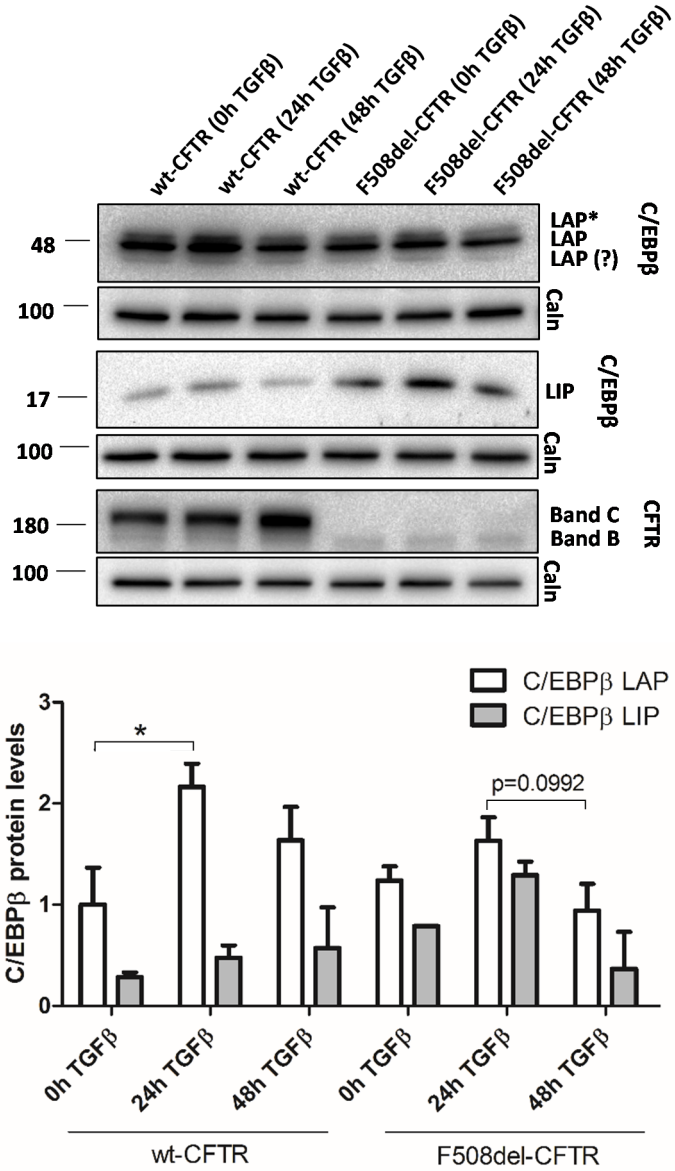

Figure 29 - C/EBPβ and CFTR protein levels in the context of TGFβ stimulation (0h, 24h, 48h). *Western blot was performed to determine protein levels. 40µL of protein were added per well. Increase in LAP levels was significant (p<0.05) for wt-CFTR cells after 24h TGFβ. Increases in CFTR were significant (p<0.05) for wt-CFTR cells at 48h TGFβ and borderline significant (p=0.0522) at 24h. (LAP and CFTR n=4; LIP n=2)*

Jonas Fuxe and collaborators also studied C/EBPβ expression levels after 48h TGFβ1 stimulation, in a different model: mouse mammary gland epithelial cells (NMuMG). Their

findings included not only EMT occurrence but also a decrease in C/EBPβ levels (both LAP and LIP). This loss of expression of C/EBPβ was inhibited by siRNA-mediated knockdown of Smad3[96]. This is consistent with findings that TGFβ signalling induces Smad3/4-dependent inhibition of C/EBPβ function[84]. Although this partly explains (and is in accordance with) the results at 48h for F508del-CFTR cells, the still increased 48h levels in wt-CFTR cells (compared to 0h) and the increases at 24h are not in agreement with this explanation.

The higher LIP levels found in F508del-CFTR cells (which are contrary to these findings) could partly help to explain the more significant LAP reduction compared to wt-CFTR cells. Accordingly, a higher LIP:LAP ratio favours the loss of the TGFβ cytostatic response and induction of EMT[77]. Since LIP levels were still increasing in wt-CFTR cells, it is possible that these cells need a more prolonged exposure to TGFβ in order for LAP knockdown to be significant. This suggests once again that F508del-CFTR cells have a reduced resistance to TGFβ1 induction, as observed in TEER measurements. These results suggest that the F508del-CFTR mutation is responsible for the involvement of other pathways which inhibit C/EBPβ and are upregulated due to the CFTR mutations in CFBE cells.

The 24h increase in C/EBPβ levels may be a homeostatic mechanisms to suppress cellular proliferation. It is important to consider that C/EBPβ can also serve as a cofactor for TGFβ signalling: induction of the cyclin-dependent kinase inhibitor p15INK4b and repression of c-Myc, both needed for the TGFβ mediated growth-arrest response, were found to depend on C/EBPβ[125]. At 24h it is possible that some of the cells still retain their growth suppressor properties and C/EBPβ is acting synergically with Smads and FoxO factors. However, prolonged exposure to TGFβ most likely shifts definitively the response from growth arrest to EMT, consistent with what is observed at 48h.

The effect of TGFβ on CFTR was surprising. An important study on primary differentiated human bronchial epithelial cells (HBEs) recently found proof that TGFβ1 inhibits CFTR biogenesis, both in cells from non-CF individuals and from patients homozygous for the F508del mutation[126]. This was the first time the TGFβ1 effect was assessed in F508del-CFTR cells. These authors also found that TGFβ did not compromise the epithelial phenotype or integrity of these cells. All of these findings are contradictory to the ones in the present work. TGFβ was found to induce EMT, wt-CFTR expression was increased and F508del-CFTR expression showed no significant differences. Since TGFβ signalling has tissue-specific and cell culture-dependent effects this could partly account for the differences observed. In addition, it has to be considered (and this could help to explain the results) that these CFBE cell lines are overexpressing CFTR and, in this respect, do not perfectly recapitulate the *in vivo* situation (as opposed to primary cells). Further studies in different cellular models are needed to establish the effects of TGFβ signalling on CFTR.

3.6. Effect of miR-155 on the levels of C/EBPβ and CFTR

Since miR-155 has been previously reported to repress C/EBPβ expression, miR-155 and its antagomiR (AmiR-155) were added to CFBE mCherry-FLAG cells and protein levels for C/EBPβ and CFTR were assessed by immunofluorescence and Western blot assays. AntagomiRs are a novel class of chemically engineered oligonucleotides which are efficient and specific silencers of endogenous miRNAs[127].

Analysis of the immunofluorescence images (Figure 30A-C) showed that miR-155 treatment increased C/EBPβ LAP levels for both wt and F508del-CFTR cells. On the other hand, treatment with antagomiR-155 (AmiR-155) had differential effects on wt and F508del-CFTR cells; whereas in wt-CFTR cells it seemed to have no effect on C/EBPβ LAP levels compared to control, on F508del-CFTR the expression increased in a similar fashion to miR-155 treatment. Most of the treatments had no effect on CFTR expression level; only for AmiR-155 in wt-CFTR cells was perceptible a slight decrease in the amount of total CFTR and an increase in CFTR at the plasma membrane were noted. However these results were not statistically significant.

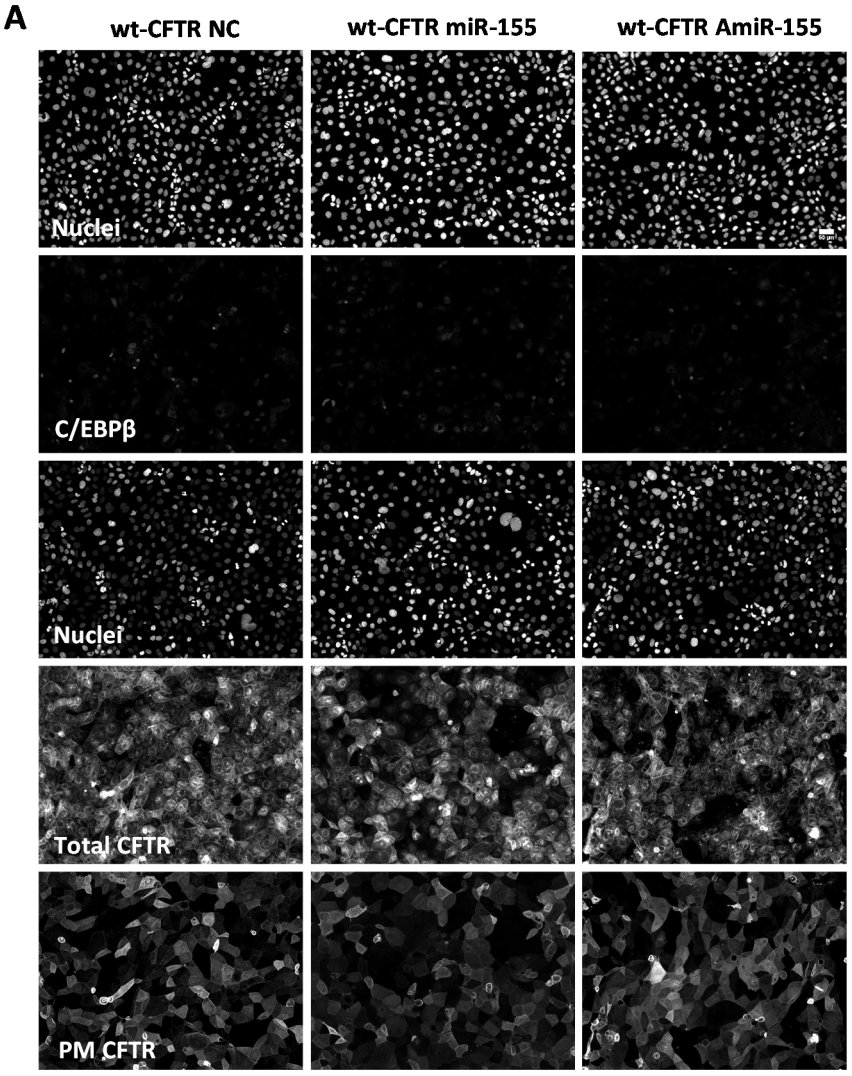

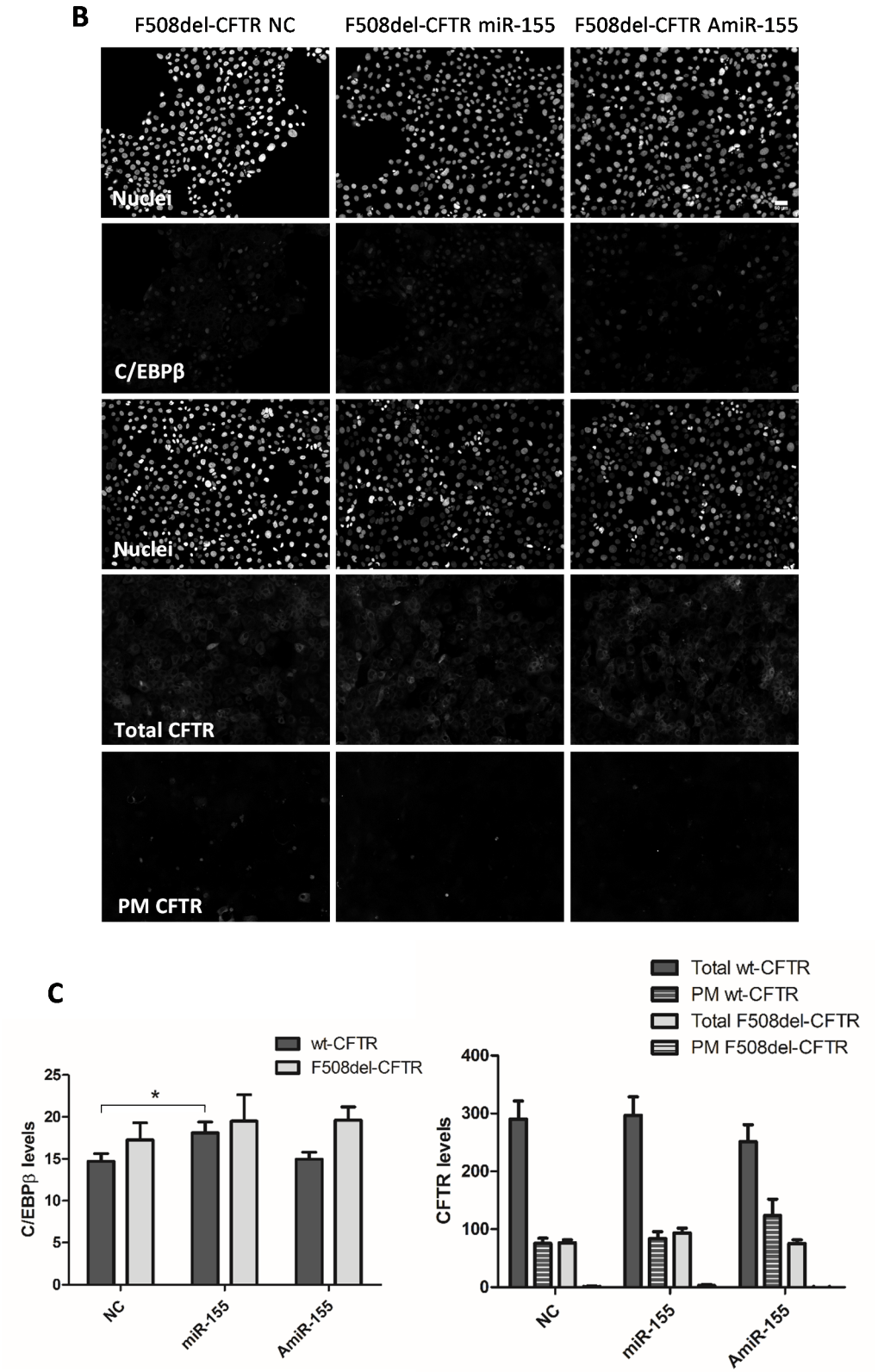

Figure 30 - A. Immunofluorescence assessment of C/EBPβ, total CFTR and plasma membrane (PM) CFTR in CFBE mCherry FLAG wt-CFTR cells, upon treatment with miR-155 and AmiR-155. B. Immunofluorescence assessment of C/EBPβ, total CFTR and plasma membrane (PM) CFTR in CFBE mCherry FLAG F508del-CFTR cells, upon treatment with miR-155 and AmiR-155. *Antibodies against C/EBPβ and FLAG were used for cell staining. Nuclei were stained with Hoechst. Scale bar represents 50 µm.* ***C. Quantification of the immunofluorescence data.*** *C/EBPβ and CFTR (total and PM) expression were analysed. The only significant difference ($p<0.05$) was found between the C/EBPβ levels on wt-CFTR cells for miR-155 treatment. (n=2, images analysed per assay=5).*

Similarly to the siRNA assay, Western blot results were not consistent with those from the immunofluorescence (Figure 31). They also proved more significant in this case. In wt-CFTR cells, LAP expression was unaltered upon treatment with miR-155 and increased (with borderline significance) following AmiR-155 treatment. On the other hand, on F508del-CFTR cells, LAP expression was significantly reduced for both treatments. As for CFTR, in wt-CFTR cells its expression increased with both treatments whereas in F508del-CFTR cells it remained unaltered.

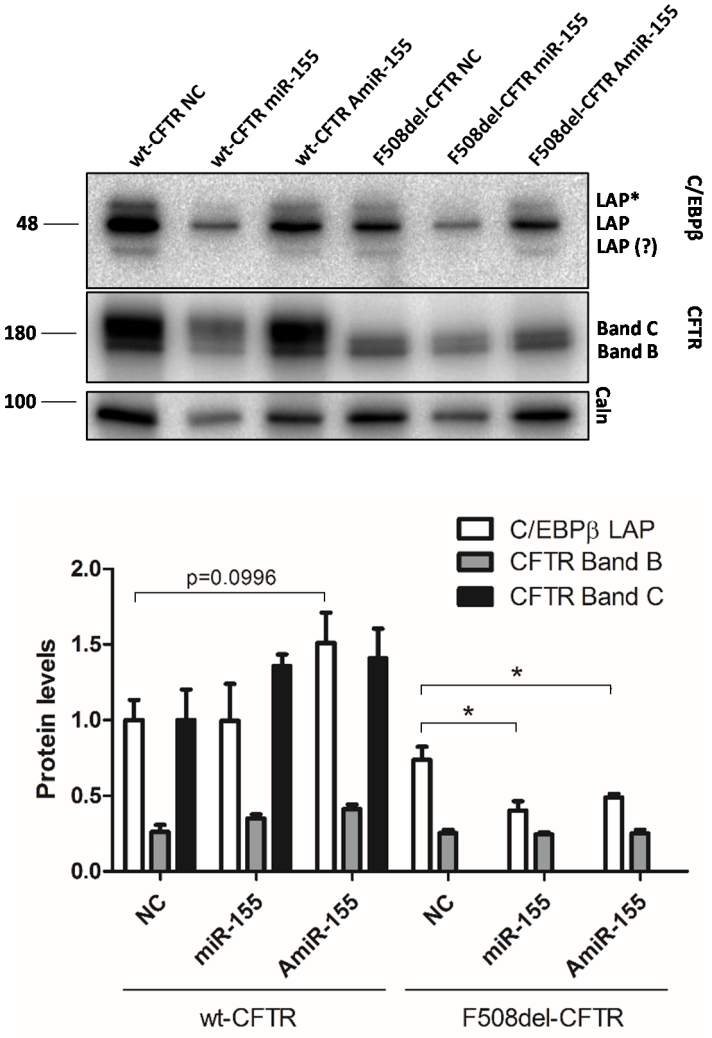

Figure 31 - Protein levels of C/EBPβ LAP and CFTR upon treatment with C/EBPβ siRNAs. *Borderline significance (p=0.0998) was found for the LAP levels upon AmiR-155 treatment. Significance (p<0.05) was found for the differences in LAP levels on F508del-CFTR cells for both treatments. (n=3).*

MiR-155 has been previously reported to repress C/EBPβ activity (see introduction). Jonas Fuxe and collaborators reported that addition of a miR-155 mimic decreased the baseline levels of C/EBPβ and that a miR-155 inhibitor increased this expression at baseline[96]. Another study, tackling inflammation in CF found miR-155 to be highly expressed by CF lung epithelial cells. This expression was related with reduced levels of phosphatidylinositol-3,4,5-trisphosphate 5-phosphatase 1 (SHIP1) and an activation of the PI3K/Akt signalling pathway. This leads to activation of downstream MAPKs with consequent stabilization of the IL-8 mRNA

and hyperexpression of the IL-8 protein. Accordingly, the addition of an antagomiR-155 to the cells reduced miR-155 and IL-8 expression. The authors also suggested that the tumour necrosis factor α (TNFα)/nuclear factor κB (NF-κB) signalling pathway (which is intrinsically activated in CF) could also be one possible mechanism by which F508del-CFTR cells activate miR-155 expression, since TNFα has also been reported to cause elevated levels of this miRNA[100].

As it was observed for the siRNA assay, the results of the immunofluorescence and the Western blot were not consistent. On the one hand, Western blot showed more statistically significant results, since the whole cell ensemble was analysed. On the other hand, due to cell-to-cell variability, in the immunofluorescence results, phenotypes were not very evident.

Some of the Western blot results are in agreement with the literature. For example, LAP levels in wt-CFTR cells were shown to increase with antagomiR-155 treatment, which is consistent with a repressive role of miR-155 on C/EBPβ. However, miR-155 treatment had no effect on this protein in these cells. This could suggest that miR-155 is a physiological mean of controlling the levels of C/EBPβ on this cells. Although blocking its effect increased C/EBPβ LAP levels, increasing its presence did not significantly dysregulate C/EBPβ, which could indicate that the baseline levels for miR-155 in these cells are quite low. On the other hand, in F508del-CFTR cells, treatment with miR-155 decreased the C/EBPβ LAP levels. This differential response suggests some dysregulation of miR-155/C/EBPβ signalling on these cells. Treatment with the antagomiR also decreased LAP levels, which was surprising. It is possible that the CFTR dysfunction in F508del-CFTR produces increased baseline levels of miR-155 which are higher in comparison to wt-CFTR cells. Hence, upon miR-155 addition, its amount has more negative effects on the cells. In addition to a decrease in the differentiation status, miR-155 could be a further mechanism by which C/EBPβ is decreased in F508del-CFTR cells. Furthermore, a higher intrinsic level of miR-155 could represent a partial mechanism which accounts for the differences in sensibility to the TGFβ treatment. More pronounced decreases in TEER and C/EBPβ expression in F508del-CFTR cells compared to wt-CFTR cells upon TGFβ treatment had suggest the involvement of other pathways which inhibit C/EBPβ and are upregulated due to the CFTR mutations. MiR-155 seems to fit this role, being reported to be upregulated in CF, which was consistent with the results found. Interestingly, TGFβ has been previously reported to induce miR-155, which supports this hypothesis[93].

Both treatments showed no effect on F508del-CFTR expression. This was expected, since according to the literature mutated CFTR increases miR-155 levels but there are no reports of the inverse. As for wt-CFTR its expression increased following both treatments. This was similar to what was found for the TGFβ treatment. Once again, it has to be considered that these CFBE cells are overexpressing CFTR and this could also help to explain these results.

4. Conclusions

Histological analysis of the CF tissue revealed areas of tissue remodelling consistent with a chronic inflammation environment in the lung. A loss of epithelial differentiation was also found. Furthermore, the presence of mesenchymal markers and loss of epithelial markers in CF lung sections supported the notion of an EMT occurrence. A replacement of E-cadherin with N-cadherin in CF tissue was one of the most striking differences and is consistent with important EMT hallmarks.

The differences in the differentiation status seem to be reflected in the C/EBPβ levels. F508del-CFTR CFBE cells show reduced C/EBPβ protein and mRNA levels. A relationship between C/EBPβ and CFTR is also apparent. Although protein interaction was not found for these two proteins, reduction of wt-CFTR at the plasma membrane when C/EBPβ was knockdown suggests an involvement of C/EBPβ in the traffic of CFTR to the plasma membrane. It is still unclear however if this role is mediated by the transcriptional activator isoform (LAP) or the transcriptional inhibitor isoform (LIP).

TGFβ treatment of polarized CFBE cells resulted in decreases in TEER and loss of E-cadherin expression, consistent with a TGFβ-induced EMT. Both wt and F508del-CFTR CFBE cells were affected by the TGFβ treatment. Despite the anti-inflammatory and anti-apoptotic roles known for TGFβ, a 48 hour exposure to this cytokine seems to definitively shift the response towards chronic inflammation and EMT induction. This response is consistent with the findings in CF lung tissue. Accordingly, decreased TEER is more pronounced for F508del-CFTR cells. C/EBPβ expression was also found to be more reduced in F508del-CFTR cells compared to wt after 48h of TGFβ treatment. This could be due to more increased LIP levels (which were observed in F508del-CFTR cells) but could also point to the involvement of other dysregulated pathways resulting from the CFTR defect. Increased LIP expression is commonly found in cells which have lost their TGFβ mediated cytostatic response and results in decreased LAP levels.

Finally, miR-155 was found to be repressing C/EBPβ on both cell types. However, on wt-CFTR cells its addition did not have any further effects on C/EBPβ levels, which suggests that the baseline physiological levels of this miRNA in these cells are not very elevated. In F508del-CFTR cells on the other hand, addition of miR-155 had a large impact on C/EBPβ levels. This could suggest that CFTR dysfunction produces increased baseline levels of miR-155 which further contribute to decreasing C/EBPβ. This is in agreement with the TGFβ results, which point to additional dysregulated pathways resulting from the CFTR defect affecting C/EBPβ levels.

Surprisingly, wt-CFTR levels increased with TGFβ and miR-155 treatment whereas F508del-CFTR showed no changes in expression. Since this is contradictory to recent findings that TGFβ impairs CFTR biogenesis, CFBE cell lines might not be the best model to assess CFTR levels in response to TGFβ treatment. This can be because these cell lines are overexpressing CFTR and, in this respect, do not perfectly recapitulate the *in vivo* situation.

Hence, from the findings of the present work, chronic inflammation and EMT were found to a part of the CF pathogenesis in the lung and were successfully replicated when cells where treated with TGFβ for 48h. Additionally, a disparity in C/EBPβ levels seems to be present as a result of CFTR dysfunction. Both TGFβ and treatment with miR-155 were shown to decrease

C/EBPβ levels in F508del-CFTR cells in a more severe manner compared to wt-CFTR cells. Thus both dysregulated miR-155 and TGFβ signalling could be present in the CF airways as a result of CFTR dysfunction and could be working synergistically to induce both EMT and loss of C/EBPβ expression. Since a decrease in C/EBPβ was shown to inhibit wt-CFTR transport to the plasma membrane, these mechanisms could be reducing the levels of mutated CFTR which reach the plasma membrane of the ciliated cells in the CF epithelium.

5. Future perspectives

One of the most important and consistent finding of these results was the loss of epithelial differentiation observed in CF tissue. A relationship between mutated CFTR and reduced differentiation status has previously been reported in other studies, but it is still unclear which pathways are involved. Assessing this could have beneficial effects for CF therapy, since new drug targets could become apparent. Hence, one of the most important aspects following this work should be to determine which proteins are involved in the loss of differentiation in CF. Ideally, a gene regulatory network which relates EMT and traffic pathways would be constructed. This could be done for example with resource to high throughput microscopy screens, which are already a common practice in systems biology.

Additionally, quantitative analysis needs to be performed to complement the immunofluorescence findings at tissue level, in order to make the results of the present work more robust. Ideally, new control samples should be collected and frozen with greater care, in order to have quantitatively comparable control and CF tissue. It should also be interesting to extract RNA from tissue and perform qPCR analysis for the epithelial and mesenchymal markers, as a way to further confirm the occurrence of EMT.

Accordingly, to validate the presence of TGFβ-induced EMT in CFBE cells, it would also be desirable to assess the levels of epithelial and mesenchymal markers, at both mRNA and protein levels, in these cells. QRT-PCR, Western blot and immunofluorescence assay could be performed on polarized CFBE cells.

Additionally, C/EBPβ seems to be a modulator of CFTR traffic. Hence, it would be instrumental to fully understand its role and relationship with CFTR. In addition to assessing the differential effects of the separate knockdown of the two C/EBPβ isoforms, the production of C/EBPβ gene knockouts is also very important. To this end, the system implemented in this work could be improved. As elucidated in the discussion, an additional step of cell sorting on cells transfected with the CRISPR system would minimize the errors that occurred in the present work. Cell sorting would not only select efficiently transfected cells but also render superfluous the hygromycin resistance plasmid, both of which could successfully determine the quality of the experiment.

Furthermore, the treatments with TGFβ and miR-155 need to be repeated and further optimized in order to obtain highly significant results which accurately show or confirm their roles in the pathology of CF disease. For example more time points could be assessed for TGFβ, as well as C/EBPβ mRNA levels. It would also be interesting to combine both treatments. Since TGFβ has been reported to regulate miR-155, such a relationship could be investigated in these cells.

6. References

1. Collins, F. S. Cystic fibrosis: molecular biology and therapeutic implications. *Science* **256,** 774–779 (1992).
2. Amaral, M. D. Novel personalized therapies for cystic fibrosis: treating the basic defect in all patients. *J. Intern. Med.* **277,** 155–166 (2015).
3. Farrell, P. M. The prevalence of cystic fibrosis in the European Union. *J. Cyst. Fibros.* **7,** 450–453 (2008).
4. Anderson, D. H. Cystic fibrosis of the pancreas and its relation to celiac disease: a clinical and pathological study. *Am J Dis Child* **56,** 344–399 (1938).
5. Boucher, R. C., Knowles, M. R., Stutts, M. J. & Gatzy, J. T. Epithelial dysfunction in cystic fibrosis lung disease. *Lung* **161,** 1–17 (1983).
6. Riordan, J. R. *et al.* Identification the Cystic Fibrosis Gene : Cloning and Characterization of Complementary DNA. *Science (80-.).* **245,** 1066–73 (1989).
7. O'Sullivan, B. P. & Freedman, S. D. Cystic fibrosis. *Lancet* **373,** 1891–1904 (2009).
8. Davies, J. C., Alton, E. W. F. W. & Bush, A. Cystic fibrosis. *BMJ* **335,** 1255–1259 (2007).
9. Gaspar, M. C., Couet, W., Olivier, J.-C., Pais, a a C. C. & Sousa, J. J. S. Pseudomonas aeruginosa infection in cystic fibrosis lung disease and new perspectives of treatment: a review. *Eur. J. Clin. Microbiol. Infect. Dis.* **32,** 1231–52 (2013).
10. Pezzulo, A. a. *et al.* Reduced airway surface pH impairs bacterial killing in the porcine cystic fibrosis lung. *Nature* **487,** 109–113 (2012).
11. Osika, E. *et al.* Distinct sputum cytokine profiles in cystic fibrosis and other chronic inflammatory airway disease. *Eur. Respir. J. Off. J. Eur. Soc. Clin. Respir. Physiol.* **14,** 339–346 (1999).
12. Rowe, S. M., Miller, S. & Sorscher, E. J. Cystic fibrosis. *N. Engl. J. Med.* **352,** 1992–2001 (2005).
13. Dean, T. P., Dai, Y., Shute, J. K., Church, M. K. & Warner, J. O. Interleukin-8 concentrations are elevated in bronchoalveolar lavage, sputum, and sera of children with cystic fibrosis. *Pediatr. Res.* **34,** 159–161 (1993).
14. Nichols, D., Chmiel, J. & Berger, M. Chronic inflammation in the cystic fibrosis lung: Alterations in inter- and intracellular signaling. *Clin. Rev. Allergy Immunol.* **34,** 146–162 (2008).
15. Carrabino, S. *et al.* Dysregulated interleukin-8 secretion and NF-κB activity in human cystic fibrosis nasal epithelial cells. *J. Cyst. Fibros.* **5,** 113–119 (2006).
16. Perez, A. *et al.* CFTR inhibition mimics the cystic fibrosis inflammatory profile. *Am. J. Physiol. Lung Cell. Mol. Physiol.* **292,** L383–L395 (2007).
17. Zielenski, J. Genotype and phenotype in cystic fibrosis. *Respiration.* **67,** 117–133 (2000).
18. Gadsby, D. C., Vergani, P. & Csanády, L. The ABC protein turned chloride channel whose failure causes cystic fibrosis. *Nature* **440,** 477–483 (2006).
19. Amaral, M. D. Processing of CFTR: Traversing the cellular maze - How much CFTR needs to go through to avoid cystic fibrosis? *Pediatr. Pulmonol.* **39,** 479–491 (2005).
20. D. Amaral, M. & M. Farinha, C. Rescuing Mutant CFTR: A Multi-task Approach to a Better Outcome in Treating Cystic Fibrosis. *Curr. Pharm. Des.* **19,** 3497–3508 (2013).
21. Ishiguro, H. *et al.* CFTR functions as a bicarbonate channel in pancreatic duct cells. *J. Gen. Physiol.* **133,** 315–326 (2009).
22. Hug, M. J., Tamada, T. & Bridges, R. J. CFTR and bicarbonate secretion by [correction of to] epithelial cells. *News Physiol. Sci.* **18,** 38–42 (2003).
23. Reddy, M. M., Light, M. J. & Quinton, P. M. Activation of the epithelial Na+ channel (ENaC) requires CFTR Cl- channel function. *Nature* **402,** 301–304 (1999).
24. Schwiebert, E. M. *et al.* CFTR regulates outwardly rectifying chloride channels through an autocrine mechanism involving ATP. *Cell* **81,** 1063–1073 (1995).

25. Kunzelmann, K. & Schreiber, R. CFTR, a regulator of channels. *J. Membr. Biol.* **168,** 1–8 (1999).
26. Mehta, A. CFTR: More than just a chloride channel. *Pediatr. Pulmonol.* **39,** 292–298 (2005).
27. Kogan, I. *et al.* CFTR directly mediates nucleotide-regulated glutathione flux. *EMBO J.* **22,** 1981–1989 (2003).
28. http://www.genet.sickkids.on.ca/app. at <http://www.genet.sickkids.on.ca/app>
29. Amaral, M. D. & Kunzelmann, K. Molecular targeting of CFTR as a therapeutic approach to cystic fibrosis. *Trends Pharmacol. Sci.* **28,** 334–341 (2007).
30. Wainwright, C. E. *et al.* Lumacaftor-Ivacaftor in Patients with Cystic Fibrosis Homozygous for Phe508del CFTR. *N. Engl. J. Med.* 1–12 (2015). doi:10.1056/NEJMoa1409547
31. Ratjen, F. & Döring, G. Cystic fibrosis. *Lancet* **361,** 681–689 (2003).
32. Accurso, F. J. & Sontag, M. K. Gene modifiers in cystic fibrosis. *Journal of Clinical Investigation* **118,** 839–841 (2008).
33. Harris, W. T., Muhlebach, M. S., Oster, R. a, Knowles, M. R. & Noah, T. L. Transforming growth factor-beta1 in bronchoalveolar lavage fluid from children with cystic fibrosis. *Pediatr. Pulmonol.* **44,** 1057–1064 (2009).
34. Drumm, M. L. *et al.* Genetic modifiers of lung disease in cystic fibrosis. *N. Engl. J. Med.* **353,** 1443–1453 (2005).
35. Massagué, J. & Gomis, R. R. The logic of TGFβ signaling. *FEBS Lett.* **580,** 2811–2820 (2006).
36. Bartram, U. & Speer, C. P. The role of transforming growth factor beta in lung development and disease. *Chest* **125,** 754–765 (2004).
37. Yang, Y. C. *et al.* Transforming growth factor-beta1 in inflammatory airway disease: A key for understanding inflammation and remodeling. *Allergy Eur. J. Allergy Clin. Immunol.* **67,** 1193–1202 (2012).
38. Derynck, R. & Zhang, Y. E. Smad-dependent and Smad-independent pathways in TGF-β family signalling. *Nature* **425,** 577–584 (2003).
39. Arkwright, P. D. *et al.* TGF-beta1 genotype and accelerated decline in lung function of patients with cystic fibrosis. *Thorax* **55,** 459–462 (2000).
40. Bremer, L. a. *et al.* Interaction between a novel TGFB1 haplotype and CFTR genotype is associated with improved lung function in cystic fibrosis. *Hum. Mol. Genet.* **17,** 2228–2237 (2008).
41. Guillot, L. *et al.* Lung disease modifier genes in cystic fibrosis. *Int. J. Biochem. Cell Biol.* **52,** 83–93 (2014).
42. Harris, W. T. *et al.* Plasma TGF-β1 in pediatric cystic fibrosis: potential biomarker of lung disease and response to therapy. *Pediatr. Pulmonol.* **46,** 688–695 (2011).
43. Wojnarowski, C. *et al.* Cytokine expression in bronchial biopsies of cystic fibrosis patients with and without acute exacerbation. *Eur. Respir. J. Off. J. Eur. Soc. Clin. Respir. Physiol.* **14,** 1136–1144 (1999).
44. Ge, Q., Moir, L. M., Black, J. L., Oliver, B. G. & Burgess, J. K. TGFβ1 induces IL-6 and inhibits IL-8 release in human bronchial epithelial cells: The role of Smad2/3. *J. Cell. Physiol.* **225,** 846–854 (2010).
45. Kelley, T. J., Elmer, H. L. & Corey, D. a. Reduced Smad3 protein expression and altered transforming growth factor-β1-mediated signaling in cystic fibrosis epithelial cells. *Am. J. Respir. Cell Mol. Biol.* **25,** 732–738 (2001).
46. Harris, W. T. *et al.* Myofibroblast Differentiation and Enhanced Tgf-B Signaling in Cystic Fibrosis Lung Disease. *PLoS One* **8,** 2–9 (2013).
47. Taylor, M. A., Parvani, J. G. & Schiemann, W. P. The Pathophysiology of Epithelial-Mesenchymal Transition Induced by Transforming Growth Factor-β in Normal and Malignant Mammary Epithelial Cells. *J. Mammary Gland Biol. Neoplasia* **15,** 169–190 (2010).
48. Willis, B. C. & Borok, Z. TGF-β-induced EMT : mechanisms and implications for fibrotic lung disease. *Am. J. Physiol. Lung Cell. Mol. Physiol.* **293,** L525–34 (2007).

49. Lamouille, S., Xu, J. & Derynck, R. Molecular mechanisms of epithelial-mesenchymal transition. *Nat. Rev. Mol. Cell Biol.* **15,** 178–96 (2014).
50. Lee, J. M. The epithelial-mesenchymal transition: new insights in signaling, development, and disease. *J. Cell Biol.* **172,** 973–981 (2006).
51. Kalluri, R. & Weinberg, R. a. The basics of epithelial-mesenchymal transition. *J. Clin. Invest.* **119,** 1420–1428 (2009).
52. Thiery, J. P., Acloque, H., Huang, R. Y. J. & Nieto, M. A. Epithelial-Mesenchymal Transitions in Development and Disease. *Cell* **139,** 871–890 (2009).
53. Zavadil, J. & Böttinger, E. P. TGF-β and epithelial-to-mesenchymal transitions. *Oncogene* **24,** 5764–5774 (2005).
54. Derynck, R., Muthusamy, P. & Saeteurn, K. Y. Signaling pathway cooperation in TGF-β-induced epithelial–mesenchymal transition. *Curr. Opin. Cell Biol.* **31,** 56–66 (2014).
55. Montrose-Rafizadeh, C., Guggino, W. B. & Montrose, M. H. Cellular differentiation regulates expression of Cl- transport and cystic fibrosis transmembrane conductance regulator mRNA in human intestinal cells. *J.Biol.Chem.* **266,** 4495–4499 (1991).
56. Sood, R. *et al.* Regulation of CFTR expression and function during differentiation of intestinal epithelial cells. *EMBO J.* **11,** 2487–94 (1992).
57. Mylona, P., Glazier, J. D., Greenwood, S. L., Sides, M. K. & Sibley, C. P. Expression of the cystic fibrosis (CF) and multidrug resistance (MDR1) genes during development and differentiation in the human placenta. *Mol.Hum.Reprod.* **2,** 693–698 (1996).
58. Larson, J. E., Delcarpio, J. B., Farberman, M. M., Morrow, S. L. & Cohen, J. C. CFTR modulates lung secretory cell proliferation and differentiation. *Am. J. Physiol. Lung Cell. Mol. Physiol.* **279,** L333–L341 (2000).
59. Bertrand, C. a & Frizzell, R. a. The role of regulated CFTR trafficking in epithelial secretion. *Am. J. Physiol. Cell Physiol.* **285,** C1–18 (2003).
60. Bebök, Z. *et al.* Activation of ΔF508 CFTR in an epithelial monolayer. *Am. J. Physiol.* **275,** C599–C607 (1998).
61. Morris, A. P., Cunningham, S. a, Benos, D. J. & Frizzell, R. a. Cellular differentiation is required for cAMP but not Ca2+- dependent Cl- secretion in colonic epithelial cells expressing high levels of cystic fibrosis transmembrane conductance regulator. *J Biol Chem* **267,** 5575–5583 (1992).
62. Hajj, R. *et al.* Human airway surface epithelial regeneration is delayed and abnormal in cystic fibrosis. *J. Pathol.* **211,** 340–350 (2007).
63. LeSimple, P., Liao, J., Robert, R., Gruenert, D. C. & Hanrahan, J. W. Cystic fibrosis transmembrane conductance regulator trafficking modulates the barrier function of airway epithelial cell monolayers. *J. Physiol.* **588,** 1195–1209 (2010).
64. Puchelle, E., Zahm, J.-M., Tournier, J.-M. & Coraux, C. Airway Epithelial Repair, Regeneration, and Remodeling after Injury in Chronic Obstructive Pulmonary Disease. *Proc. Am. Thorac. Soc.* **3,** 726–733 (2006).
65. Dupuit, F. *et al.* CFTR and differentiation markers expression in non-CF and delta F 508 homozygous CF nasal epithelium. *J. Clin. Invest.* **96,** 1601–1611 (1995).
66. Leigh, M. W., Kylander, J. E., Yankaskas, J. R. & Boucher, R. C. Cell proliferation in bronchial epithelium and submucosal glands of cystic fibrosis patients. *Am. J. Respir. Cell Mol. Biol.* **12,** 605–612 (1995).
67. Schiller, K. R., Maniak, P. J. & O'Grady, S. M. Cystic fibrosis transmembrane conductance regulator is involved in airway epithelial wound repair. *AJP Cell Physiol.* **299,** C912–C921 (2010).
68. Trinh, N. T. N. *et al.* Improvement of defective cystic fibrosis airway epithelial wound repair after CFTR rescue. *Eur. Respir. J.* **40,** 1390–1400 (2012).
69. Bonvin, E. *et al.* Congenital tracheal malformation in cystic fibrosis transmembrane conductance regulator-deficient mice. *J. Physiol.* **586,** 3231–3243 (2008).

70. Meyerholz, D. K. *et al.* Loss of Cystic Fibrosis Transmembrane Conductance Regulator Function Produces Abnormalities in Tracheal Development in Neonatal Pigs and Young Children. *Am. J. Respir. Crit. Care Med.* **182,** 1251–1261 (2010).
71. Maisonneuve, P., Marshall, B. C., Knapp, E. a. & Lowenfels, A. B. Cancer Risk in Cystic Fibrosis: A 20-Year Nationwide Study From the United States. *JNCI J. Natl. Cancer Inst.* **105,** 122–129 (2013).
72. Zhang, J. T. *et al.* Downregulation of CFTR promotes epithelial-to-mesenchymal transition and is associated with poor prognosis of breast cancer. *Biochim. Biophys. Acta - Mol. Cell Res.* **1833,** 2961–2969 (2013).
73. Xie, C. *et al.* CFTR suppresses tumor progression through miR-193b targeting urokinase plasminogen activator (uPA) in prostate cancer. *Oncogene* **32,** 2282–2291 (2013).
74. Li, Y. *et al.* Cystic fibrosis transmembrane conductance regulator gene mutation and lung cancer risk. *Lung Cancer* **70,** 14–21 (2010).
75. SON, J. W. *et al.* Promoter hypermethylation of the CFTR gene and clinical/pathological features associated with non-small cell lung cancer. *Respirology* **16,** 1203–1209 (2011).
76. Tsukada, J., Yoshida, Y., Kominato, Y. & Auron, P. E. The CCAAT/enhancer (C/EBP) family of basic-leucine zipper (bZIP) transcription factors is a multifaceted highly-regulated system for gene regulation. *Cytokine* **54,** 6–19 (2011).
77. Zahnow, C. a. CCAAT/enhancer-binding protein β: its role in breast cancer and associations with receptor tyrosine kinases. *Expert Rev. Mol. Med.* **11,** e12 (2009).
78. RAMJI, D. P. & FOKA, P. CCAAT/enhancer-binding proteins: structure, function and regulation. *Biochem. J.* **365,** 561–575 (2002).
79. Mcknight, S. L., Graves, B. & Johnson, P. McBindall — A Better Name for CCAAT/Enhancer Binding Proteins ? *Cell* **107,** 259–261 (2001).
80. Roos, A. Regulation of Gene Expression in Pulmonary Inflammation and Differentiation: A Role for C/EBP Transcription Factors. (Karolinska Institutet, 2012).
81. Hu, B., Wu, Z., Nakashima, T. & Phan, S. H. Mesenchymal-Specific Deletion of C/EBPβ Suppresses Pulmonary Fibrosis. *Am. J. Pathol.* **180,** 2257–2267 (2012).
82. Jundi, K. & Greene, C. Transcription of Interleukin-8: How Altered Regulation Can Affect Cystic Fibrosis Lung Disease. *Biomolecules* **5,** 1386–1398 (2015).
83. Yan, C. *et al.* Critical Role for CCAAT/Enhancer-Binding Protein in Immune Complex-Induced Acute Lung Injury. *J. Immunol.* **189,** 1480–1490 (2012).
84. Nerlov, C. C/EBPs: recipients of extracellular signals through proteome modulation. *Curr. Opin. Cell Biol.* **20,** 180–185 (2008).
85. Gomis, R. R., Alarcón, C., Nadal, C., Van Poznak, C. & Massagué, J. C/EBPβ at the core of the TGFβ cytostatic response and its evasion in metastatic breast cancer cells. *Cancer Cell* **10,** 203–214 (2006).
86. Zahnow, C. a, Cardiff, R. D., Laucirica, R., Medina, D. & Rosen, J. M. A role for CCAAT/enhancer binding protein beta-liver-enriched inhibitory protein in mammary epithelial cell proliferation. *Cancer Res.* **61,** 261–269 (2001).
87. Li, J. *et al.* EGF-induced C/EBP participates in EMT by decreasing the expression of miR-203 in esophageal squamous cell carcinoma cells. *J. Cell Sci.* **127,** 3735–3744 (2014).
88. Bundy, L. M. & Sealy, L. CCAAT/enhancer binding protein beta (C/EBPβ)-2 transforms normal mammary epithelial cells and induces epithelial to mesenchymal transition in culture. *Oncogene* **22,** 869–883 (2003).
89. Shuman, J. D. *et al.* Cell Cycle-Dependent Phosphorylation of C/EBP Mediates Oncogenic Cooperativity between C/EBP and H-RasV12. *Mol. Cell. Biol.* **24,** 7380–7391 (2004).
90. Mo, X., Kowenz-Leutz, E., Xu, H. & Leutz, A. Ras Induces Mediator Complex Exchange on C/EBPβ. *Mol. Cell* **13,** 241–250 (2004).
91. Lamb, J. *et al.* A Mechanism of Cyclin D1 Action Encoded in the Patterns of Gene Expression in Human Cancer. *Cell* **114,** 323–334 (2003).

92. Faraoni, I., Antonetti, F. R., Cardone, J. & Bonmassar, E. miR-155 gene: A typical multifunctional microRNA. *Biochim. Biophys. Acta - Mol. Basis Dis.* **1792,** 497–505 (2009).
93. Kong, W. *et al.* MicroRNA-155 Is Regulated by the Transforming Growth Factor/Smad Pathway and Contributes to Epithelial Cell Plasticity by Targeting RhoA. *Mol. Cell. Biol.* **28,** 6773–6784 (2008).
94. Mattiske, S., Suetani, R. J., Neilsen, P. M. & Callen, D. F. The Oncogenic Role of miR-155 in Breast Cancer. *Cancer Epidemiol. Biomarkers Prev.* **21,** 1236–1243 (2012).
95. Rodriguez, A. *et al.* Requirement of bic/microRNA-155 for Normal Immune Function. *Science (80-.).* **316,** 608–611 (2007).
96. Johansson, J. *et al.* MiR-155-mediated loss of C/EBPβ shifts the TGF-β response from growth inhibition to epithelial-mesenchymal transition, invasion and metastasis in breast cancer. *Oncogene* **32,** 5614–5624 (2013).
97. He, M., Xu, Z., Ding, T., Kuang, D.-M. & Zheng, L. MicroRNA-155 Regulates Inflammatory Cytokine Production in Tumor-associated Macrophages via Targeting C/EBPβ. *Cell. Mol. Immunol.* **6,** 343–352 (2009).
98. Worm, J. *et al.* Silencing of microRNA-155 in mice during acute inflammatory response leads to derepression of c/ebp Beta and down-regulation of G-CSF. *Nucleic Acids Res.* **37,** 5784–5792 (2009).
99. Yang, M. *et al.* High expression of miR-21 and miR-155 predicts recurrence and unfavourable survival in non-small cell lung cancer. *Eur. J. Cancer* **49,** 604–615 (2013).
100. Bhattacharyya, S. *et al.* Elevated miR-155 Promotes Inflammation in Cystic Fibrosis by Driving Hyperexpression of Interleukin-8. *J. Biol. Chem.* **286,** 11604–11615 (2011).
101. Cong, L. *et al.* Multiplex Genome Engineering Using CRISPR/Cas Systems. *Science (80-.).* **339,** 819–823 (2013).
102. Singh, P., Schimenti, J. C. & Bolcun-Filas, E. A Mouse Geneticist's Practical Guide to CRISPR Applications. *Genetics* **199,** 1–15 (2015).
103. Mali, P. *et al.* RNA-Guided Human Genome Engineering via Cas9. *Science (80-.).* **339,** 823–826 (2013).
104. NCBI - CEBPB gene. at <http://www.ncbi.nlm.nih.gov/gene/1051>
105. Ehrhardt, C. *et al.* Towards an in vitro model of cystic fibrosis small airway epithelium: characterisation of the human bronchial epithelial cell line CFBE41o-. *Cell Tissue Res.* **323,** 405–415 (2006).
106. Bebok, Z. *et al.* Failure of cAMP agonists to activate rescued ΔF508 CFTR in CFBE41o - airway epithelial monolayers. *J. Physiol.* **569,** 601–615 (2005).
107. Botelho, H. M. *et al.* Protein Traffic Disorders: an Effective High-Throughput Fluorescence Microscopy Pipeline for Drug Discovery. *Sci. Rep.* **5,** 9038 (2015).
108. Van de Lest, C. H., Versteeg, E. M., Veerkamp, J. H. & Van Kuppevelt, T. H. Elimination of autofluorescence in immunofluorescence microscopy with digital image processing. *J. Histochem. Cytochem.* **43,** 727–730 (1995).
109. Ross, M. & Pawlina, W. *Histology: A Text and Atlas. Uma ética para quantos?* **XXXIII,** (2011).
110. Scouten, C. W. & Cunningham, M. Freezing Biological Samples. (2012). at <http://www.leicabiosystems.com/pathologyleaders/freezing-biological-samples/>
111. Polosukhin, V. V. Ultrastructure of the Bronchial Epithelium in Chronic In ammation. *Ultrastruct. Pathol.* 119–128 (2001).
112. Scholzen, T. & Gerdes, J. The Ki-67 protein: From the known and the unknown. *J. Cell. Physiol.* **182,** 311–322 (2000).
113. Raschperger, E. *et al.* The coxsackie- and adenovirus receptor (CAR) is an in vivo marker for epithelial tight junctions, with a potential role in regulating permeability and tissue homeostasis. *Exp. Cell Res.* **312,** 1566–1580 (2006).

114. Salon, C. *et al.* The E-cadherin–β-catenin complex and its implication in lung cancer progression and prognosis. *Futur. Oncol.* **1,** 649–660 (2005).
115. Wijnhoven, B. P. L., Dinjens, W. N. M. & Pignatelli, M. E-cadherin-catenin cell-cell adhesion complex and human cancer. *Br. J. Surg.* **87,** 992–1005 (2000).
116. Piorunek, T. *et al.* Correlation between the stage of cystic fibrosis and the level of morphological changes in adult patients. *J. Physiol. Pharmacol.* **59 Suppl 6,** 565–572 (2008).
117. Clarke, L. a, Sousa, L., Barreto, C. & Amaral, M. D. Changes in transcriptome of native nasal epithelium expressing F508del-CFTR and intersecting data from comparable studies. *Respir. Res.* **14,** 38 (2013).
118. Dearth, L. R., Hutt, J., Sattler, a, Gigliotti, a & DeWille, J. Expression and function of CCAAT/enhancer binding proteinbeta (C/EBPbeta) LAP and LIP isoforms in mouse mammary gland, tumors and cultured mammary epithelial cells. *J. Cell. Biochem.* **82,** 357–70 (2001).
119. McCarthy, V. a. & Harris, A. The CFTR gene and regulation of its expression. *Pediatr. Pulmonol.* **40,** 1–8 (2005).
120. Torres-Padilla, M.-E. & Chambers, I. Transcription factor heterogeneity in pluripotent stem cells: a stochastic advantage. *Development* **141,** 2173–2181 (2014).
121. Natoli, M. *et al.* Cell growing density affects the structural and functional properties of Caco-2 differentiated monolayer. *J. Cell. Physiol.* **226,** 1531–1543 (2011).
122. Stewart, C. E., Torr, E. E., Mohd Jamili, N. H., Bosquillon, C. & Sayers, I. Evaluation of Differentiated Human Bronchial Epithelial Cell Culture Systems for Asthma Research. *J. Allergy* **2012,** 1–11 (2012).
123. Rahimi, R. a & Leof, E. B. TGF-β signaling: A tale of two responses. *J. Cell. Biochem.* **102,** 593–608 (2007).
124. Blobe, G. C., Schiemann, W. P. & Lodish, H. F. Role of transforming growth factor beta in human disease. *N. Engl. J. Med.* **342,** 1350–1358 (2000).
125. Gomis, R. R. *et al.* A FoxO-Smad synexpression group in human keratinocytes. *Proc. Natl. Acad. Sci.* **103,** 12747–12752 (2006).
126. Snodgrass, S. M., Cihil, K. M., Cornuet, P. K., Myerburg, M. M. & Swiatecka-Urban, A. Tgf-β1 Inhibits Cftr Biogenesis and Prevents Functional Rescue of ΔF508-Cftr in Primary Differentiated Human Bronchial Epithelial Cells. *PLoS One* **8,** (2013).
127. Krützfeldt, J. *et al.* Silencing of microRNAs in vivo with 'antagomirs'. *Nature* **438,** 685–689 (2005).

7. Appendices

7.1. C/EBPβ leaky ribosome scanning

Figure 32 – Amino acid sequence for the LAP, LAP* and LIP isoforms. ** indicates the consensus region for all isoforms. Leaky ribosome scanning in translation in apparent.*

7.2. Antibodies and primers

Table 1 - Primary antibodies used in the present work. *Information like the experiment they were used in, the respective dilution, the host and the company and reference are clarified.*

Target	Use	Dilution	Host	Company	Reference
C/EBPβ	IHC	1:200	Rabbit	Santa Cruz	sc-150
	IF	1:500			
	WB/coIP	1:500 or 1:750			
CFTR	IHC	1:500	Mouse	CFF	570
	WB/coIP	1:3000	Mouse	CFF	596
FLAG	IF	1:500	Mouse	Sigma-Aldrich	F1804
Calnexin	WB	1:3000	Mouse	BD Transduction Lab	610523
E-cadherin	IHC	1:200	Mouse	BD Transduction Lab	610181
	IF filters	1:100			
Cytokeratin-18	IHC	1:100	Mouse	Santa Cruz	sc-32329
Vimentin	IHC	1:200	Rabbit	Santa Cruz	sc-7557-r
KI67	IHC	1:100	Rabbit	Abcam	ab16667
CAR	IHC	1:200	Rabbit	Atlas Antibodies	HPA003342
β-catenin	IHC	1:200	Rabbit	Abcam	Ab12221
N-cadherin	IHC	1:200	Rabbit	Abcam	Ab32572

Table 2 - Secondary antibodies used in the present work. *Information like the target, the experiment they were used in, the respective dilution, the host and the company and reference are clarified.*

Antibody	Target	Use	Dilution	Host	Company	Reference
Alexa Fluor 488	Mouse IgG	IHC IF filters	1:500	Donkey	Life Technologies	A21202
Alexa Fluor 488	Rabbit IgG	IHC	1:500			A21206
Alexa Fluor 568	Rabbit IgG	IHC	1:500			A10042
Cy5	Mouse IgG	IHC IF	1:500	Goat	Life Technologies	A10524
Alex Fluor 647	Rabbit IgG	IHC IF	1:500			A21244
(H+L)-HRP Conjugate	Mouse IgG	WB	1:3000	Goat	Bio-Rad	170-6515
(H+L)-HRP Conjugate	Rabbit IgG	WB	1:3000			170-6516

Table 3 - Description of the primers used in qRT-PCR in the present work. *Sequence information is clarified. The C/EBPβ primer was ordered from Qiagen and its sequence was not disclosed.*

Target	Forward/reverse primer	Sequence (5'-3')
β-actin	Forward	CTCTTCCAGCCTTCCTTCCT
	Reverse	AGCACTGTGTTGGCGTACAG
C/EBPβ	mix	QT00237580

7.3. CRISPR system

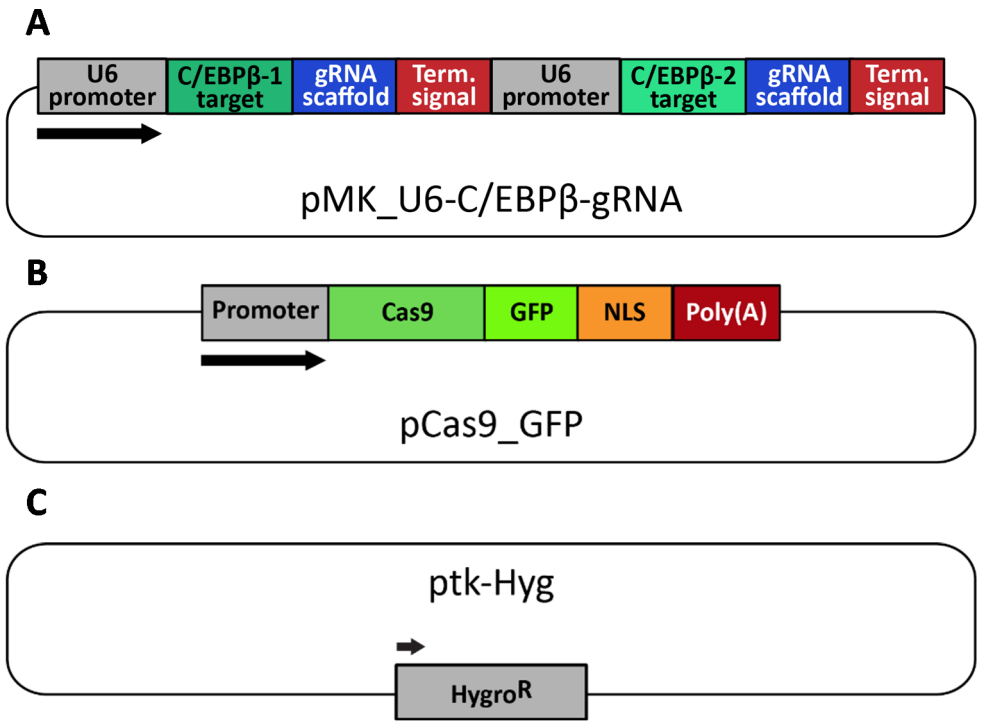

Figure 33 – Vector maps for the three plasmids used in the CRISPR transfection. *A. gRNA expression plasmid for C/EBPβ. B. Expression plasmid for Cas9-GFP. C. Hygromycin selection vector. Image kindly provided by Ines Pankonien.*

7.4. siRNA assay

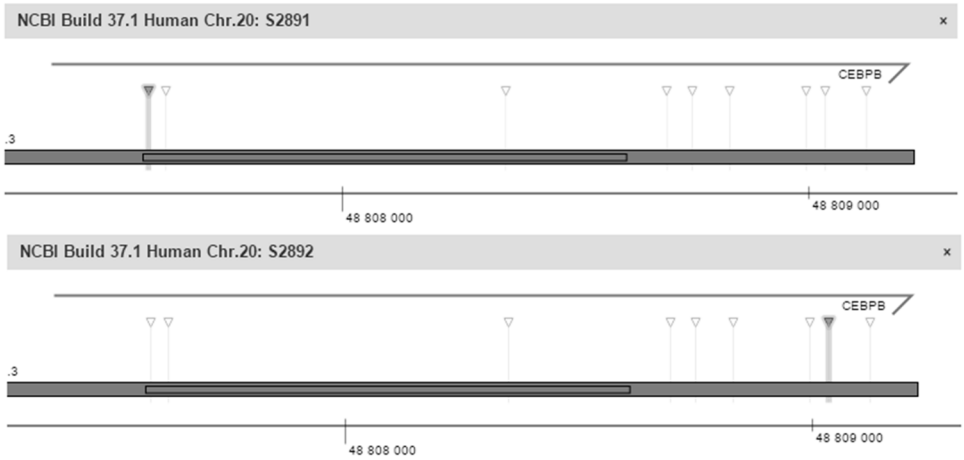

Figure 34 - Map of the C/EBPβ gene areas targeted by the siRNAs used. *S2891 targets the 3' region of the gene (coding region) and s2892 targets the 5' UTR region of the gene.*

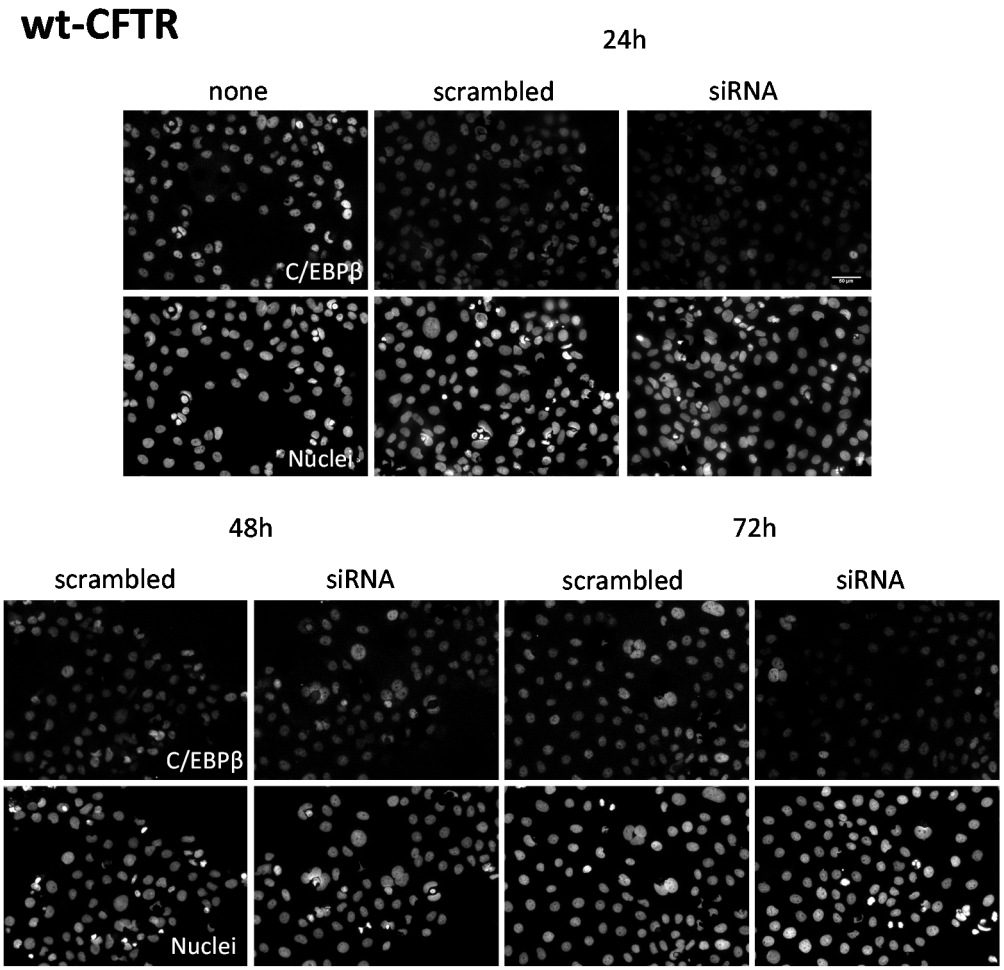

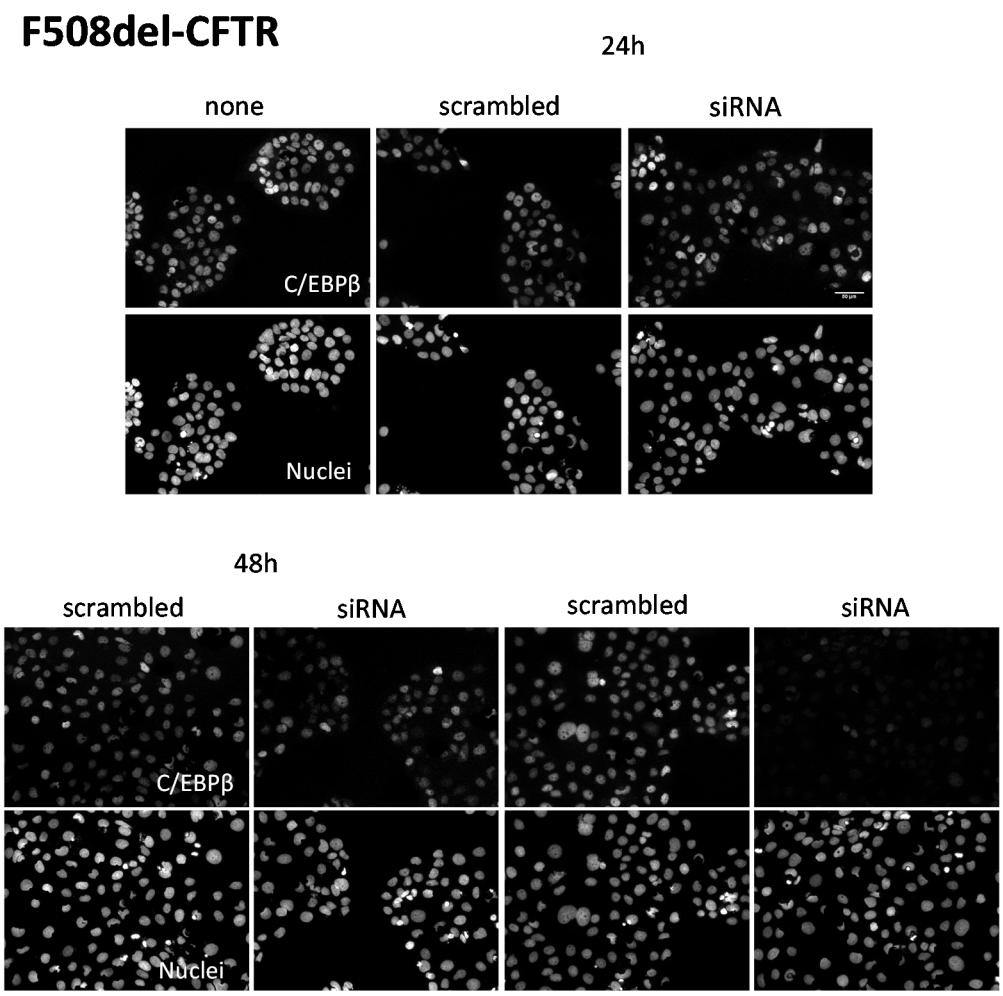

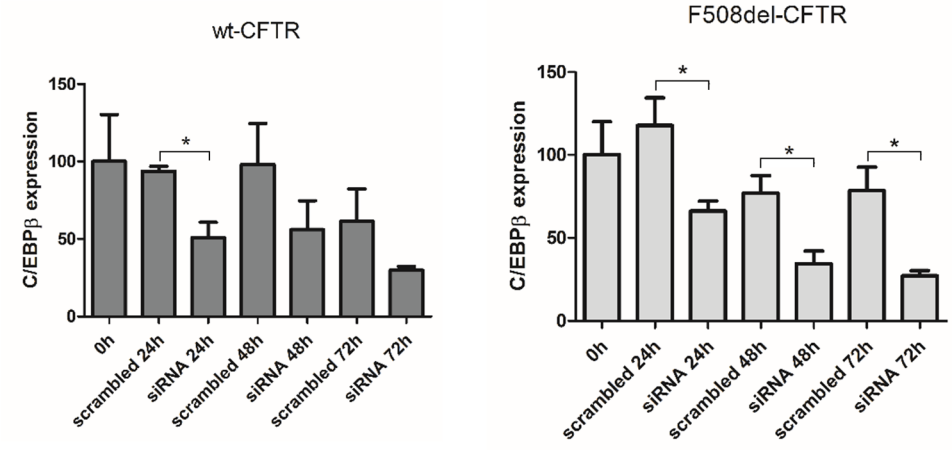

(caption on the next page)

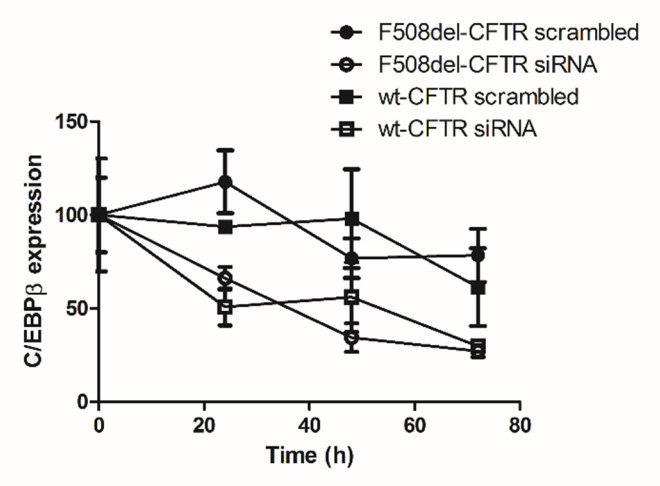

Figure 35 – Effect of siRNAs for C/EBPβ on C/EBPβ expression throughout 72h - immunofluorescence images and respective quantification. *Cells were stained for C/EBPβ. Nuclei were stained with Hoechst. Scale bar represents 50µm. Differences were significant (p<0.05) for 24h, 48h and 72h siRNA effect on F508del-CFTR cells and for 24h siRNA effect on wt-CFTR cells. Results are depicted in % and normalized for 0h C/EBPβ expression. (n=3)*